

Lectures on Cosmological Correlations

Daniel Baumann^{1,2} and Austin Joyce³

¹ *Center for Theoretical Physics, National Taiwan University, Taipei 10617, Taiwan*

² *Institute of Physics, University of Amsterdam, Amsterdam, 1098 XH, The Netherlands*

³ *Kavli Institute for Cosmological Physics, Department of Astronomy and Astrophysics, University of Chicago, Chicago, IL 60637, USA*

Abstract

In these lecture notes, we present three approaches to compute cosmological correlation functions: 1) the in-in formalism, 2) the wavefunction approach, and 3) the cosmological bootstrap. We include over 40 exercises, with detailed solutions, to help the students get proficient with the first-principles computations of cosmological correlators.

Work in progress.

September 1, 2022

Please email corrections to: dbaumann@uva.nl

Contents

1	Introduction	5
2	Basics of Cosmology	7
2.1	Homogeneous Cosmology	7
2.2	Cosmological Perturbations	9
2.3	Inflation and de Sitter Space	13
2.4	Quantum Initial Conditions	14
2.5	Primordial Non-Gaussianity	20
3	The In-In Formalism	23
3.1	In-In Correlators	23
3.1.1	A Master Formula	24
3.1.2	Perturbative Expansion	27
3.1.3	Feynman Rules	29
3.2	Correlators in Flat Space	30
3.3	Correlators in de Sitter	34
4	The Wavefunction Approach	42
4.1	Wavefunction of the Universe	42
4.2	Warmup in Quantum Mechanics	43
4.2.1	Harmonic Oscillator	43
4.2.2	Time-Dependent Oscillator	44
4.3	Free Fields in de Sittter	45
4.4	Interactions	48
4.4.1	Anharmonic Oscillator	48
4.4.2	Wavefunction in Field Theory	51
4.4.3	Perturbation Theory	54
4.4.4	Correlators in Flat Space	57
4.4.5	Correlators in de Sitter	59
4.5	A Challenge	61
5	The Cosmological Bootstrap	64
5.1	Bootstrap Philosophy	64
5.1.1	S-matrix Bootstrap	65
5.1.2	Cosmological Bootstrap	66
5.2	Symmetries	66
5.2.1	De Sitter Isometries	66
5.2.2	Unitary Representations	68
5.2.3	Realization on Bulk Fields	70
5.2.4	Boundary Conformal Symmetry	72
5.2.5	Conformal Ward Identities	74

5.3	Singularities	79
5.3.1	Flat-Space Examples	79
5.3.2	Generalization to de Sitter	81
5.3.3	Singularities as Input	81
5.4	Example: Massive Exchange	82
5.4.1	Ward Identities	82
5.4.2	Contact Solutions	83
5.4.3	Exchange Solutions	84
5.4.4	Particle Production	91
5.5	Unitarity	92
5.5.1	Optical Theorem	92
5.5.2	Cutting Rules	92
5.6	Example: Boostbreaking Correlators	92
5.7	Summary of Recent Progress	92
6	Conclusions and Outlook	93
A	Some Facts About De Sitter	94
A.1	Different Coordinates	94
A.2	Unitary Representations	94
B	Solutions to the Exercises	99
B.1	Solution to Exercise 2.1	99
B.2	Solution to Exercise 2.2	100
B.3	Solution to Exercise 3.1	103
B.4	Solution to Exercise 3.2	104
B.5	Solution to Exercise 3.3	106
B.6	Solution to Exercise 3.4	107
B.7	Solution to Exercise 3.5	109
B.8	Solution to Exercise 3.6	111
B.9	Solution to Exercise 3.7	112
B.10	Solution to Exercise 3.8	112
B.11	Solution to Exercise 4.1	114
B.12	Solution to Exercise 4.2	115
B.13	Solution to Exercise 4.3	115
B.14	Solution to Exercise 4.4	116
B.15	Solution to Exercise 4.5	117
B.16	Solution to Exercise 4.6	118
B.17	Solution to Exercise 4.7	119
B.18	Solution to Exercise 4.8	121
B.19	Solution to Exercise 4.9	121
B.20	Solution to Exercise 4.10	122
B.21	Solution to Exercise 4.11	123

B.22 Solution to Exercise 4.12	124
B.23 Solution to Exercise 4.13	124
B.24 Solution to Exercise 5.1	126
B.25 Solution to Exercise 5.2	127
B.26 Solution to Exercise 5.3	128
B.27 Solution to Exercise 5.4	128
B.28 Solution to Exercise 5.5	129
B.29 Solution to Exercise 5.6	130
B.30 Solution to Exercise 5.7	130
B.31 Solution to Exercise 5.8	130
B.32 Solution to Exercise 5.9	130
B.33 Solution to Exercise 5.10	130
B.34 Solution to Exercise 5.11	130
B.35 Solution to Exercise 5.12	130
B.36 Solution to Exercise 5.13	130
B.37 Solution to Exercise 5.14	130
B.38 Solution to Exercise A.1	130
References	131

1 Introduction

One of the biggest questions in all of science is the origin of structure in the Universe. What created everything that we see around us? An important clue lies in the fact that the structures in the Universe aren't distributed randomly, but displays large-scale correlations. These correlations are a fossil record of the early universe, and by measuring them we hope to uncover how the cosmological perturbations formed and evolved.

Our earliest snapshot of the large-scale structure of the Universe comes from measurements of the cosmic microwave background (CMB), whose intensity varies as a function of position on the sky. These CMB anisotropies reflect variations in the matter density at the time when the first atoms formed, about 380 000 years after the Big Bang. Over time, the density fluctuations grew, until clouds of gas started to collapse into stars and galaxies. In principle, the distribution of the collapsed objects still contains correlations that carry information about the primordial universe. Extracting that information is a fundamental challenge of modern cosmology.

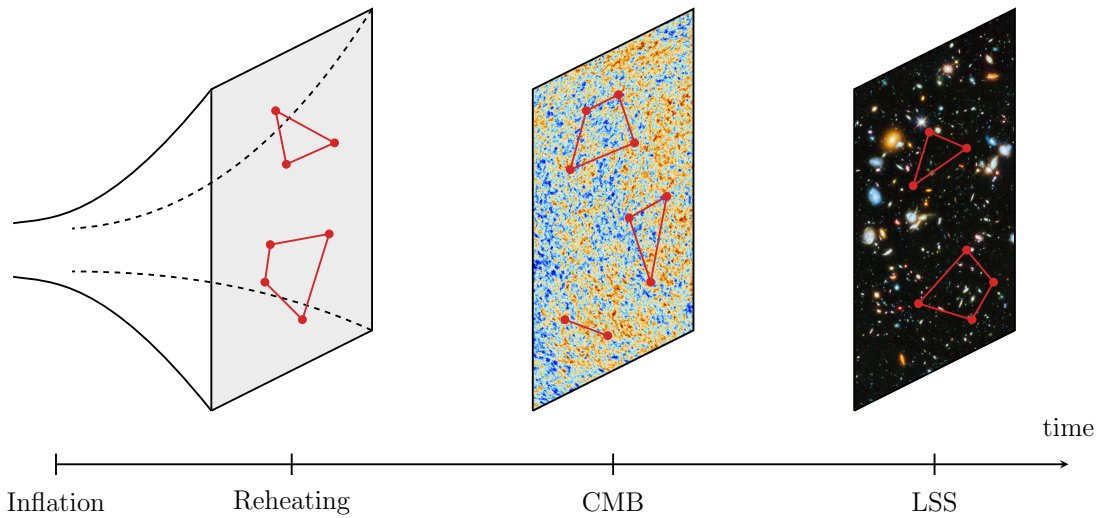


Figure 1: The correlations in late-time cosmological observables—like the distribution of the large-scale structure (LSS) or the anisotropies of the cosmic microwave background (CMB)—can be traced back in time to primordial correlations on the “reheating surface” (marking the initial surface of the hot Big Bang universe or the final surface at the end of inflation). Imprinted in these correlations is the physics of the inflationary era. (Figure adapted from [1].)

We understand the late-time evolution of the Universe well enough to trace back until the beginning of the hot Big Bang. While doing this, cosmologists recently discovered a remarkable fact: the initial fluctuations which ultimately led to the large-scale structure of the Universe must have been created *before* the hot Big Bang. The conventional Big Bang was therefore *not* the beginning of time, but the end of an earlier high-energy period, and the primordial fluctuations were created in this pre-Big Bang phase. But, how exactly did this happen? The challenge is to extract this information from the pattern of correlations in the late universe.

We have some evidence for a period of inflationary expansion before the hot Big Bang. The details of inflation are still uncertain, but it provides an elegant mechanism to convert quantum

vacuum fluctuations into large-scale cosmological perturbations. The main observable predictions of inflation are spatial correlation functions and our goal in these lectures is to explain how these are computed.

We will describe three different approaches to compute cosmological correlation functions:

- *In-in formalism*.—In cosmology, we compute “in-in correlators” (rather than in-out transition amplitudes). This means we are interested in the expectation values of quantum operators, $\mathcal{O}(t)$ at some fixed time, $\langle \mathcal{O}(t) \rangle \equiv \langle \Omega | \mathcal{O}(t) | \Omega \rangle$, where $|\Omega\rangle$ is a specific state that we evolve from some initial time t_i to t .
- *Wavefunction approach*.—Alternatively, we first define a wavefunctional for the late-time fluctuations, $\Psi[\phi]$, which determines the probability for a given field configuration $\phi(\mathbf{x})$ at the end of inflation. From this wavefunctional we can then compute all correlations of the late-time field ϕ .
- *Cosmological bootstrap*.—A drawback to the in-in and wavefunction methods is that they involve complex time integrals that typically cannot be performed analytically. Since the time evolution during inflation is not actually observable, it stands to reason that the late-time correlators can be determined more directly without having to follow this evolution directly. The main idea of the cosmological bootstrap is to infer the static boundary correlations from consistency conditions alone.

Our goal is to explain in very explicit detail how to perform computations in all three of these approaches.

Outline The outline of these notes is as follows: In Section 2, we provide a lightning review of elementary concepts of modern cosmology. For most readers, this will hopefully just be a reminder of material they have seen before, and experts can skip this section. The following three sections then present three different ways of computing cosmological correlation functions from first principles: In Section 3, we review the in-in formalism and use it to compute correlation functions both in flat space and in de Sitter space. In Section 4, we introduce the wavefunction approach and use it to compute a wide variety of correlators. We show in detail how the wavefunction computations reproduce the results from the in-in computation. Finally, in Section 5, we present a new “bootstrap” approach to the problem of cosmological correlations. Instead of struggling with complex time integrals, the bootstrap method tries to infer the spatial correlators directly by imposing consistency requirements. The cosmological bootstrap is still an active area of research and we therefore only provide a limited pedagogical introduction to the bootstrapping of simple scalar correlators. We end, in Section 6, with an outlook on the future.

Further reading These lecture notes are *not* meant to be a review, but rather are intended as a tutorial that teaches students how to compute cosmological correlators. For further reading, we recommend [2, 3] (on the in-in formalism) and [1, 4, 5] (on the cosmological bootstrap).

2 Basics of Cosmology

We begin with a lightning review of cosmology, focusing on the elements most relevant for the study of cosmological correlations. Readers who are familiar with the basic concepts of cosmology may skip this section.

2.1 Homogeneous Cosmology

Averaged over long enough distances, the Universe is homogeneous (translation invariant) and isotropic (rotation invariant). The Robertson–Walker metric of such a homogenous and isotropic spacetime is

$$ds^2 = -dt^2 + a^2(t) g_{ij} dx^i dx^j, \quad (2.1)$$

where g_{ij} denotes the metric of a maximally symmetric 3-space and $a(t)$ is the scale factor. Homogeneity and isotropy allow three possibilities for the curvature of the spatial slices (positive, negative or flat), but observations favor a flat universe, $g_{ij} \rightarrow \delta_{ij}$, which we will assume throughout these lectures.

The evolution of the metric is determined by the Einstein equations, which in this context take the form of the Friedmann equation for the scale factor

$$H^2 = \frac{8\pi G}{3}\rho, \quad (2.2)$$

where $H \equiv \dot{a}/a$ is the expansion rate (also called the Hubble parameter) and $\rho = \sum_i \rho_i$ is the total energy density of all the constituents of the Universe. The present value of the Hubble parameter is $H_0 \approx 70 \text{ km s}^{-1} \text{Mpc}^{-1}$ and the average density today is

$$\begin{aligned} \rho_0 &= \frac{3H_0^2}{8\pi G} = 0.8 \times 10^{-29} \text{ g cm}^{-3} \\ &\approx 5 \text{ protons m}^{-3}. \end{aligned}$$

In comparison, the best vacuum on Earth has a density of about $1000 \text{ atoms cm}^{-3}$, so the universe is pretty empty.

The universe is filled with several different species of particles:

$$\underbrace{\text{photons } (\gamma) \quad \text{neutrinos } (\nu)}_{\text{radiation } (r)} \quad \underbrace{\text{baryons } (b)}_{\substack{\text{electrons } (e) \quad \text{protons } (p)}} \quad \underbrace{\text{cold dark matter } (c)}_{\text{matter } (m)}.$$

For most of the history of the Universe, these particles can be treated in a fluid approximation and each homogeneous matter species is characterized by an energy density, ρ , and a pressure, P . In an expanding universe, these fluid components satisfy the continuity equation

$$\frac{d\rho}{dt} = -3H(\rho + P). \quad (2.3)$$

The two equations (2.2) and (2.3) together fully specify the homogeneous evolution of the combined metric-matter system once we posit an equation of state relating the density and pressure

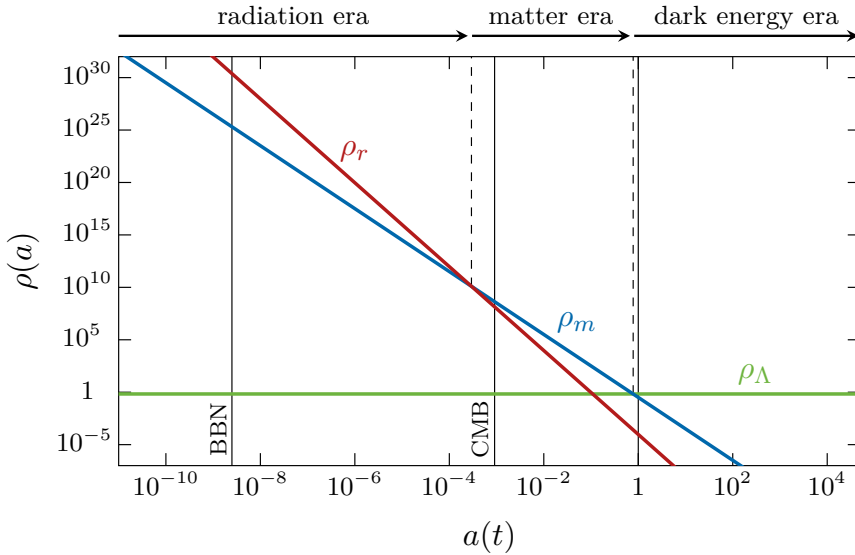


Figure 2: Evolution of the energy densities in the Universe. We see that the Universe was first dominated by radiation, then matter and today dark energy.

of the fluid components. (Typically, this specifies the pressure in terms of the energy as $P = w\rho$, for some constant w , which is called the equation of state parameter.)

Non-relativistic matter is pressureless ($w = 0$) and from (2.3) we infer that its energy density evolves as $\rho_m \propto a^{-3}$. This scaling is fairly intuitive since the energy of non-relativistic particles in a fixed volume is constant, while the latter increases as $V \propto a^3$. In contrast, the energy density of relativistic particles (or “radiation”, with $w = 1/3$) decreases as $\rho_r \propto a^{-4}$. The extra dilution comes from the fact that the energy of relativistic particles isn’t constant, but redshifts as $E \propto a^{-1}$. Feeding these scalings into the Friedmann equation (2.2) gives $a(t) \propto t^{2/3}$ and $a(t) \propto t^{1/2}$ during the matter and radiation eras, respectively.

In 1998, it was discovered that the universe is accelerating. The source of the acceleration is unknown, and we call it “dark energy.” The simplest form of dark energy is a cosmological constant (or “vacuum energy”), with $\rho_\Lambda = \text{const}$. Feeding this into the Friedmann equation leads to exponential expansion of the scale factor, $a(t) \propto e^{H_\Lambda t}$.

It is conventional to measure the contribution of each species i as a fraction of the total energy density today, $\Omega_i \equiv \rho_i/\rho_0$. The measured ΛCDM parameters then are

$$\Omega_r = 9.4 \times 10^{-5}, \quad \Omega_b = 0.04, \quad \Omega_m = 0.32, \quad \Omega_\Lambda = 0.68.$$

We see that the present Universe has comparable amounts of (dark) matter and dark energy. Why today is a mystery call the “coincidence problem.” Figure 2 shows the evolution of the three main energy components in the Universe. We see that although the Universe today is dominated by dark energy, in past matter and radiation were more important. Many interesting things happened during the early radiation phase of the universe, most notably the formation of the light elements during Big Bang nucleosynthesis (BBN). The fascinating history of the primordial universe is told in any cosmology textbook, but is beyond the scope of these lectures.

2.2 Cosmological Perturbations

Of course, the Universe is not perfectly homogeneous and cosmologists have learned a great deal about the structure and evolution of the Universe by studying its large-scale structure. Mathematically, we describe these inhomogeneities by perturbations of the energy-momentum tensor, $\delta T_{\mu\nu}(t, \mathbf{x})$, and the spacetime metric, $\delta g_{\mu\nu}(t, \mathbf{x})$. The Einstein equations—together with fluid or Boltzmann equations for the matter—then relate these fluctuations and determine their evolution. Not all fluctuations, however, are physical since they can transform under a change of coordinates. This gauge problem is addressed either by working with a fixed set of coordinates—and tracking all fluctuations—or by defining gauge-invariant combinations of perturbations and following their evolution. Irrespective of which approach is being used, in the end, the result must be related to unambiguous physical observables.

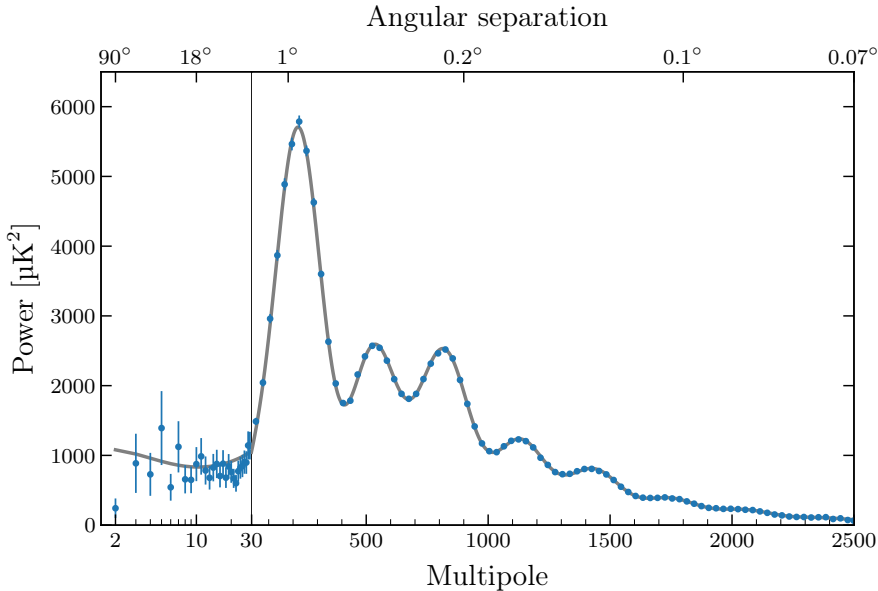


Figure 3: Power spectrum of CMB temperature anisotropies as measured by the Planck satellite [?].

Late-time correlations

We measure cosmological perturbations by observing different *tracers* of the distribution of structure in the Universe. For example, we observe the positions and redshifts of galaxies to determine the late-time distribution of matter, or the angular variations in the CMB temperature to infer the primordial density perturbations at the time of recombination. We will collectively denote the different cosmological observables by $\mathcal{O}(t, \mathbf{x})$. It is a crucial fact that the large-scale structure in the Universe isn't distributed randomly, but has interesting correlations between spatially separated points:¹

$$\langle \mathcal{O}(t, \mathbf{x}_1) \mathcal{O}(t, \mathbf{x}_2) \dots \mathcal{O}(t, \mathbf{x}_N) \rangle. \quad (2.4)$$

¹The expectation value $\langle \dots \rangle$ denotes an *ensemble average* of the stochastic process that created the random field $\mathcal{O}(\mathbf{x})$ (e.g. quantum fluctuations during inflation). While the ensemble average is the natural object to compute from a theory of the initial conditions, it is not what we actually measure in observations. The observed large-scale structure of the Universe is a single realization of a random process. To relate these observations to our theoretical

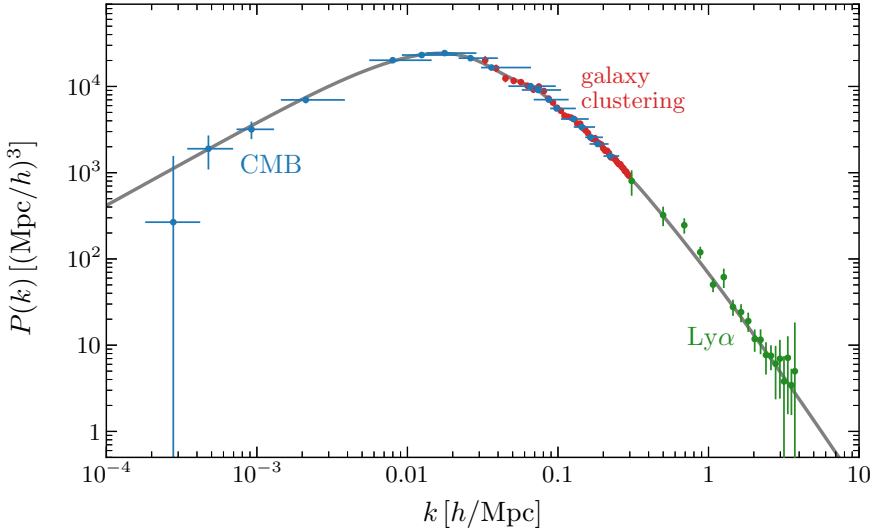


Figure 4: Measurements of the linear matter power spectrum (figure adapted from [?]). The “galaxy clustering” constraints are from the luminous red galaxy sample of the Sloan Digital Sky Survey (SDSS), the “CMB” constraints are derived from the Planck measurements of the CMB anisotropies, and “Ly α ” refers to the Lyman-alpha forest.

These N -point correlators are to the cosmologist what N -point scattering amplitudes are to the particle physicist.

Figure 3 shows the two-point correlation function of the CMB temperature anisotropies, $\langle \delta T(\boldsymbol{\theta}_1) \delta T(\boldsymbol{\theta}_2) \rangle$. The importance of this graph for cosmology cannot be overstated. The shape of the CMB power spectrum depends sensitively on the cosmological parameters and CMB measurements have therefore been used to determine the parameters of the Λ CDM cosmology to great precision.

Figure 4 displays measurements of the two-point function of matter density fluctuations, $\langle \delta \rho_m(\mathbf{x}_1) \delta \rho_m(\mathbf{x}_2) \rangle$, using different tracers of the matter perturbations. The shape of this two-point function can be understood from the difference in the clustering of subhorizon mode during the radiation and matter eras. (Matter only starts to cluster significantly when the universe becomes matter dominated.)

Initial conditions

Under relatively mild assumptions, the cosmological perturbations can be traced back in time to the origin of the hot Big Bang (or the reheating surface after inflation). In principle, the initial fluctuations can be very complicated, with independent fluctuations in each component of the primordial plasma. In practice, however, all fluctuations are synchronized and can be described

predictions, we assume *ergodicity*, which states that ensemble averages are equal to spatial averages as the volume becomes infinitely large. In that case, different parts of the Universe can be viewed as different realizations of the underlying random process. The volume average therefore approximates the average over different members of the ensemble. Of course, in reality, we don’t measure an infinite volume which introduces an irreducible *cosmic variance* in the measurements.

by a single fluctuating degree of freedom (we call this *adiabatic initial conditions*). We will describe the initial fluctuations at the beginning of the hot Big Bang by the so-called *curvature perturbation*, $\zeta(t_i, \mathbf{x})$, which is defined as a local, isotropic rescaling of the spatial metric

$$g_{ij}(t, \mathbf{x}) = a^2(t) e^{2\zeta(t, \mathbf{x})} \delta_{ij}. \quad (2.5)$$

The name curvature perturbation follows from the fact that the three-dimensional Ricci curvature on the spatial slices is $a^2 R_{(3)} = 4\nabla^2 \zeta$. We assume that the initial fluctuations were drawn from a probability distribution $\mathbb{P}[\zeta]$ and that their correlation functions can therefore be written as

$$\langle \zeta(\mathbf{x}_1) \cdots \zeta(\mathbf{x}_N) \rangle = \int \mathcal{D}\zeta \, \zeta(\mathbf{x}_1) \cdots \zeta(\mathbf{x}_N) \mathbb{P}[\zeta], \quad (2.6)$$

where the integral is a functional integral (or path integral) over field configurations. By tracing the observed correlations $\langle \mathcal{O}_1 \mathcal{O}_2 \dots \mathcal{O}_N \rangle$ back in time, cosmologists try to measure the initial correlations $\langle \zeta_1 \zeta_2 \dots \zeta_N \rangle$ and use them to extract information about the initial probability distribution $\mathbb{P}(\zeta)$ and about the physics that gave rise to it.

If the initial perturbations were drawn from a Gaussian probability distribution then all statistical information is captured by the two-point function, $\langle \zeta(\mathbf{x}) \zeta(\mathbf{x}') \rangle$. Statistical homogeneity and isotropy demand that the two-point function is invariant under translations and rotations, and can therefore only depend on the distance between two points, $r \equiv |\mathbf{x} - \mathbf{x}'|$.

It is also convenient to describe the field $\zeta(\mathbf{x})$ in terms of its Fourier modes:

$$\zeta(t_i, \mathbf{x}) = \int \frac{d^3 k}{(2\pi)^3} \zeta_{\mathbf{k}}(t_i) e^{i\mathbf{k} \cdot \mathbf{x}}. \quad (2.7)$$

Since $\zeta(\mathbf{x})$ is a real field, its Fourier components satisfy $\zeta_{\mathbf{k}} = \zeta_{-\mathbf{k}}^*$. The two-point correlator of the Fourier modes is the *power spectrum*:

$$\langle \zeta_{\mathbf{k}} \zeta_{\mathbf{k}'} \rangle = (2\pi)^3 \delta^{(3)}(\mathbf{k} + \mathbf{k}') P_{\zeta}(k), \quad (2.8)$$

where the delta function is a consequence of translation invariance. Rotational invariance demands that the power spectrum is a function only of $k \equiv |\mathbf{k}|$ and doesn't depend on the direction of the wavevector. Substituting (2.8) into the definition of the two-point function (in position space), we find

$$\begin{aligned} \langle \zeta(\mathbf{x}) \zeta(\mathbf{x}') \rangle &= \int \frac{d^3 k}{(2\pi)^3} \int \frac{d^3 k'}{(2\pi)^3} \langle \zeta_{\mathbf{k}} \zeta_{\mathbf{k}'} \rangle e^{i\mathbf{k} \cdot \mathbf{x}} e^{i\mathbf{k}' \cdot \mathbf{x}'} \\ &= \int \frac{d^3 k}{(2\pi)^3} P_{\zeta}(k) e^{i\mathbf{k} \cdot (\mathbf{x} - \mathbf{x}')}. \end{aligned} \quad (2.9)$$

We see that the power spectrum is the Fourier transform of the two-point function. Performing the angular integral, we find

$$\langle \zeta(\mathbf{x}) \zeta(\mathbf{x}') \rangle = \int d \log k \frac{k^3}{2\pi^2} P_{\zeta}(k) j_0(k|\mathbf{x} - \mathbf{x}'|), \quad (2.10)$$

where $j_0(x) = \sin(x)/x$ is a spherical Bessel function of order zero. Equation (2.10) motivates us to define the dimensionless power spectrum:

$$\Delta_\zeta^2(k) = \frac{k^3}{2\pi^2} P_\zeta(k). \quad (2.11)$$

The variance of the field is $\langle \zeta^2(\mathbf{x}) \rangle = \int d\log k \Delta_\zeta^2(k)$. A *scale-invariant* spectrum has $\Delta_\zeta^2(k) = \text{const.}$ and the variance receives equal contributions from every logarithmic integral of k . (In position space, this translates into $\langle \zeta(\lambda\mathbf{x})\zeta(\lambda\mathbf{x}') \rangle = \langle \zeta(\mathbf{x})\zeta(\mathbf{x}') \rangle$, for a constant λ .) Deviations from scale invariance are often parameterized by a power-law ansatz

$$\Delta_\zeta^2(k) = A_s \left(\frac{k}{k_0} \right)^{n_s - 1}, \quad (2.12)$$

where n_s is the *scalar spectral index* defined relative to a reference scale k_0 . By a historical accident, the scale-invariant spectrum corresponds to $n_s = 1$. The measured spectral index in our Universe is [?]

$$n_s = 0.9667 \pm 0.0040. \quad (2.13)$$

We see that there is a statistically significant deviation from the scale-invariant spectrum.

Transfer functions

As long as the fluctuations are small (i.e. at early times or on large scales), their evolution equations can be linearized. It is convenient to describe this linear evolution in Fourier space, since the individual Fourier modes evolve independently. Each observable \mathcal{O} is then related to the primordial perturbations $\zeta_{\mathbf{k}}(t_i)$ by a *transfer function*:

$$\mathcal{O}(\mathbf{x}, t) = \int \frac{d^3k}{(2\pi)^3} T_{\mathcal{O}}(k; t, t_i) \zeta_{\mathbf{k}}(t_i) e^{i\mathbf{k}\cdot\mathbf{x}}. \quad (2.14)$$

As indicated by the notation, there are different transfer functions $T_{\mathcal{O}}$ for each component of the Universe (photons, baryons, dark matter, etc.) At early times, photons and baryons were strongly coupled and acted as a single fluid. The large pressure of the radiation supported sound waves in the primordial plasma that left an imprint in the pattern of CMB anisotropies that we can still observe today. All of this interesting physics is captured by the CMB transfer function. Dark matter, on the other hand, is pressureless and therefore started to cluster earlier than the baryons. Only after recombination, did the baryons lose their pressure support and started collapsing into denser structure. It is important that the clustering of dark matter had a head start and then assisted the formation of baryonic structures (like stars and galaxies). Without the scaffolding provided by the dark matter structures wouldn't have formed fast enough to produce the Universe we see around us. All of this is encoded in the (dark) matter transfer function. More on the linear transfer functions for cosmological fluctuations can be found in any cosmology textbook, e.g. [6, 7]. For the purpose of these lectures, it is only important to know that the physics of the linear evolution is extremely well-understood, so that the fluctuations can be traced back to their primordial origins, $\zeta_{\mathbf{k}}(t_i)$.²

²At some point—at late times and on small scales—the fluctuations become large and the linearize approximation breaks down. The relation between the observables \mathcal{O} and the initial conditions ζ then isn't described by linear transfer functions, but instead must be described by a phenomenological model.

2.3 Inflation and de Sitter Space

A promising (but still speculative) framework for explaining the cosmological initial conditions is the theory of *inflation*, which posits that the early universe experience a brief period of accelerated expansion, $\ddot{a} > 0$. During this phase, small quantum fluctuations were stretched to cosmic scales and became the seeds for the formation of structure in the Universe. Accelerated expansion can occur in GR if the Universe is filled with a substance with nearly constant energy density (like a temporary cosmological constant). The expansion rate is then nearly constant, $H \approx \text{const.}$, and the scale factor grows exponentially $a(t) \approx e^{Ht}$. The metric during inflation is approximately that of *de Sitter space*:

$$\begin{aligned} ds^2 &= -dt^2 + e^{2Ht} d\mathbf{x}^2 \\ &= \frac{1}{H^2 \eta^2} (-d\eta^2 + d\mathbf{x}^2), \end{aligned} \tag{2.15}$$

where we have introduced conformal time, $d\eta = dt/a(t)$. The deviation from the perfect de Sitter limit is characterized by the parameter

$$\varepsilon \equiv -\frac{\dot{H}}{H^2} \ll 1. \tag{2.16}$$

Inflationary models are characterized by the history of the nearly constant Hubble parameter, $H(t)$. The spontaneous breaking of time translation symmetry leads to a scalar Goldstone mode, $\pi(t, \mathbf{x})$, whose quantum fluctuations may have been the seeds for density fluctuations in the early universe. Differential inflationary models can be classify by their symmetry breaking patterns and the associated Goldstone interactions [8, 9].

An influential toy model for the inflationary dynamics is *slow-roll inflation*. In these models, a scalar field ϕ (the *inflaton*) dominates the energy density of the universe and dictates the evolution of the background spacetime. The action of the field, minimally coupled to gravity, is

$$S = \int d^4x \sqrt{-g} \left(\frac{M_{\text{Pl}}^2}{2} R - \frac{1}{2} g^{\mu\nu} \partial_\mu \phi \partial_\nu \phi - V(\phi) \right). \tag{2.17}$$

The expansion rate of the universe is then determined by the Friedmann equation

$$H^2 = \frac{1}{3M_{\text{Pl}}^2} \left(\frac{1}{2} \dot{\phi}^2 + V(\phi) \right), \tag{2.18}$$

which during inflation has to remain approximately constant. This inflationary condition is satisfied if a nearly constant potential energy density, $V(\phi)$, dominates over the kinetic energy density of the field. For successful inflation, this slow-roll evolution has to be maintained for a sufficiently long amount of time, which requires the acceleration of the field to be small. We assess this by considering the Klein–Gordon equation

$$\ddot{\phi} + 3H\dot{\phi} = -\frac{dV}{d\phi}. \tag{2.19}$$

Sustained slow-roll inflation occurs when the Hubble friction term, $3H\dot{\phi}$, is large compared to the acceleration of the field, $\ddot{\phi}$. Many models of inflation have been constructed that satisfy these slow-roll conditions (see e.g. [? ?] for more details).

2.4 Quantum Initial Conditions

So far, we have only discussed the homogeneous dynamics of inflation. One of the most fascinating features of the theory, however, is that it automatically contains a mechanism to explain the origin of fluctuations in the Universe. In this section, we will describe a simplified toy model for this process. More details can be found in [6, 10].

For concreteness, we will describe the quantization of fluctuations in slow-roll inflation, but the same procedure applies to the fluctuations in more general models of inflation. Consider the perturbed inflaton field:

$$\phi(\eta, \mathbf{x}) = \bar{\phi}(\eta) + \varphi(\eta, \mathbf{x}). \quad (2.20)$$

In GR, the field fluctuations will not be independent from metric fluctuations, but will be coupled to them through the Einstein equations. These gravitational couplings are gauge dependent, i.e. depend on the choice of coordinates used to describe the fluctuations. A convenient gauge to describe the quantization of the inflaton fluctuations is the spatially-flat gauge, with $g_{ij} = a^2(\eta)\delta_{ij}$. In this gauge, the mixing between φ and the metric perturbations $\delta g_{0\mu}$ vanishes in the limit $\varepsilon \rightarrow 0$. The inflaton self-interactions are also suppressed due to the flatness of the slow-roll potential. The leading behaviour in the limit $\varepsilon \rightarrow 0$ therefore is that of a free massless scalar in exact de Sitter space, described by the action

$$S = \int d^4x \sqrt{-g} \left(-\frac{1}{2} g^{\mu\nu} \partial_\mu \varphi \partial_\nu \varphi \right) \quad (2.21)$$

$$= \frac{1}{2} \int d\eta d^3x a^2(\eta) \left((\varphi')^2 - (\nabla \varphi)^2 \right), \quad (2.22)$$

where $a(\eta) = -(H\eta)^{-1}$. Our goal is to compute the variance of the field fluctuations induced by quantum mechanics.

Classical dynamics

We begin by studying the classical dynamics of the field φ . From the action (4.58), we obtain the following equation of motion:

$$\varphi'' + 2\frac{a'}{a}\varphi' - \nabla^2\varphi = 0, \quad (2.23)$$

so that each Fourier mode satisfies

$$\varphi''_{\mathbf{k}} - \frac{2}{\eta}\varphi'_{\mathbf{k}} + k^2\varphi_{\mathbf{k}} = 0. \quad (2.24)$$

In order to cast this equation in a more familiar form, we define $\varphi_{\mathbf{k}} \equiv a(\eta)^{-1}u_{\mathbf{k}}$, where the function $u_{\mathbf{k}}(\eta)$ obeys

$$u''_{\mathbf{k}} + \left(k^2 - \frac{2}{\eta^2} \right) u_{\mathbf{k}} = 0.$$

(2.25)

This is the equation of a harmonic oscillator, with a frequency given by the wavenumber k and a time-dependent (tachyonic) mass term.

Before solving (2.25), it is useful to determine the limiting behavior of the solutions:

- At *early times*, most modes of interest had wavelengths much smaller than the comoving Hubble scale, $k^{-1} \ll (aH)^{-1} = -\eta$. In this regime, the mass term can be dropped and equation (2.25) simplifies to

$$u''_{\mathbf{k}} + k^2 u_{\mathbf{k}} = 0, \quad (2.26)$$

which is exactly the same as the equation satisfied by a massless scalar field in Minkowski space.³ The solutions to this equation are the standard solutions of the simple harmonic oscillator

$$u_{\mathbf{k}} \xrightarrow{k\eta \rightarrow -\infty} \frac{1}{\sqrt{2k}} e^{\pm ik\eta}, \quad (2.27)$$

where we have chosen the overall normalization, so that the solutions have Wronskian $\pm i$.

- At *late times*, the tachyonic mass term becomes relevant, and the fluctuations are amplified. In this limit, equation (2.25) becomes

$$u''_{\mathbf{k}} - \frac{2}{\eta^2} u_{\mathbf{k}} = 0, \quad (2.28)$$

which is solved by

$$u_{\mathbf{k}} = c_1 \eta^{-1} + c_2 \eta^2 \xrightarrow{k\eta \rightarrow 0} c_1 \eta^{-1}. \quad (2.29)$$

The growing mode solution implies $\varphi_{\mathbf{k}} = a^{-1} u_{\mathbf{k}} \propto \eta \times \eta^{-1} = \text{const}$, so that the original field fluctuations are *frozen*.

Of course, we can also solve (2.25) directly to find

$$u_{\mathbf{k}}(\eta) = c_1 \frac{1}{\sqrt{2k}} \left(1 + \frac{i}{k\eta} \right) e^{ik\eta} + c_2 \frac{1}{\sqrt{2k}} \left(1 - \frac{i}{k\eta} \right) e^{-ik\eta}, \quad (2.30)$$

where the free coefficients c_1, c_2 will be fixed by boundary conditions. From these solutions, we can explicitly see that there is a crossover in behavior when the wavelength of a mode becomes larger than the comoving Hubble radius, where the mode goes from being oscillatory to growing like a power law, reproducing the behaviors we saw above in the relevant regimes. Translating back into the original field, $\varphi_{\mathbf{k}} = a^{-1} u_{\mathbf{k}}$, the solutions are

$$\varphi_{\mathbf{k}} = \frac{H}{\sqrt{2k^3}} (1 \pm ik\eta) e^{\mp ik\eta}. \quad (2.31)$$

Now that we have a handle on the classical dynamics, we turn to the quantization of this field.

Canonical quantization

We have seen that, at early times, the field fluctuations $u_{\mathbf{k}}$ satisfy the equation of a simple harmonic oscillator. Quantum zero-point fluctuations of this collection of oscillators produce a nonzero variance of the field. The expansion of the Universe amplifies these fluctuations and stretches them to large scales. In the following, we will compute the spectrum of these quantum fluctuations.

³Physically, this is a manifestation of the equivalence principle, which states that at scales much smaller than the radius of curvature of de Sitter space, the effects of the geometry are invisible.

We start with the action for the canonically-normalized field $u \equiv a(\eta)\varphi$:

$$S = \frac{1}{2} \int d\eta d^3x \left((u')^2 - (\nabla u)^2 + \frac{a''}{a} u^2 \right), \quad (2.32)$$

whose equation of motion reproduces (2.25). The canonical momentum conjugate to u is

$$\pi \equiv \frac{\delta \mathcal{L}}{\delta u'} = u'. \quad (2.33)$$

We quantize the theory by promoting the classical fields u and π to quantum operators \hat{u} and $\hat{\pi}$, and impose the canonical commutation relation

$$[\hat{u}(\eta, \mathbf{x}), \hat{\pi}(\eta, \mathbf{x}')] = i\delta^{(3)}(\mathbf{x} - \mathbf{x}'), \quad (2.34)$$

in units where $\hbar \equiv 1$. The delta function is required by locality: modes at different points in space are independent and the corresponding operators therefore must commute. In Fourier space, the commutator becomes

$$\begin{aligned} [\hat{u}_{\mathbf{k}}(\eta), \hat{\pi}_{\mathbf{k}'}(\eta)] &= \int d^3x \int d^3x' \underbrace{[\hat{u}(\eta, \mathbf{x}), \hat{\pi}(\eta, \mathbf{x}')]}_{i\delta^{(3)}(\mathbf{x} - \mathbf{x}')} e^{-i\mathbf{k}\cdot\mathbf{x}} e^{-i\mathbf{k}'\cdot\mathbf{x}'} \\ &= i \int d^3x e^{-i(\mathbf{k}+\mathbf{k}')\cdot\mathbf{x}} \\ &= i(2\pi)^3 \delta^{(3)}(\mathbf{k} + \mathbf{k}'), \end{aligned} \quad (2.35)$$

and we see that modes with different wavelengths commute. We then decompose the field operator in terms of creation and annihilation operators

$$\hat{u}(\eta, \mathbf{x}) = \int \frac{d^3k}{(2\pi)^3} \left(u_k^*(\eta) \hat{a}_{\mathbf{k}} + u_k(\eta) \hat{a}_{-\mathbf{k}}^\dagger \right) e^{i\mathbf{k}\cdot\mathbf{x}}, \quad (2.36)$$

where the mode function $u_k(\eta)$ is a solution to the classical equation of motion (2.25), and $u_k^*(\eta)$ is its complex conjugate.⁴ The commutator of the ladder operators is

$$[\hat{a}_{\mathbf{k}}, \hat{a}_{\mathbf{k}'}^\dagger] = (2\pi)^3 \delta^{(3)}(\mathbf{k} - \mathbf{k}'), \quad (2.37)$$

which is the direct analogue of the commutator for the ladder operators in the ordinary harmonic oscillator. The field operator and its conjugate momentum operator then satisfy the commutation relation (2.35), as long as the mode functions obey the *Wronskian condition*:

$$\partial_\eta u_k(\eta) u_k^*(\eta) - u_k(\eta) \partial_\eta u_k^*(\eta) = i. \quad (2.38)$$

Up to an irrelevant phase, this fixes the normalization of the solution $u_k(\eta)$.

⁴Because the evolution is isotropic, the mode functions depend only on the magnitude of the wavevector, $k \equiv |\mathbf{k}|$, and not its direction. The creation and annihilation operators, on the other hand, do depend on direction and only their statistical properties have to be isotropic.

Vacuum choice

At this point, we have not yet picked a particular solution for the mode function $u_k(\eta)$. In fact, there is a one-parameter family of solutions that satisfy the Wronskian condition (2.38), and our selection of $u_k(\eta)$ is related to choosing the vacuum state of the theory. As in the ordinary harmonic oscillator, the vacuum state is defined to be the state that satisfies

$$\hat{a}_{\mathbf{k}}|0\rangle = 0. \quad (2.39)$$

Effectively, different choices of u_k in (2.36) correspond to different choices of vacuum state. In flat space, there is a natural choice, which is to choose the vacuum to be the (unique) state of lowest energy. However, in de Sitter space there is no time translation invariance, and so no bounded operator that we can use as the Hamiltonian.

The most natural vacuum choice is to require that modes at large k (or, equivalently, in the infinite past) reduce to their Minkowski space counterparts (see Exercise 2.1):

$$\lim_{k\eta \rightarrow -\infty} u_k(\eta) = \frac{1}{\sqrt{2k}} e^{ik\eta}, \quad (2.40)$$

which is known as the *Bunch–Davies* vacuum.⁵ This additional boundary condition fixes the solution to be

$$u_k(\eta) = \frac{1}{\sqrt{2k}} \left(1 + \frac{i}{k\eta} \right) e^{ik\eta}. \quad (2.41)$$

This specifies the ground state of the system and fixes the operator (2.36), so that we can compute its variance.

Exercise 2.1. Consider a simple harmonic oscillator whose action is

$$S = \int dt \left(\frac{1}{2} \dot{q}^2 - \frac{1}{2} \omega^2 q^2 \right), \quad (2.42)$$

where q is the deviation from equilibrium and ω is a constant frequency. The mass of the oscillator has been set to unity, $m \equiv 1$. The position operator is written as

$$\hat{q}(t) = q^*(t) \hat{a} + q(t) \hat{a}^\dagger. \quad (2.43)$$

where $q(t)$ is a solution to the classical equations of motion:

$$q(t) = c_1 \frac{1}{\sqrt{2\omega}} e^{i\omega t} + c_2 \frac{1}{\sqrt{2\omega}} e^{-i\omega t}. \quad (2.44)$$

⁵This vacuum state has numerous names. Other common ones are the Euclidean vacuum, adiabatic vacuum, and the Hartle–Hawking state. In principle we did not have to choose this as the ground state. In contrast to what happens in flat space, there is a one-parameter family of de Sitter-symmetric vacua, where we take $u_k(\eta)$ to be any linear combination of (2.41) and its complex conjugate satisfying the Wronskian condition. These different linear combinations are conventionally labeled by a parameter α , and so are typically called α -vacua [11, 12]. It should be noted that these states are somewhat peculiar and it is unclear whether they make sense beyond free theory.

The Wronskian of the solution is $q^* \dot{q} - \dot{q}^* q = i$, so that $[\hat{a}, \hat{a}^\dagger] = 1$. By considering the vacuum expectation value of the Hamiltonian, $\langle 0 | \hat{H} | 0 \rangle$, show that the vacuum $|0\rangle$ is the minimum energy state iff $c_1 = 1$ and $c_2 = 0$.

Power spectrum

We now want to compute the two-point function of the field φ :

$$\langle 0 | \hat{\varphi}(\eta, \mathbf{x}) \hat{\varphi}(\eta, \mathbf{0}) | 0 \rangle = \int \frac{d^3 k}{(2\pi)^3} \frac{d^3 k'}{(2\pi)^3} \langle 0 | \hat{\varphi}_{\mathbf{k}}(\eta) \hat{\varphi}_{\mathbf{k}'}(\eta) | 0 \rangle e^{i\mathbf{k}\cdot\mathbf{x}}, \quad (2.45)$$

where we have taken advantage of the translation invariance of spatial slices to place one of the points at the origin. Using

$$\hat{\varphi}_{\mathbf{k}}(\eta) = f_k^*(\eta) \hat{a}_{\mathbf{k}} + f_k(\eta) \hat{a}_{-\mathbf{k}}^\dagger, \quad (2.46)$$

with $f_k(\eta) = u_k(\eta)/a(\eta)$, we can then compute

$$\begin{aligned} \langle 0 | \hat{\varphi}_{\mathbf{k}}(\eta) \hat{\varphi}_{\mathbf{k}'}(\eta) | 0 \rangle &= \langle 0 | \left(f_k^*(\eta) \hat{a}_{\mathbf{k}} + f_k(\eta) \hat{a}_{-\mathbf{k}}^\dagger \right) \left(f_{k'}^*(\eta) \hat{a}_{\mathbf{k}'} + f_{k'}(\eta) \hat{a}_{-\mathbf{k}'}^\dagger \right) | 0 \rangle \\ &= (2\pi)^3 \delta^{(3)}(\mathbf{k} + \mathbf{k}') f_k^*(\eta) f_{k'}(\eta), \end{aligned} \quad (2.47)$$

where we have used the commutator (2.37). The *power spectrum* is therefore simply the square of the mode function:

$$P_\varphi(k) \equiv |f_k(\eta)|^2. \quad (2.48)$$

Substituting (2.47) back into (2.45), we get

$$\langle 0 | \hat{\varphi}(\eta, \mathbf{x}) \hat{\varphi}(\eta, \mathbf{0}) | 0 \rangle = \int \frac{d^3 k}{(2\pi)^3} P_\varphi(k) e^{i\mathbf{k}\cdot\mathbf{x}} \quad (2.49)$$

$$= \int d \log k \frac{k^3}{2\pi^2} P_\varphi(k) \frac{\sin(kr)}{kr}, \quad (2.50)$$

where $r \equiv |\mathbf{x}|$. The first line shows that the two-point function (in position space) is the Fourier transform of the power spectrum, and in the second line we have done the integral over the angular directions of \mathbf{k} . It is also often useful to define the *dimensionless power spectrum*

$$\Delta_\varphi^2(k) \equiv \frac{k^3}{2\pi^2} P_\varphi(k). \quad (2.51)$$

We now want to compute these power spectra explicitly for the massless scalar (2.21). Substituting the solution (2.41) into (2.48), we find

$$P_\varphi(k) = \frac{|u_k(\eta)|^2}{a^2(\eta)} = \frac{H^2}{2k^3} (1 + k^2 \eta^2) \xrightarrow{k\eta \rightarrow 0} \frac{H^2}{2k^3}. \quad (2.52)$$

It is these late-time statistics that are relevant for our Universe. The fluctuations generated during inflation that survive until late times are the things that serve as the initial conditions for the evolution of the universe at the onset of the hot Big Bang. In terms of the dimensionless power spectrum, we find at late times

$$\boxed{\Delta_\varphi^2 = \left(\frac{H}{2\pi} \right)^2}. \quad (2.53)$$

The fact that this is independent of k is typically called *scale invariance*. Looking back at (2.50) we see that this scale invariance means that there is equal power per logarithmic interval in fluctuations of φ . The (near) scale-invariance of fluctuations is one of the critical predictions of the inflationary universe.⁶

Exercise 2.2. Repeat the canonical quantization procedure for a massive scalar field in de Sitter space, starting from the action

$$S = \int d^4x \sqrt{-g} \left(-\frac{1}{2}(\partial\chi)^2 - \frac{m^2}{2}\chi^2 \right). \quad (2.54)$$

You should find that:

- The Bunch–Davies mode function is

$$\chi_k(\eta) = H \sqrt{\frac{\pi}{4}} e^{-\frac{i\pi}{4}(1+2\nu)} (-\eta)^{3/2} H_\nu^{(2)}(-k\eta), \quad \nu \equiv \sqrt{\frac{9}{4} - \frac{m^2}{H^2}}, \quad (2.55)$$

where $H_\nu^{(2)}(x)$ is a Hankel function of the second kind.

- The power spectrum is

$$P_\chi(\eta, k) = \frac{\pi}{4} H^2(-\eta)^3 H_\nu^{(2)}(-k\eta) H_\nu^{(1)}(-k\eta). \quad (2.56)$$

- The late-time limit of the power spectrum is

$$\lim_{k\eta \rightarrow 0} P_\chi(\eta, k) = \frac{H^2(-\eta)^3}{4\pi} \left[\Gamma[-\nu]^2 \left(\frac{k^2\eta^2}{4} \right)^\nu + \Gamma[\nu]^2 \left(\frac{k^2\eta^2}{4} \right)^{-\nu} - \frac{2\pi \cot(\pi\nu)}{\nu} \right]. \quad (2.57)$$

Plot the power spectrum as a function of $k\eta$ for some mass values between $0 \leq m \leq 3H/2$ and for $m > 3H/2$. What is the qualitative difference?

Curvature perturbations

As we described above, the primordial fluctuations are usually characterized in terms of the comoving curvature perturbation ζ . Performing a gauge transformation from the spatially flat gauge to comoving gauge gives the following relation between the inflaton fluctuations and the curvature perturbations:

$$\zeta = -\frac{H}{\dot{\phi}}\varphi. \quad (2.58)$$

⁶This scale invariance follows directly from the symmetries of de Sitter space (as we will see in Section 5). This is one of the amazing aspects of inflation, features of the bulk time evolution get encoded in objects that live on the future boundary and which make no reference to the inflationary spacetime. In this case, the symmetries of the power spectrum are encoding the dilatation (essentially time translation) invariance of de Sitter dynamics.

From the result (2.53), we then obtain

$$\boxed{\Delta_\zeta^2(k) = \left(\frac{H}{\dot{\phi}}\right)^2 \left(\frac{H}{2\pi}\right)^2 \Big|_{k=aH}}, \quad (2.59)$$

where the right-hand side is evaluated at the horizon crossing of each mode. Since $H(t)$ and $\dot{\phi}(t)$ are weakly time-dependent during inflation, the dimensionless power spectrum $\Delta_\zeta^2(k)$ inherits a weak scale-dependence.

2.5 Primordial Non-Gaussianity

We have seen that inflation predicts that the initial correlations are highly Gaussian and therefore described well by the power spectrum. Nevertheless, in principle, a significant amount of information about the physics of inflation can be encoded in small levels of non-Gaussianity. In particular, the higher-order correlations associated with non-Gaussian initial conditions are sensitive to nonlinear interactions, while the power spectrum only probes the free theory. Measurements of primordial non-Gaussianity would therefore probe the particle content and the interactions during inflation.⁷

The leading signature of non-Gaussianity is a nonzero three-point correlation function, or its Fourier equivalent, the *bispectrum*:

$$\langle \zeta_{\mathbf{k}_1} \zeta_{\mathbf{k}_2} \zeta_{\mathbf{k}_3} \rangle = (2\pi)^3 \delta^{(3)}(\mathbf{k}_1 + \mathbf{k}_2 + \mathbf{k}_3) \frac{(2\pi^2)^2}{(k_1 k_2 k_3)^3} B_\zeta(k_1, k_2, k_3), \quad (2.60)$$

where the delta function is again a consequence of the homogeneity of the background. The sum of the three wavevectors must therefore form a closed triangle and the strength of the signal will depend on the shape of the triangle. As indicated by the notation, the bispectrum is a function of the magnitudes of the wavevectors, $k_{n=1,2,3}$, as required by the isotropy of the background. The factor of $(k_1 k_2 k_3)^{-2}$ has been extracted in to make the function $B_\zeta(k_1, k_2, k_3)$ dimensionless. The *amplitude* of the non-Gaussianity is then defined as the size of the bispectrum in the equilateral configuration:

$$f_{\text{NL}}(k) \equiv \frac{5}{18} \frac{B_\zeta(k, k, k)}{\Delta_\zeta^4(k)}, \quad (2.61)$$

where the numerical factor is a historical accident. In general, the parameter f_{NL} can depend on the overall wavenumber (or the size of the triangle), but for scale-invariant initial conditions it would be a constant. The bispectrum can then be written as

$$B_\zeta(k_1, k_2, k_3) = \frac{18}{5} f_{\text{NL}} \times S(x_2, x_3) \times \Delta_\zeta^4, \quad (2.62)$$

⁷An analogy with particle physics may be informative: the measurements of the power spectrum are the analog of measuring the propagators of particles. While these propagators are important features of long-lived particles, their form is completely fixed by Lorentz symmetry and therefore doesn't contain dynamical information. To learn about the dynamics of the theory we collide particles and study the resulting interactions. Measurements of higher-order correlations (or non-Gaussianity) are the analog of measuring collisions in particle physics. The study of non-Gaussianity therefore also goes by the name of “cosmological collider physics” [13].

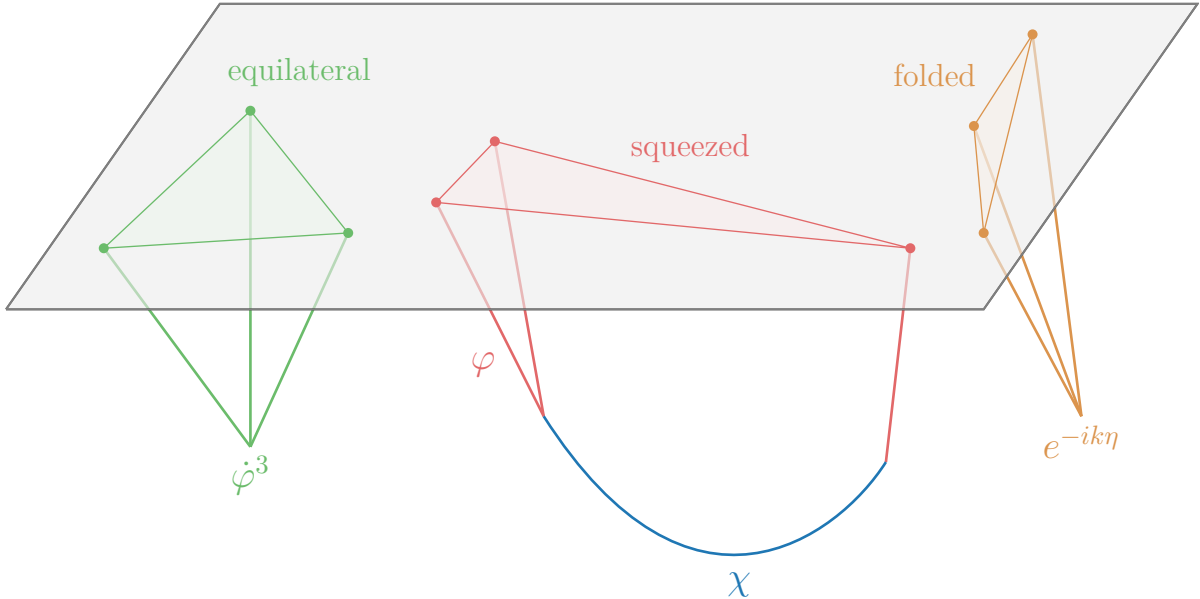


Figure 5: Illustration of the different types of non-Gaussianity described in the text: 1) Local interactions in the bulk produce the “equilateral” shape; 2) Excited initial states create an enhanced signal in the “folded” configuration; and 3) The production and decay of massive particles leave an imprint in the “squeezed” limit.

where $x_2 \equiv k_2/k_1$ and $x_3 \equiv k_3/k_1$. The shape function $S(x_2, x_3)$ is normalized so that $S(1, 1) \equiv 1$. As we will see below, the *shape* of the non-Gaussianity contains a lot of information about the microphysics of inflation (see Fig. 5). This is to be contrasted with the power spectrum, which is described by just two numbers, A_s and n_s , and not a whole function.

Equilateral In slow-roll inflation, the flatness of the inflationary potential constrains the size of the inflaton self-interactions. However, interesting models of inflation have been suggested in which higher-derivative corrections—such as $(\partial\phi)^4$ —play an important role during inflation. These interactions lead to cubic interactions of the inflaton perturbations—like $\dot{\varphi}^3$ and $\dot{\varphi}(\partial_i\varphi)^2$ —and hence a nonzero bispectrum.⁸ Since the inflaton fluctuations interact locally at points in the bulk spacetime, this produces a bispectrum with an enhanced signal for “equilateral” triangles, with $k_1 \approx k_2 \approx k_3$.

Folded The Gaussianity of slow-roll inflation also relies on the fact that we evaluated the quantum fluctuations in the Bunch–Davies vacuum (corresponding to the ground state of the harmonic oscillator). In contrast, starting from an excited initial state would lead to non-Gaussianity. The detailed shape of this non-Gaussianity depends on the model for the excited initial state. A universal feature is that the correlations are enhanced for “folded” triangles where two of the wavevectors become colinear, so that $k_1 + k_2 \approx k_3$. The signal in the folded configuration also provides an interesting test of the quantum origin of the fluctuations [?]. While classical fluctuations would generically have non-vanishing correlations in the folded limit, quantum fluctuations in the Bunch–Davies vacuum are characterized by the absence of such a signal.

⁸A systematic way to classify these derivative interactions is in terms of an EFT for the inflationary fluctuations [?].

Squeezed Finally, non-Gaussianity is a sensitive detector of new particles during inflation. These particles are created by the rapid expansion of the spacetime and, through their decays, produce distinct correlations in the primordial fluctuations. The massive particles can decay at widely separated points in the bulk spacetime, leading to an imprint in the so-called “squeezed” limit, $k_3 \ll k_1 \approx k_2$.

In the rest of these lectures, we will describe three methods for computing cosmological correlators: 1) the in-in formalism, 2) the wavefunction approach, and 3) the cosmological bootstrap.

3 The In-In Formalism

The standard way to compute cosmological correlation functions uses the so-called “in-in” (or Schwinger–Keldysh) formalism [14–18]. In this section, we will introduce the in-in formalism and apply it to a few illustrative examples. The use of the in-in formalism in cosmology was reinvigorated by Maldacena, who applied it to compute the three-point function in slow-roll inflation [19]. The approach was further systematized by Weinberg [20] in order to study loop corrections. Nice reviews of the in-in formalism with cosmological applications in mind can be found in [2, 3].⁹

3.1 In-In Correlators

In flat-space quantum field theory, one is often interested in the transition amplitudes between some specified initial (“in”) and final (“out”) states, $S = \langle \text{out} | \text{in} \rangle$.¹⁰ More precisely, we can write this “ S -matrix” as

$$S_{\beta\alpha} = \langle \beta | \alpha \rangle, \quad (3.1)$$

which captures the probability for the state prepared in the far past with particles α to evolve into a state with particles β in the far future. In order to actually compute the S -matrix, we specify the initial state in the asymptotic past, $|\alpha_0\rangle \equiv |\alpha_0(t_i)\rangle$, where the theory is effectively free and evolve this state using the interaction Hamiltonian H_{int} :

$$|\alpha_0(t_f)\rangle = T \exp \left(-i \int_{t_i}^{t_f} dt H_{\text{int}} \right) |\alpha_0(t_i)\rangle. \quad (3.2)$$

where T denotes time-ordering. We then measure the overlap of $|\alpha_0(t_f)\rangle$ with some other multi-particle final state, $|\beta_0\rangle \equiv |\beta_0(t_f)\rangle$, specified again in the free theory. The S -matrix for this process is

$$S_{\beta\alpha} = \langle \beta_0 | T e^{-i \int_{-\infty}^{\infty} dt H_{\text{int}}} | \alpha_0 \rangle. \quad (3.3)$$

Importantly, to specify the S -matrix we choose boundary conditions for our measurement *both* in the past and in the future.

In cosmology, the situation is different. Roughly speaking, none of the conditions we require to define the S -matrix hold in cosmological backgrounds. It is not possible to localize wave packets and separate them asymptotically in order to map interacting states to free states (at least not for light fields). Relatedly, the gravitational production of particles cannot be shut off in asymptotic regions, so in and out states with definite particle numbers are not particularly well-defined. Moreover, in de Sitter space a single observer cannot access an entire Cauchy slice of the spacetime, so they cannot even in principle set up a scattering experiment. Finally, as far as we know, the Universe did not start in some state specified by an experimentalist, so even if they could be defined, transition amplitudes are of questionable practical utility.¹¹

⁹ Aside from cosmology, the in-in formalism is useful any time one is interested in a question where only the initial state can be prepared, and is frequently used in the study of thermal [?] or out-of-equilibrium systems [?].

¹⁰ See Chapter 3 of [21] for an authoritative discussion.

¹¹ Such an object would still be of formal interest. See [?], for some attempts to define an S -matrix-like quantity in de Sitter space.

This motivates us to ask a different question. Given some initial “in-state” of the Universe, $|0\rangle$, which we evolve from an early time t_i to a late time t , what is the quantum-mechanical expectation value of an operator $\mathcal{O}(t)$ in this (time-evolved) state? This expectation value is called an *in-in correlator* and can be written as

$$\langle \mathcal{O}(t) \rangle = \langle 0 | \bar{T} e^{i \int_{-\infty}^t dt' H_{\text{int}}} \mathcal{O}(t) T e^{-i \int_{-\infty}^t dt' H_{\text{int}}} | 0 \rangle, \quad (3.4)$$

where again T denotes time-ordering and \bar{T} denotes anti time-ordering. While this formula bears some formal similarity to (3.3), the important difference is that we can only specify the initial state of the system, and compute expectation values sandwiched between this in-state on both sides (hence the name “in-in”).

We now elaborate on the the meaning and derivation of the formula (3.4), and then utilize it to compute expectation values in a number of situations.

3.1.1 A Master Formula

The fundamental quantities that we are interested in computing are expectation values of quantum operators, $\mathcal{O}(t)$ at some time t in a state $|\Omega\rangle$:

$$\langle \mathcal{O}(t) \rangle \equiv \langle \Omega | \mathcal{O}(t) | \Omega \rangle. \quad (3.5)$$

The operator \mathcal{O} can be either a single operator or a string of operators evaluated at the same time.¹² Typically, we take the state $|\Omega\rangle$ to be the in vacuum state of the full interacting theory. Much as in the construction of the S -matrix, we compute these expectation values by envisioning $|\Omega\rangle$ as the time-evolution of some state specified in the infinite past as a state of the corresponding free theory (typically the free vacuum).

In the Heisenberg picture, states are time-independent and operators evolve according to the full Hamiltonian H of the theory:

$$\mathcal{O}(t) = U^\dagger(t, t_i) \mathcal{O}(t_i) U(t, t_i), \quad (3.6)$$

where t_i is some initial time, and the unitary time-evolution operator $U(t, t_i)$ satisfies

$$\frac{dU}{dt} = -iHU, \quad \text{with} \quad U(t_i, t_i) = 1. \quad (3.7)$$

The exact evolution of $\mathcal{O}(t)$ is complicated by the fact that H contains interaction terms (when written in terms of the field perturbations), which leads to nonlinear equations of motion. We deal with this by working in the *interaction picture*, where operators evolve according to the free Hamiltonian H_0 and states according to the interaction Hamiltonian $H_{\text{int}} = H - H_0$. The interaction picture operator at time t is then given by

$$\mathcal{O}_I(t) = U_0^\dagger(t, t_i) \mathcal{O}(t_i) U_0(t, t_i), \quad (3.8)$$

¹²It is not difficult to generalize the formalism to compute expectation values involving operator insertions at different times. One just inserts time evolution operators between the various operator insertions. We will specialize to equal-time correlators though because they are typically the observables of interest in cosmology.

where $U_0(t, t_i)$ satisfies

$$\frac{dU_0}{dt} = -iH_0 U_0, \quad \text{with} \quad U_0(t_i, t_i) = 1. \quad (3.9)$$

The main idea is that (3.8) encodes the leading evolution in terms of interaction picture fields and the effects of interactions will be treated perturbatively as a power series in H_{int} .

We now write (3.5) in terms of interaction-picture operators as

$$\begin{aligned} \langle \Omega | \mathcal{O}(t) | \Omega \rangle &= \langle \Omega | U^\dagger(t, t_i) \mathcal{O}(t_i) U(t, t_i) | \Omega \rangle \\ &= \langle \Omega | F^\dagger(t, t_i) U_0^\dagger(t, t_i) \mathcal{O}(t_i) U_0(t, t_i) F(t, t_i) | \Omega \rangle \\ &= \langle \Omega | F^\dagger(t, t_i) \mathcal{O}_I(t) F(t, t_i) | \Omega \rangle, \end{aligned} \quad (3.10)$$

where we have defined

$$F(t, t_i) \equiv U_0^\dagger(t, t_i) U(t, t_i). \quad (3.11)$$

Using (3.7) and (3.9), we find that

$$\begin{aligned} \frac{dF}{dt} &= \frac{d}{dt}(U_0^\dagger U) = \frac{dU_0^\dagger}{dt} U + U_0^\dagger \frac{dU}{dt} = (iH_0 U_0^\dagger) U + U_0^\dagger (-iH U) \\ &= -iU_0^\dagger (H - H_0) U_0 U_0^\dagger U \\ &= -i(U_0^\dagger H_{\text{int}} U_0) U_0^\dagger U \\ &= -iH_{\text{int}}^I F, \end{aligned} \quad (3.12)$$

where the superscript on H_{int}^I indicates that the fields inside H_{int} are evolved in the interaction picture (using the free Hamiltonian H_0). We can think of F as evolving the state using the interaction Hamiltonian: $|\Omega_I(t)\rangle = F(t, t_i)|\Omega_I(t_i)\rangle$, where $|\Omega_I(t_i)\rangle \equiv |\Omega\rangle$. Equation (3.10) then implies consistency of the expectation value in the Heisenberg and interaction pictures: $\langle \Omega | \mathcal{O}(t) | \Omega \rangle = \langle \Omega_I(t) | \mathcal{O}_I(t) | \Omega_I(t) \rangle$.

A formal solution of (3.12) is

$$F(t, t_i) = T \exp \left(-i \int_{t_i}^t dt' H_{\text{int}}^I(t') \right), \quad (3.13)$$

where T denotes the time-ordering operation. The expectation value (3.5) can then be written as

$$\langle \mathcal{O}(t) \rangle = \langle \Omega | \overline{T} e^{i \int_{t_i}^t dt' H_{\text{int}}^I(t')} \mathcal{O}_I(t) T e^{-i \int_{t_i}^t dt' H_{\text{int}}^I(t')} | \Omega \rangle, \quad (3.14)$$

where \overline{T} denotes anti time-ordering.

We would like the state $|\Omega\rangle$ to be the “in” vacuum of the *interacting theory*. In the interaction picture, all states can be expressed in terms of the Fock states of the free Hamiltonian (which can be constructed by applying creation operators on the free vacuum $|0\rangle$). We would therefore like to express the interacting vacuum at early times in terms of this Fock (or *Bunch–Davies*) vacuum $|0\rangle$. We first write $|0\rangle$ in terms of a complete set of energy eigenstates of the *full* theory:

$$|0\rangle = \sum_N |N\rangle \langle N|0\rangle. \quad (3.15)$$

Near $t_i \rightarrow -\infty$, the evolution of the Fock vacuum with the full Hamiltonian H gives

$$\begin{aligned} e^{-iH(t-t_i)}|0\rangle &= \sum_N e^{-iE_N(t-t_i)}|N\rangle\langle N|0\rangle \\ &= e^{-iE_\Omega(t-t_i)}|\Omega\rangle\langle\Omega|0\rangle + \sum_{N' \neq \Omega} e^{-iE_{N'}(t-t_i)}|N'\rangle\langle N'|0\rangle, \end{aligned} \quad (3.16)$$

where $|N'\rangle$ denotes all states excluding the vacuum. We can now employ the same trick as in standard in-out field theory: we rotate time slightly into the imaginary direction, so that

$$t \mapsto t(1 - i\epsilon) \equiv t^-, \quad (3.17)$$

where $\epsilon > 0$ is an infinitesimal constant. Near $t_i \rightarrow -\infty$, the $i\epsilon$ factor leads to factors of the form $e^{-\infty \times \epsilon E_N}$. Since E_Ω is the smallest eigenvalue of the Hamiltonian H , only the state $|\Omega\rangle$ survives in this limit, and will project the interacting vacuum onto the free vacuum:

$$e^{-iH(t^- - t_i^-)}|\Omega\rangle = \frac{e^{-iH(t^- - t_i^-)}|0\rangle}{\langle\Omega|0\rangle}. \quad (3.18)$$

Equation (3.14) can then be written as

$$\langle\Omega|\mathcal{O}(t)|\Omega\rangle = \frac{1}{|\langle\Omega|0\rangle|^2} \langle 0 | \overline{T} e^{i \int_{-\infty+}^t dt' H_{\text{int}}^I(t')} \mathcal{O}_I(t) T e^{-i \int_{-\infty-}^t dt' H_{\text{int}}^I(t')} | 0 \rangle, \quad (3.19)$$

where we have introduced the shorthand $-\infty^\pm \equiv -\infty(1 \pm i\epsilon)$. Note that the anti-time-ordering changes the sign of the $i\epsilon$ prescription. Taking $\mathcal{O}(t)$ to be the identity operator, equation (3.19) implies

$$|\langle\Omega|0\rangle|^2 = \frac{\langle 0 | F^\dagger F | 0 \rangle}{\langle\Omega|\Omega\rangle} = \frac{\langle 0 | 0 \rangle}{\langle\Omega|\Omega\rangle} = 1. \quad (3.20)$$

We can therefore drop the prefactor in (3.19) and obtain our final *master in-in formula*

$$\langle\mathcal{O}(t)\rangle = \langle 0 | \overline{T} e^{i \int_{-\infty+}^t dt' H_{\text{int}}(t')} \mathcal{O}(t) T e^{-i \int_{-\infty-}^t dt' H_{\text{int}}(t')} | 0 \rangle. \quad (3.21)$$

To avoid clutter, we have dropped the labels I on the right-hand side, but evolution in the interaction picture will always be implied. A graphical illustration of the in-in contour is given in Figure 6. Operators will be time-ordered on \mathcal{C}_+ and anti-time-ordered on \mathcal{C}_- .

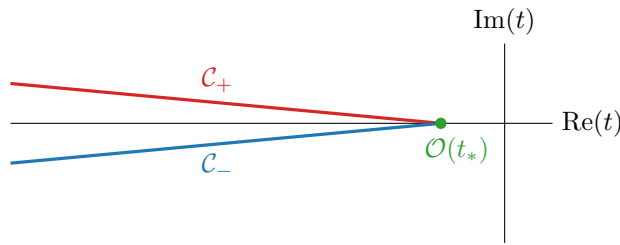


Figure 6: Graphical illustration of the in-in contour. The contour has small imaginary parts at early times to project the interacting vacuum onto the free vacuum.

3.1.2 Perturbative Expansion

Equation (3.21) is the in-in analogue of Dyson's formula. In practice, we use it to compute correlation functions in perturbation theory by expanding in powers of H_{int} and evaluating the resulting expressions by writing a mode expansion of the field operators in canonical quantization.

At lowest order, we find that the expectation value of \mathcal{O} is given by

$$\langle \mathcal{O}(t) \rangle = 2 \text{Im} \left(\int_{-\infty}^t dt' \langle 0 | \mathcal{O}(t) H_{\text{int}}(t') | 0 \rangle \right). \quad (3.22)$$

This expression captures the leading-order perturbative effect of interactions, which from a diagrammatic viewpoint correspond to contact interactions. To make this less abstract, we work out an explicit example in the box below.

Example To show how to use (3.22), let us consider the three-point function coming from a ϕ^3 interaction in an arbitrary FRW spacetime. We take the interaction Lagrangian to be

$$L_{\text{int}} = -\frac{1}{3!} g \phi^3. \quad (3.23)$$

In this case, the interaction Hamiltonian is then just minus the interaction Lagrangian

$$\begin{aligned} H_{\text{int}}(t) &= \frac{g}{3!} \int d^3x a^3(t) \phi^3(\mathbf{x}, t) \\ &= \frac{g}{3!} a^3(t) \int d^3x \int \frac{d^3q_1}{(2\pi)^3} \frac{d^3q_2}{(2\pi)^3} \frac{d^3q_3}{(2\pi)^3} \phi_{\mathbf{q}_1}(t) \phi_{\mathbf{q}_2}(t) \phi_{\mathbf{q}_3}(t) e^{-i(\mathbf{q}_1 + \mathbf{q}_2 + \mathbf{q}_3)\mathbf{x}} \\ &= \frac{g}{3!} a^3(t) \int \frac{d^3q_1}{(2\pi)^3} \frac{d^3q_2}{(2\pi)^3} \frac{d^3q_3}{(2\pi)^3} \phi_{\mathbf{q}_1}(t) \phi_{\mathbf{q}_2}(t) \phi_{\mathbf{q}_3}(t) (2\pi)^3 \delta^{(3)}(\mathbf{q}_1 + \mathbf{q}_2 + \mathbf{q}_3), \end{aligned} \quad (3.24)$$

where g is the coupling constant. Equation (3.22) then implies

$$\langle \phi_{\mathbf{k}_1}(t) \phi_{\mathbf{k}_2}(t) \phi_{\mathbf{k}_3}(t) \rangle = 2 \text{Im} \left(\int_{-\infty}^t dt' \langle 0 | \phi_{\mathbf{k}_1}(t) \phi_{\mathbf{k}_2}(t) \phi_{\mathbf{k}_3}(t) H_{\text{int}}(t') | 0 \rangle \right), \quad (3.25)$$

and we therefore need to compute the following expectation value

$$\langle 0 | \phi_{\mathbf{k}_1}(t) \phi_{\mathbf{k}_2}(t) \phi_{\mathbf{k}_3}(t) \phi_{\mathbf{q}_1}(t') \phi_{\mathbf{q}_2}(t') \phi_{\mathbf{q}_3}(t') | 0 \rangle. \quad (3.26)$$

The computation should be familiar from your courses on quantum field theory. Each field operator is written in terms of annihilation and creation operators,

$$\phi_{\mathbf{k}}(t) = f_k^*(t) \hat{a}_{\mathbf{k}} + f_k(t) \hat{a}_{-\mathbf{k}}^\dagger, \quad (3.27)$$

and we evaluate (3.26) like we did the two-point function in Section 2.4 by shuffling the $\hat{a}_{\mathbf{k}}$ s all the way to the right using the commutator (2.37), so that they can annihilate the vacuum. This somewhat tedious procedure can be streamlined using Wick's theorem.¹³ We define the *Wick contraction* between two operators as

$$\overline{\phi_{\mathbf{k}}(t) \phi_{\mathbf{q}}(t')} = f_k^*(t) f_k(t') \delta^{(3)}(\mathbf{k} + \mathbf{q}) \equiv W_k(t, t') \delta^{(3)}(\mathbf{k} + \mathbf{q}), \quad (3.28)$$

where W_k is the *Wightman function*. Wick's theorem then says that (3.26) is equal to the sum of all possible such contractions. We are interested in the *connected* part of the correlation function, which consists of contractions between the external legs (i.e., one of the $\phi_{\mathbf{k}}$'s) and the vertex (i.e., one of the $\phi_{\mathbf{q}}$'s). Here is an example:

$$\begin{aligned} & \langle 0 | \overbrace{\phi_{\mathbf{k}_1}(t) \phi_{\mathbf{k}_2}(t) \phi_{\mathbf{k}_3}(t) \phi_{\mathbf{q}_1}(t') \phi_{\mathbf{q}_2}(t') \phi_{\mathbf{q}_3}(t')} | 0 \rangle \\ &= f_{k_1}^*(t) f_{k_1}(t') \delta^{(3)}(\mathbf{k}_1 + \mathbf{q}_3) f_{k_2}^*(t) f_{k_2}(t') \delta^{(3)}(\mathbf{k}_2 + \mathbf{q}_1) f_{k_3}^*(t) f_{k_3}(t') \delta^{(3)}(\mathbf{k}_3 + \mathbf{q}_2). \end{aligned} \quad (3.29)$$

Integrating over the \mathbf{q} 's, the delta function $\delta^{(3)}(\mathbf{q}_1 + \mathbf{q}_2 + \mathbf{q}_3)$ in (3.24) becomes $\delta^{(3)}(\mathbf{k}_1 + \mathbf{k}_2 + \mathbf{k}_3)$. It doesn't matter how the \mathbf{q} 's are paired with the \mathbf{k} 's, they will all lead to the same result. As there are $3!$ different ways of pairing the \mathbf{q} 's and the \mathbf{k} 's, we just need to multiply the result of one way of contracting fields by $3!$. After this, (3.25) becomes

$$\langle \phi_{\mathbf{k}_1}(t) \phi_{\mathbf{k}_2}(t) \phi_{\mathbf{k}_3}(t) \rangle' = 2g \operatorname{Im} \left[f_{k_1}^*(t) f_{k_2}^*(t) f_{k_3}^*(t) \int_{-\infty}^t dt' a^3(t') f_{k_1}(t') f_{k_2}(t') f_{k_3}(t') \right]. \quad (3.30)$$

In a specific theory, with some given scale factor $a(t)$ and mode functions $f_k(t)$, we could compute the time integral and get an explicit answer for the correlator.

In order to compute to higher orders in perturbation theory—which is necessary to capture the effects of exchanges or loops—we need to expand (3.21) to higher order. For example, to compute the tree-level four-point function in ϕ^3 theory, we have to expand (3.21) to second order in H_{int} , which leads to

$$\begin{aligned} \langle \mathcal{O}(t) \rangle &= \int_{-\infty}^t dt' \int_{-\infty}^t dt'' \langle 0 | H_{\text{int}}(t') \mathcal{O}(t) H_{\text{int}}(t'') | 0 \rangle \\ &\quad - 2 \operatorname{Re} \left(\int_{-\infty}^t dt' \int_{-\infty}^{t'} dt'' \langle 0 | H_{\text{int}}(t') H_{\text{int}}(t'') \mathcal{O}(t) | 0 \rangle \right). \end{aligned} \quad (3.31)$$

In principle, this expression can be evaluated using Wick contractions as in the example above. However, like in ordinary QFT, this operator-based approach is somewhat cumbersome and it pays to work with Feynman diagrams and associated Feynman rules to simplify calculations.

Exercise 3.1. Derive (3.22) and (3.31). Verify that they are equivalent to

$$\langle \mathcal{O}(t) \rangle = i \int_{-\infty}^t dt' \langle 0 | [H_{\text{int}}(t'), \mathcal{O}(t)] | 0 \rangle, \quad (3.32)$$

$$\langle \mathcal{O}(t) \rangle = - \int_{-\infty}^t dt' \int_{-\infty}^{t'} dt'' \langle 0 | [H_{\text{int}}(t''), [H_{\text{int}}(t'), \mathcal{O}(t)]] | 0 \rangle, \quad (3.33)$$

respectively. Try to find an all-orders expression for the expansion of (3.21) of this form.

3.1.3 Feynman Rules

Diagrammatic rules for the computation of in-in correlation functions were developed in [20, 23]. We will state these rules without explicit derivation and then illustrate them in a few examples.

1. Draw the final time surface ($t = t_*$).
2. Draw all diagrams contributing to the relevant process, allowing vertices both above and below this surface.
3. Lines that cross or end on the time surface represent a *Wightman propagator*,

$$W_k(t, t') = f_k^*(t) f_k(t'), \quad (3.34)$$

where the left argument is given by the time of the uppermost vertex and the right argument is given by the lowermost vertex. Lines which lie entirely below the fixed time surface represent *Feynman propagators*,

$$G_F(k; t, t') = W_k(t, t') \theta(t - t') + W_k(t', t) \theta(t' - t), \quad (3.35)$$

while lines which lie entirely above the surface are replaced with time-reversed Feynman propagators, $G_F(k; t', t) = G_F^*(k; t, t')$.

4. Vertices below the time surface get vertex factors $-iV$, where V is obtained by functional differentiation of the interaction Hamiltonian.¹⁴ Vertices above the time surface get factors of iV^\dagger . In Fourier space, momentum is conserved at each vertex, and there is an overall momentum-conserving delta function.
5. All vertex insertions must be integrated over time, using the measure $Dt \equiv dt a^3(t)$. If the diagram involves loops, integrate over the loop momenta.
6. If there are symmetry factors in diagrams, divide by them. In the second step above, we can mod out by reflections across the final time surface, but then we have to take 2Re of the answer.

Example Let us apply these rules to the three-point example worked out in Section 3.1.2. We are instructed to consider two diagrams—one with the interaction vertex above and one with it below the final time surface. Using the Feynman rules presented above, the first diagram gives

$$I_+ \equiv \begin{array}{c} \text{Diagram of } I_+ \text{ (three vertices connected by lines)} \end{array} = -iV \int_{-\infty}^{t_*} Dt W_{k_1}(t_*, t) W_{k_2}(t_*, t) W_{k_3}(t_*, t) \quad (3.36)$$

$$= -iV f_{k_1}^*(t_*) f_{k_2}^*(t_*) f_{k_3}^*(t_*) \int_{-\infty}^{t_*} Dt f_{k_1}(t) f_{k_2}(t) f_{k_3}(t), \quad (3.37)$$

¹⁴For example, a theory with $L_{\text{int}} = -g\phi^n/n!$ would get a factor of $-iV = -ig$ at an n -point vertex.

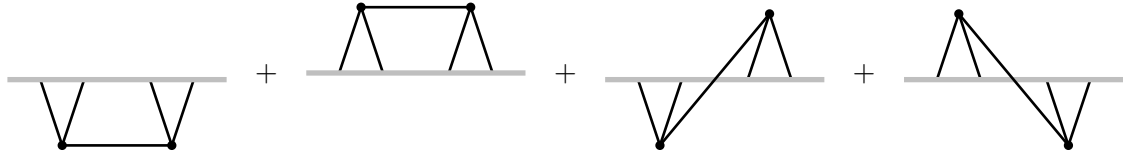
where we are being a bit schematic about the meaning of the vertex factor V . In cases that involve derivatives, we have to include the relevant factors of spatial momenta and appropriately act with time derivatives on the mode functions inside the integral. Similarly, the second diagram leads to

$$I_- \equiv \begin{array}{c} \text{Diagram of a triangle with vertices on a horizontal line} \\ \text{with two internal vertical lines} \end{array} = +iV \int_{-\infty}^{t_*} Dt W_{k_1}(t, t_*) W_{k_2}(t, t_*) W_{k_3}(t, t_*) \quad (3.38)$$

$$= +iV f_{k_1}(t_*) f_{k_2}(t_*) f_{k_3}(t_*) \int_{-\infty}^{t_*} Dt f_{k_1}^*(t) f_{k_2}^*(t) f_{k_3}^*(t). \quad (3.39)$$

The sum of the two diagrams, $\langle\phi\phi\phi\rangle = I_+ + I_-$, therefore indeed reproduces the result in (3.30).

Things become more interesting for exchange diagrams. For the tree-level four-point function in ϕ^3 theory, there are four different time orderings for the two vertices of the exchange diagram, corresponding to four distinct diagrams (in the s -channel):



Rather than writing complicated abstract formulas for each of the contributions, we will evaluate them in specific examples.

3.2 Correlators in Flat Space

Though our primary interest is in cosmology, an instructive warmup is to consider in-in correlators in flat space. In that case, the mode functions are simple enough that all time integrals can be evaluated explicitly. The computation in de Sitter space will then be conceptually exactly the same, but just algebraically more complicated.

We assume that the correlations are computed at a fixed time $t_* = 0$. This time slice is the analog of the future boundary in the de Sitter case.¹⁵ The interactions which create the late-time correlations live at $-\infty < t < 0$. For simplicity, we first consider a massless ϕ^3 theory, with the action

$$S = \int d^4x \left(-\frac{1}{2}(\partial\phi)^2 - \frac{g}{3!}\phi^3 \right). \quad (3.40)$$

The flat-space mode function for this massless scalar is

$$f_k(t) = \frac{e^{ikt}}{\sqrt{2k}}, \quad (3.41)$$

¹⁵Unlike the de Sitter case, there is no privileged time slice in Minkowski space. The choice of such a slice does break the time translation symmetry of the spacetime, but all such constant time slices are equivalent because they can be transformed into each other by time translations. It is therefore convenient to choose the slice $t_* = 0$.

which implies that the Wightman and Feynman propagators are given by

$$W_k(t, t') = \frac{1}{2k} e^{-ik(t-t')}, \quad (3.42)$$

$$G_F(k; t, t') = \frac{1}{2k} \left(e^{-ik(t-t')} \theta(t - t') + e^{ik(t-t')} \theta(t' - t) \right). \quad (3.43)$$

The vertex factors are simple because $H_{\text{int}} = -L_{\text{int}}$, so that $V = g$. We can now combine together these building blocks to compute some example correlators.

Three-point function We first compute the three-point function $\langle \phi \phi \phi \rangle$. Substituting the flat-space mode function into the expressions (3.37) and (3.39), and taking the limit $t_* \rightarrow 0$, gives

$$I_+ = -\frac{ig}{8k_1 k_2 k_3} \int_{-\infty}^0 dt e^{iKt} = -\frac{g}{8k_1 k_2 k_3} \frac{1}{K}, \quad (3.44)$$

$$I_- = \frac{ig}{8k_1 k_2 k_3} \int_{-\infty}^0 dt e^{-iKt} = -\frac{g}{8k_1 k_2 k_3} \frac{1}{K}, \quad (3.45)$$

where we have defined the sum of energies $K \equiv k_1 + k_2 + k_3$. Notice that in order to get these oscillatory integrals to converge as $t \rightarrow -\infty$, we have implicitly implemented the $i\epsilon$ prescription of (3.21) and rotated the contour slightly. Summing these answers, we get the final correlator

$$\boxed{\langle \phi_{\mathbf{k}_1} \phi_{\mathbf{k}_2} \phi_{\mathbf{k}_3} \rangle' = -\frac{g}{4k_1 k_2 k_3} \frac{1}{(k_1 + k_2 + k_3)}}.$$

(3.46)

Notice from (3.37) and (3.39) that I_+ and I_- in general are complex conjugates of each other. In this specific case, however, both contributions are purely real, so we just get two times the contribution of one of the graphs.

Four-point function As a more nontrivial example, we next compute the four-point function $\langle \phi \phi \phi \phi \rangle$, which involves the exchange of a particle.¹⁶ In the s -channel, there are four relevant diagrams (corresponding to the four different time orderings of the interaction vertices), which we will now evaluate in turn.

We first consider the diagram where both vertices are below the final time surface. Using the Feynman rules, we find

$I_{++} \equiv$



$= (-ig)^2 \int_{-\infty}^0 dt' dt'' W_{k_1}(0, t') W_{k_2}(0, t') G_F(k_I; t', t'') W_{k_3}(0, t'') W_{k_4}(0, t'')$
 $= -\frac{g^2}{16k_1 k_2 k_3 k_4} \int_{-\infty}^0 dt' dt'' e^{ik_{12}t'} G_F(k_I; t', t'') e^{ik_{34}t''},$

(3.47)

¹⁶There can, of course, also be contributions to the four-point function coming from contact interactions, which will involve a single insertion of the quartic interaction Hamiltonian. See Section 3.3, for an example.

where we have defined $k_{12} \equiv k_1 + k_2$, $k_{34} \equiv k_3 + k_4$ and $k_I \equiv |\mathbf{k}_1 + \mathbf{k}_2|$. (Due to momentum conservation at the bulk vertices, the momentum of the internal line is $\mathbf{k}_I = \mathbf{k}_1 + \mathbf{k}_2 = -\mathbf{k}_3 - \mathbf{k}_4$.) Substituting the Feynman propagator (3.43), this becomes

$$\begin{aligned} I_{++} &= -\frac{g^2}{16k_1k_2k_3k_4}\frac{1}{2k_I}\int_{-\infty}^0 dt' dt'' e^{ik_{12}t'} e^{-ik_I(t'-t'')} \theta(t' - t'') e^{ik_{34}t''} + (k_{12} \leftrightarrow k_{34}) \\ &= -\frac{g^2}{16k_1k_2k_3k_4}\frac{1}{2k_I}\int_{-\infty}^0 dt' e^{i(k_{12}-k_I)t'} \int_{-\infty}^{t'} dt'' e^{i(k_{34}+k_I)t''} + (k_{12} \leftrightarrow k_{34}) \\ &= -\frac{g^2}{16k_1k_2k_3k_4}\frac{1}{2k_I}\int_{-\infty}^0 dt' \frac{e^{i(k_{12}+k_{34})t'}}{i(k_{34}+k_I)} + (k_{12} \leftrightarrow k_{34}) \\ &= \frac{g^2}{16k_1k_2k_3k_4}\frac{1}{2k_I}\frac{1}{k_{12}+k_{34}}\left(\frac{1}{k_{12}+k_I} + \frac{1}{k_{34}+k_I}\right) \end{aligned} \quad (3.48)$$

$$= \frac{g^2}{16k_1k_2k_3k_4}\left(\frac{1}{EE_L E_R} + \frac{1}{2k_I E_L E_R}\right), \quad (3.49)$$

where we have defined $E \equiv k_{12} + k_{34}$, $E_L \equiv k_{12} + k_I$ and $E_R \equiv k_{34} + k_I$. While in more general situations in cosmology these nested time integrals are challenging to compute, in this flat-space example the final result is a relatively simple rational function of the energies involved in the process.

Similarly, when both vertices are above the final time surface, the relevant integral is

$$\begin{aligned} I_{--} &\equiv \text{Diagram showing two vertices above the final time surface connected by a horizontal line.} \\ &= (ig)^2 \int_{-\infty}^0 dt' dt'' W_{k_1}(t', 0) W_{k_2}(t', 0) G_F(k_I; t'', t') W_{k_3}(t'', 0) W_{k_4}(t'', 0). \end{aligned} \quad (3.50)$$

Note the difference in the orderings of the arguments of the propagators in (3.47) and (3.50). Using that $W_k(t', t) = W_k^*(t, t')$ and $G_F(k; t'', t') = G_F^*(k; t', t'')$, we see that $I_{--} = I_{++}^*$ and hence $I_{++} + I_{--} = 2 \operatorname{Re}(I_{++})$. In this specific case, both contributions are purely real (so $I_{--} = I_{++}$) and the sum of the two diagrams is just twice the answer in (3.49):

$$I_{++} + I_{--} = \frac{g^2}{8k_1k_2k_3k_4}\left(\frac{1}{EE_L E_R} + \frac{1}{2k_I E_L E_R}\right). \quad (3.51)$$

We have separated the answer into a “connected part” (with an $E = 0$ pole) and a “disconnected part” (without an $E = 0$ pole).

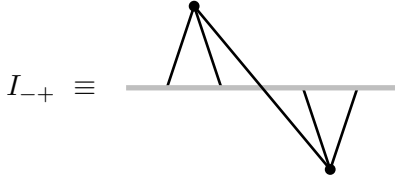
Next, we consider the case where one vertex is below the final time surface and one is above:

$$I_{+-} \equiv \text{Diagram showing one vertex above and one below the final time surface connected by a diagonal line.}$$

$$\begin{aligned}
&= (-ig)(ig) \int_{-\infty}^0 dt' dt'' W_{k_1}(0, t') W_{k_2}(0, t') W_{k_I}(t'', t') W_{k_3}(t'', 0) W_{k_4}(t'', 0) \\
&= \frac{g^2}{16k_1 k_2 k_3 k_4} \frac{1}{2k_I} \int_{-\infty}^0 dt' dt'' e^{ik_{12}t'} e^{-ik_I(t''-t')} e^{-ik_{34}t''} \\
&= \frac{g^2}{16k_1 k_2 k_3 k_4} \frac{1}{2k_I} \int_{-\infty}^0 dt' e^{i(k_{12}+k_I)t'} \int_{-\infty}^0 dt'' e^{-i(k_{34}+k_I)t''} \\
&= \frac{g^2}{16k_1 k_2 k_3 k_4} \frac{1}{2k_I} \frac{1}{(k_{12}+k_I)(k_{34}+k_I)} \\
&= \frac{g^2}{16k_1 k_2 k_3 k_4} \frac{1}{2k_I E_L E_R}. \tag{3.52}
\end{aligned}$$

Since all propagators are Wightman propagators, the two time integrations decoupled and could be performed separately. The answer therefore only includes a “disconnected part.” We will see later that it is useful to combine this with the disconnect part inside I_{++} .

Finally, we consider the contribution I_{-+} , with opposite time ordering of the interaction vertices:



$$\begin{aligned}
I_{-+} &\equiv \text{Diagram above} \\
&= ig(-ig) \int_{-\infty}^0 dt' dt'' W_{k_1}(t', 0) W_{k_2}(t', 0) W_{k_I}(t', t'') W_{k_3}(t'', 0) W_{k_4}(t'', 0). \tag{3.54}
\end{aligned}$$

It is straightforward to check that $I_{-+} = I_{+-}^*$, and since I_{+-} is purely real, it will just give us a factor of 2:

$$I_{+-} + I_{-+} = \frac{g^2}{8k_1 k_2 k_3 k_4} \frac{1}{2k_I E_L E_R}. \tag{3.55}$$

Notice that this contribution to the correlator only has the singularities when the energy flowing into a vertex is conserved, but does not have a singularity when the total energy is conserved.

Putting everything together, the final result is then the sum of (3.51) and (3.55):

$$\langle \phi_{\mathbf{k}_1} \phi_{\mathbf{k}_2} \phi_{\mathbf{k}_3} \phi_{\mathbf{k}_4} \rangle' = \frac{g^2}{8k_1 k_2 k_3 k_4} \left[\frac{1}{E E_L E_R} + \frac{1}{k_I E_L E_R} \right]. \tag{3.56}$$

One of the benefits of this simplified situation is that we can obtain completely explicit expressions for all the constituent pieces of the correlator, and get a sense of how they fit together in the final answer. When it comes time to examine the singularity structure of correlation functions, we will see that this is enormously useful.

One can proceed to compute higher-point correlation functions in this model, or consider more nontrivial types of interactions. One such example is given in the following exercise.

Exercise 3.2. Compute the four-point function arising from a cubic interaction involving derivatives

$$S = \int d^4x \left(-\frac{1}{2}(\partial\Phi)^2 - \frac{\dot{\Phi}^3}{6\Lambda^2} \right). \quad (3.57)$$

Note that the interaction involves $\dot{\Phi}$, so be careful about the definition of H_{int} .

3.3 Correlators in de Sitter

Having gained some experience with the computation of in-in correlators in flat space, we are now ready to attack the corresponding computations in de Sitter space. Conceptually, these computations are exactly the same, only algebraically do they become a bit more involved. In fact, in many cases, the resulting time integrals cannot be performed explicitly in de Sitter space, which will motivate us to develop a bootstrap method that avoids these integrals altogether (see Section 5).

For concreteness, we again consider Φ^3 theory, where the field Φ is a generic scalar field of mass m . As we showed in Exercise 2.2, the Bunch–Davies mode function of a massive field is

$$f_k(\eta) = H \sqrt{\frac{\pi}{4}} e^{-\frac{i\pi}{4}(1+2\nu)} (-\eta)^{3/2} H_\nu^{(2)}(-k\eta), \quad \text{where } \nu = \sqrt{\frac{9}{4} - \frac{m^2}{H^2}}. \quad (3.58)$$

We will often specialize to *conformally coupled scalars*, with $m^2 = 2H^2$. In that case, the order of the Hankel function becomes $\nu = 1/2$ and the mode function is almost as simple as in flat space:

$$f_k(\eta) = H(-\eta) \frac{e^{ik\eta}}{\sqrt{2k}}. \quad (3.59)$$

The in-in computations simplify drastically for conformally coupled scalars and can often be performed explicitly.¹⁷

Three-point function We first compute the three-point function $\langle\phi\phi\phi\rangle$. Equation (3.37) still applies, so we have

$$I_+ = I_-^* = -ig f_{k_1}^*(\eta_*) f_{k_2}^*(\eta_*) f_{k_3}^*(\eta_*) \int_{-\infty}^{\eta_*} D\eta f_{k_1}(\eta) f_{k_2}(\eta) f_{k_3}(\eta), \quad (3.60)$$

where $D\eta \equiv d\eta a^4(\eta)$. One conceptual difference with the flat-space case is that there is a distinguished time slice in de Sitter space ($\eta_* = 0$), where it is most natural to compute correlators. This future boundary is particularly nice because it is mapped to itself under de Sitter transformations. In the following we will always compute correlators in the $\eta_* \rightarrow 0$ limit for this reason.

¹⁷ Aside from being simple to compute, it is often possible to transform the correlation functions of conformally coupled scalar fields into those of fields with other mass values, corresponding to half-integer values of ν , by a “weight-shifting” procedure [24]. The correlators of conformal scalars therefore become seeds for more complicated correlators.

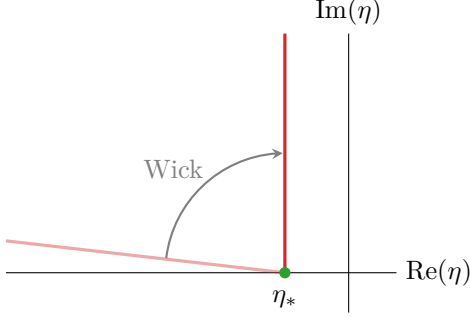


Figure 7: Graphical illustration of Wick rotation of the contour used in the integral in (3.61).

For the totally generic case involving massive fields, this involves an integral over a product of three Hankel functions. This integral can be evaluated in terms of Appell's F_4 function [25], but unfortunately the properties of this special function are still somewhat mysterious, making this representation somewhat less useful than it could be. However, for special masses the integral simplifies and can be evaluated explicitly.

One such example is the three-point function of conformally coupled scalars. In this case, the relevant integral (in the limit $\eta_* \rightarrow 0$) is

$$I_+ = -\frac{ig}{8} \frac{H^2 \eta_*^3}{k_1 k_2 k_3} \int_{-\infty^-}^{\eta_*} \frac{d\eta}{\eta} e^{iK\eta} = -\frac{ig}{8} \frac{H^2 \eta_*^3}{k_1 k_2 k_3} \log(iK\eta_*), \quad (3.61)$$

where again $K \equiv k_1 + k_2 + k_3$. Two aspects of this expression merit discussion. First, this is our first encounter with a correlator that diverges as $\eta_* \rightarrow 0$. We regulate this IR divergence by cutting the integration off at finite $\eta = \eta_*$. Second, the answer has a factor of i in the argument of the log. This arises from the $i\epsilon$ prescription used to define the integral (see Fig. 7 for a graphical illustration of the Wick rotation of the integration contour).¹⁸

Combining I_+ with its complex conjugate I_- , we obtain the full correlator

$$\langle \phi_{\mathbf{k}_1} \phi_{\mathbf{k}_2} \phi_{\mathbf{k}_3} \rangle' = -\frac{g}{8} \frac{H^2 \eta_*^3}{k_1 k_2 k_3} \left(i \log(iK\eta_*) - i \log(-iK\eta_*) \right) = \boxed{\frac{\pi}{8} g \frac{H^2 \eta_*^3}{k_1 k_2 k_3}}. \quad (3.62)$$

Notice that the two branches of the in-in contour conspire to cancel the $\log \eta_*$ divergence, and to remove the singularity as $K \rightarrow 0$ that I_+ and I_- have individually.

Another particularly relevant mass value is $m^2 = 0$, where the field Φ is related to the fluctuations of the inflaton field in the conformal limit, $\varepsilon \rightarrow 0$. This means that correlation functions in slow-roll inflation can often be obtained from those involving massless scalars.

¹⁸The $i\epsilon$ prescription for I_+ selects a contour that extends to infinity above the x -axis. Since the integrand does not have any singularities in the upper left quadrant of the complex plane, we can rotate it to run along the imaginary axis, $\eta \rightarrow -i\eta$.

Exercise 3.3. Consider a massless scalar field with a Φ^3 interaction in de Sitter space. Show that the bispectrum, in the limit $\eta_* \rightarrow 0$, is

$$\begin{aligned} B(k_1, k_2, k_3) &\equiv \frac{(k_1 k_2 k_3)^2}{(2\pi^2)^2} \langle \phi_{\mathbf{k}_1} \phi_{\mathbf{k}_2} \phi_{\mathbf{k}_3} \rangle' \\ &= \frac{g}{H^4} \frac{(k_1^3 + k_2^3 + k_3^3) (\gamma + \log(|K\eta_*|)) - K(k_1^2 + k_2^2 + k_3^2) + k_1 k_2 k_3}{12 (k_1 k_2 k_3)^3}, \end{aligned} \quad (3.63)$$

where γ is the Euler–Mascheroni constant.

It is also possible to directly integrate (3.60) when two of the fields involved are conformally coupled and the third has an arbitrary mass, as you will see in the following exercise. This correlator is useful as a building block to construct more complicated processes, and gives us some intuition for how correlators involving massive fields behave.

Exercise 3.4. Derive an expression for the three-point function of two conformally coupled scalars and one scalar of generic mass. You should find

$$\begin{aligned} \langle \phi \phi \chi \rangle &= \frac{g(H\eta_*)^2}{16\sqrt{\pi}} \frac{1}{k_1 k_2 k_3^2} \Gamma[\frac{1}{2} - \nu] \Gamma[\frac{1}{2} + \nu] P_{\nu - \frac{1}{2}}^0(u^{-1}) \\ &\times \left[\cos\left(\frac{\pi}{4}(1+2\nu)\right) \Gamma[\nu] \left(\frac{-k_3\eta_*}{2}\right)^{\frac{3}{2}-\nu} + \cos\left(\frac{\pi}{4}(1-2\nu)\right) \Gamma[-\nu] \left(\frac{-k_3\eta_*}{2}\right)^{\frac{3}{2}+\nu} \right], \end{aligned} \quad (3.64)$$

where $u \equiv k_3/(k_1 + k_2)$ and $P_\nu^\mu(x)$ is an associated Legendre function. You may find the following integral representation of the Hankel function useful (see equation (5.11.1) of [?])

$$H_\nu^{(2)}(x) = \frac{2^{\nu+1} e^{i\nu\pi} x^\nu}{i\sqrt{\pi} \Gamma[\nu + \frac{1}{2}]} \int_0^\infty ds e^{-i(1+2s)x} s^{\nu-\frac{1}{2}} (1+s)^{\nu-\frac{1}{2}}. \quad (3.65)$$

Show that you recover (3.62) in the appropriate limit.

So far, we have only considered the simplest ϕ^3 interaction. If the cubic coupling between the scalar fields respects de Sitter symmetry, this choice is actually fully general—any de Sitter invariant scalar cubic interaction can be reduced to this form via integration by parts and field redefinitions [26]. However, during inflation, the self-interactions of the inflaton generically break de Sitter symmetry, essentially because it can be thought of as a Nambu–Goldstone mode for the breaking of these symmetries. It is therefore interesting to consider more general cubic interactions that violate de Sitter symmetry, while keeping the background spacetime de Sitter. In the following exercise, you will investigate the simplest such interactions that arise in the effective field theory description of inflation [8, 9, 27].

Exercise 3.5. Consider the following action for a massless scalar field, π , in de Sitter space:

$$S = \int d^4x a^3(t) \left(\frac{1}{2} \dot{\pi}^2 - \frac{1}{2a^2(t)} (\nabla\pi)^2 + \frac{c_{\dot{\pi}^3}}{f_\pi^2} \dot{\pi}^3 + \frac{c_{\dot{\pi}(\nabla\pi)^2}}{f_\pi^2} \frac{1}{a^2(t)} \dot{\pi}(\nabla\pi)^2 \right), \quad (3.66)$$

where $c_{\dot{\pi}^3}$ and $c_{\dot{\pi}(\nabla\pi)^2}$ are dimensionless constants and f_π has mass dimension one. Compute the in-in three-point function arising from each of these interactions.

Four-point function We next consider the four-point function $\langle \phi\phi\phi\phi \rangle$. The simplest such four-point functions arise from contact interactions, much like the three-point functions that have studied so far. In terms of (3.21), they arise from a single insertion of the quartic interactions inside H_{int} , such as the bulk interaction Φ^4 . As a concrete example, we can consider the four-point function of a conformally coupled scalar field. From the Feynman rules, we find that the I_+ contribution is given by

$$\begin{aligned} I_+ &= \begin{array}{c} \diagup \\ \diagdown \\ \diagup \\ \diagdown \\ \diagup \\ \diagdown \end{array} = -iV \int_{-\infty}^{\eta_*} D\eta W_{k_1}(\eta_*, \eta) W_{k_2}(\eta_*, \eta) W_{k_3}(\eta_*, \eta) W_{k_4}(\eta_*, \eta) \\ &= -i \frac{\lambda(H\eta_*)^4}{16 k_1 k_2 k_3 k_4} \int_{-\infty}^{\eta_*} d\eta e^{i(k_1+k_2+k_3+k_4)\eta} \\ &= -\frac{\lambda(H\eta_*)^4}{16 k_1 k_2 k_3 k_4 (k_1 + k_2 + k_3 + k_4)}. \end{aligned} \quad (3.67)$$

This contribution is again purely real, so the full correlator is just twice the above answer:

$$\langle \phi_{\mathbf{k}_1} \phi_{\mathbf{k}_2} \phi_{\mathbf{k}_3} \phi_{\mathbf{k}_4} \rangle' = -\frac{\lambda(H\eta_*)^4}{8 k_1 k_2 k_3 k_4} \frac{1}{E}, \quad (3.68)$$

where $E \equiv k_1 + k_2 + k_3 + k_4$. In this particular case, the flat-space version of the correlator is very simply related to the one that we have just calculated—one just removes the $(H\eta_*)^4 = a^{-4}(\eta_*)$ factor. This is special to four dimensions where the theory is conformal.¹⁹ Notice that (3.67) decays as $\eta_* \rightarrow 0$, but the coefficient of this power-law decay is still physically meaningful, as we will see more explicitly in Section 5.

Exercise 3.6. Consider a conformally coupled scalar field in D -dimensional de Sitter space with a quartic interaction

$$S = \int d^Dx \sqrt{-g} \left(-\frac{1}{2} (\partial\Phi)^2 - \frac{D(D-2)H^2}{8} \Phi^2 - \frac{\lambda}{4!} \Phi^4 \right). \quad (3.69)$$

Compute the in-in four-point function at tree level. Do you notice a difference between even and odd D ?

We can also compute tree-level exchange contributions to four-point functions in the same way that we did in flat space. It is again useful to begin by considering a conformally coupled

¹⁹Since a conformally coupled scalar with a $\lambda\Phi^4$ interaction is conformally invariant, it can be related to the corresponding flat-space theory by a Weyl rescaling with $g_{\mu\nu}^{\text{dS}} = a^2(\eta)\eta_{\mu\nu}$ and $\Phi_{\text{flat}} = a(\eta)\Phi_{\text{dS}}$.

scalar. We can write the Wightman and Feynman propagators explicitly using (3.59):

$$W_k(\eta, \eta') = H^2 \eta \eta' \frac{1}{2k} e^{-ik(\eta-\eta')}, \quad (3.70)$$

$$G_F(k; \eta, \eta') = H^2 \eta \eta' \frac{1}{2k} \left(e^{-ik(\eta-\eta')} \theta(\eta - \eta') + e^{ik(\eta-\eta')} \theta(\eta' - \eta) \right). \quad (3.71)$$

Notice that these are exactly $H^2 \eta \eta'$ times their flat-space counterparts (3.42) and (3.43). (This is another manifestation of the conformal invariance of the conformally coupled scalar.) The I_{++} contribution is

$$\begin{aligned} I_{++} &\equiv \text{Diagram: Two vertical lines meeting at a central horizontal line, forming a V-shape.} \\ &= (-ig)^2 \int_{-\infty}^{\eta_*} D\eta' D\eta'' W_{k_1}(\eta_*, \eta') W_{k_2}(\eta_*, \eta') G_F(k_I; \eta', \eta'') W_{k_3}(\eta_*, \eta'') W_{k_4}(\eta_*, \eta'') \\ &= -\frac{g^2 H^2 \eta_*^4}{16k_1 k_2 k_3 k_4} \int_{-\infty}^{\eta_*} \frac{d\eta'}{\eta'} \int_{-\infty}^{\eta_*} \frac{d\eta''}{\eta''} e^{ik_{12}\eta'} G_F^{(\text{flat})}(k_I; \eta', \eta'') e^{ik_{34}\eta''}, \end{aligned} \quad (3.72)$$

where, in the second line, we have suggestively written the expression in terms of the flat-space Feynman propagator (3.43). This integral is a bit tricky to evaluate because it is divergent. As we will see, the divergences in I_{--} and I_{++} cancel against similar divergences in I_{-+} and I_{+-} . In order to isolate the divergent piece, it is therefore useful to add and subtract a contribution to the integral (3.72) as

$$I_{++} = -\frac{g^2 H^2 \eta_*^4}{16k_1 k_2 k_3 k_4} \int_{-\infty}^{\eta_*} \frac{d\eta'}{\eta'} \int_{-\infty}^{\eta_*} \frac{d\eta''}{\eta''} e^{ik_{12}\eta'} \left(G_B^{(\text{flat})}(k_I; \eta', \eta'') + \frac{1}{2k_I} e^{ik_I(\eta'+\eta'')} \right) e^{ik_{34}\eta''}, \quad (3.73)$$

where we have defined²⁰

$$G_B^{(\text{flat})}(k_I; \eta', \eta'') = G_F^{(\text{flat})}(k_I; \eta', \eta'') - \frac{1}{2k_I} e^{ik_I(\eta'+\eta'')}. \quad (3.74)$$

We can now perform the integral involving G_B via a trick. We note that

$$-i \int_a^\infty dx e^{ix\eta} = \frac{1}{\eta} e^{ia\eta}, \quad (3.75)$$

so that (3.73) can be written as

$$\begin{aligned} I_{++} &= \frac{g^2 H^2 \eta_*^4}{16k_1 k_2 k_3 k_4} \left[\int_{k_{12}}^\infty dx \int_{k_{34}}^\infty dy \int_{-\infty}^{\eta_*} d\eta' d\eta'' e^{ix\eta'} e^{iy\eta''} G_B^{(\text{flat})}(k_I; \eta', \eta'') \right. \\ &\quad \left. - \frac{1}{2k_I} \int_{-\infty}^{\eta_*} \frac{d\eta'}{\eta'} \int_{-\infty}^{\eta_*} \frac{d\eta''}{\eta''} e^{i(k_{12}+s)\eta'} e^{i(k_{34}+s)\eta''} \right], \end{aligned} \quad (3.76)$$

The time integrals in the first line now only involve flat-space quantities and can therefore easily be computed

$$I(x, y) \equiv \int_{-\infty}^0 d\eta' d\eta'' e^{ix\eta'} e^{iy\eta''} G_B^{(\text{flat})}(k_I; \eta', \eta'') = -\frac{1}{(x+y)(x+k_I)(y+k_I)}. \quad (3.77)$$

²⁰In Section 4, we will encounter this object as the *bulk-to-bulk propagator*.

It is then useful to split I_{++} into two pieces: a “connected” component, $I_{++}^{(c)}$, which is the energy integral of $I(x, y)$, and a “disconnected” component, $I_{++}^{(d)}$, which involves un-ordered time integrals.

Performing the energy integrals, the connected piece becomes [13]

$$\begin{aligned} I_{++}^{(c)} &\equiv \frac{g^2 H^2 \eta_*^4}{16 k_1 k_2 k_3 k_4} \int_{k_{12}}^\infty dx \int_{k_{34}}^\infty dy I(x, y) \\ &= \boxed{\frac{g^2 H^2 \eta_*^4}{32 k_1 k_2 k_3 k_4 k_I} \left[\text{Li}_2\left(\frac{E - E_L}{E}\right) + \text{Li}_2\left(\frac{E - E_R}{E}\right) + \log\left(\frac{E_L}{E}\right) \log\left(\frac{E_R}{E}\right) - \frac{\pi^2}{6} \right]}, \end{aligned} \quad (3.78)$$

where Li_2 is the dilogarithm and we have defined the variables $E_L \equiv k_{12} + k_I$ (the energy flowing into the left vertex), $E_R \equiv k_{34} + k_I$ (same for the right vertex) and the total energy $E \equiv k_{12} + k_{34}$.

Exercise 3.7. Derive the result (3.78).

In order to compute the disconnected piece, it is simplest to do the time integrals directly, rather than trying to write them as energy integrals of the flat-space result. This is because we have to be careful about the $i\epsilon$ prescriptions for the contours, much like we did for (3.61). In this case, we can rotate the contours in the same direction as (3.61), so we get

$$\begin{aligned} I_{++}^{(d)} &\equiv -\frac{g^2 H^2 \eta_*^4}{32 k_1 k_2 k_3 k_4 k_I} \int_{-\infty}^{\eta_*} \frac{d\eta'}{\eta'} e^{i(k_{12}+s)\eta'} \int_{-\infty}^{\eta_*} \frac{d\eta''}{\eta''} e^{i(k_{34}+s)\eta''} \\ &= -\frac{g^2 H^2 \eta_*^4}{32 k_1 k_2 k_3 k_4 k_I} \log(iE_L \eta_*) \log(iE_R \eta_*). \end{aligned} \quad (3.79)$$

As advertised, this contribution is divergent as $\eta_* \rightarrow 0$, which is why we split it off from $I_{++}^{(c)}$ to begin with. These divergences cancel with the $I_{\mp\pm}$ pieces, which we now want to calculate.

Using the Feynman rules, we find

$$\begin{aligned} I_{+-} &\equiv \begin{array}{c} \text{Diagram: A horizontal line with a V-shape below it, meeting at a point above the line.} \end{array} \\ &= g^2 \int_{-\infty}^{\eta_*} D\eta' D\eta'' W_{k_1}(\eta_*, \eta') W_{k_2}(\eta_*, \eta') W_{k_I}(\eta'', \eta') W_{k_3}(\eta'', \eta_*) W_{k_4}(\eta'', \eta_*) \\ &= \frac{g^2 H^2 \eta_*^4}{32 k_1 k_2 k_3 k_4 k_I} \int_{-\infty}^{\eta_*} \frac{d\eta'}{\eta'} e^{i(k_{12}+k_I)\eta'} \int_{-\infty}^{\eta_*} \frac{d\eta''}{\eta''} e^{-i(k_{34}+k_I)\eta''} \\ &= \frac{g^2 H^2 \eta_*^4}{32 k_1 k_2 k_3 k_4 k_I} \log(iE_L \eta_*) \log(-iE_R \eta_*). \end{aligned} \quad (3.80)$$

In the last line, we evaluated the integrals, noting that the different $i\epsilon$ prescriptions required for convergence of the integrals lead to different signs of the arguments of the log for the η' and η''

integrals. Adding (3.80) to the result (3.79) for $I_{++}^{(d)}$, we get

$$I_{++}^{(d)} + I_{+-} = \frac{g^2 H^2 \eta_*^4}{32 k_1 k_2 k_3 k_4 k_I} (-i\pi \log(iE_L \eta_*)) . \quad (3.81)$$

Notice that this is similar in structure to what we found for the three-point function in (3.61). The sum of the $I_{--}^{(d)}$ and I_{-+} contributions gives the complex conjugate of (3.81)). Putting everything together, we therefore find

$$I_{++}^{(d)} + I_{+-} + I_{--}^{(d)} + I_{-+} = \boxed{\frac{g^2 H^2 \eta_*^4}{32 k_1 k_2 k_3 k_4 k_I} \pi^2} . \quad (3.82)$$

Note that there is a similar effect as in (3.62) where the kinematic part of the log drops out and we are left with just factors of π .

Assembling all the pieces, the full correlator is

$$\begin{aligned} \langle \phi_{\mathbf{k}_1} \phi_{\mathbf{k}_2} \phi_{\mathbf{k}_3} \phi_{\mathbf{k}_4} \rangle' &= I_{++}^{(c)} + (I_{++}^{(d)} + I_{+-}) + \text{c.c.} \\ &= \boxed{\frac{g^2 H^2 \eta_*^4}{16 k_1 k_2 k_3 k_4 k_I} \left[\text{Li}_2\left(\frac{E - E_L}{E}\right) + \text{Li}_2\left(\frac{E - E_R}{E}\right) + \log\left(\frac{E_L}{E}\right) \log\left(\frac{E_R}{E}\right) + \frac{\pi^2}{3} \right]} . \end{aligned} \quad (3.83)$$

Notice that this correlator has transcendentality two, compared to its flat-space counterpart (3.56), which is a rational function. This is rather interesting, and is in some sense a signature of the time evolution of the spacetime that gave rise to it. Aside from its intrinsic interest, and serving as a useful testing ground, this correlator is closely related to many correlation functions of practical interest, including those involving exchanges of massless particles with spin, which can be generated by differentiating this correlator in a suitable way [24, 28].

As a last example, we consider the four-point function that arises from the exchange of a massive particle $m > \frac{3}{2}H$ between two pairs of conformally coupled scalar fields. In this case, the order ν of the Hankel function in (3.58) is purely imaginary, so it is useful to write the mode functions as

$$f_k(\eta) = e^{-\frac{i\pi}{4}} H \sqrt{\frac{\pi}{4}} (-\eta)^{3/2} e^{\frac{\pi}{2}\mu} H_{i\mu}^{(2)}(-k\eta) , \quad \text{where } i\mu = \sqrt{\frac{9}{4} - \frac{m^2}{H^2}} . \quad (3.84)$$

The definition of μ is such that it is a real number for $m > \frac{3}{2}H$. From this mode function, we can build the Wightman and Feynman propagators:²¹

$$W_k(\eta, \eta') = \frac{H^2 \pi}{4} (\eta \eta')^{3/2} H_{i\mu}^{(1)}(-k\eta) H_{i\mu}^{(2)}(-k\eta') , \quad (3.86)$$

$$G_F(k; \eta, \eta') = W_k(\eta, \eta') \theta(\eta - \eta') + W_k(\eta', \eta) \theta(\eta' - \eta) . \quad (3.87)$$

²¹Here, we have used the fact that

$$\left(H_{i\mu}^{(2)}(x) \right)^* = H_{-i\mu}^{(1)}(x) = e^{-\pi\mu} H_{i\mu}^{(1)}(x) , \quad (3.85)$$

which causes the explicit exponential factors of μ to cancel in the Wightman function.

With these building blocks, we can write down the various exchange contributions. For example, I_{++} is

$$I_{++} = -\frac{g^2 \eta_*^4}{16k_1 k_2 k_3 k_4} \int_{-\infty}^{\eta_*} \frac{d\eta'}{(\eta')^2} \int_{-\infty}^{\eta_*} \frac{d\eta''}{(\eta'')^2} e^{ik_{12}\eta'} G_F(k_I; \eta', \eta'') e^{ik_{34}\eta''}, \quad (3.88)$$

and I_{--} is just the complex conjugate of this expression. Similarly, I_{+-} is

$$I_{+-} = \frac{g^2 \eta_*^4}{16k_1 k_2 k_3 k_4} \int_{-\infty}^{\eta_*} \frac{d\eta'}{(\eta')^2} \int_{-\infty}^{\eta_*} \frac{d\eta''}{(\eta'')^2} e^{ik_{12}\eta'} W_{k_I}(\eta'', \eta') e^{-ik_{34}\eta''}, \quad (3.89)$$

whose complex conjugate is I_{-+} .

The integral in (3.89) can be done by the same method employed in Exercise 3.4, but doing the nested time integrals involved in (3.88) is a challenge that we will return to later. However, in the limit that the exchanged momentum is small $k_I \rightarrow 0$, the computation is quite tractable.

Exercise 3.8. In the long-wavelength limit $k_I \rightarrow 0$, there is no difference between the Wightman and Feynman propagators:

$$\begin{aligned} \lim_{k_I \rightarrow 0} G(k_I; \eta', \eta'') &= \lim_{k_I \rightarrow 0} W_{k_I}(\eta', \eta'') \\ &= \frac{H^2}{4\pi} (\eta' \eta'')^{3/2} \left[\Gamma[-i\mu]^2 \left(\frac{k_I^2 \eta' \eta''}{4} \right)^{i\mu} + \Gamma[i\mu]^2 \left(\frac{k_I^2 \eta' \eta''}{4} \right)^{-i\mu} \right]. \end{aligned} \quad (3.90)$$

This is basically because we are probing separations where the two vertices are outside each others' lightcones, so that the time-ordering does not matter. (This still captures the interesting non-analytic signature of particle exchange.) Use this fact to perform the time integrals (3.88)–(3.88) and combine them together with I_{--} and I_{-+} into the in-in correlator in the $k_I \rightarrow 0$ limit.

4 The Wavefunction Approach

Cosmological correlations can also be computed by means of the so-called “wavefunction of the universe.” The wavefunction is a slightly more primitive object than correlators themselves—the relation between them is roughly the same as that between the S -matrix and scattering cross-sections. As a result, the wavefunction is somewhat simpler than correlators in certain ways that we will see. In this section, we will describe the wavefunction approach and show, in specific examples, how it reproduces the in-in results of the previous section.

4.1 Wavefunction of the Universe

Consider a set of bulk fields, $\Phi(t, \mathbf{x})$, which can include both matter fields (such as the inflaton) and metric fluctuations (such as the graviton). We are interested in their spatial correlations. The information about these correlations is contained in the quantum-mechanical state of the system at a given time. It is convenient to describe states in the basis of field eigenstates, which (in the Heisenberg picture) satisfy

$$\hat{\Phi}(t, \mathbf{x})|\phi(\mathbf{x})\rangle = \phi(\mathbf{x})|\phi(\mathbf{x})\rangle, \quad (4.1)$$

where $\hat{\Phi}$ is a field operator and $\phi(\mathbf{x}) \equiv \phi(t, \mathbf{x})$ is the spatial profile of the field at a given time t . Any state of the system can be projected onto this basis, but we will primarily be interested in the (interacting) vacuum state of the system. Writing this state in the basis of field eigenstates, the overlap coefficients are

$$\Psi[\phi(\mathbf{x})] \equiv \langle \phi(\mathbf{x}) | 0 \rangle. \quad (4.2)$$

This *wavefunctional* expresses the overlap between the vacuum state and a given state of the late-time fluctuations, and therefore provides a probability density for spatial field configurations. Equal-time correlation functions of the field are then defined as

$$\langle \phi(\mathbf{x}_1) \cdots \phi(\mathbf{x}_n) \rangle = \int \mathcal{D}\phi \phi(\mathbf{x}_1) \cdots \phi(\mathbf{x}_n) |\Psi[\phi]|^2, \quad (4.3)$$

which is a familiar formula from quantum mechanics applied to this field theory setup. This formula makes it clear that the wavefunctional and (equal-time) correlation functions contain the same information, though the translation between the two can be somewhat complicated in general. The fact that the wavefunction is in a sense a “square root” of correlation functions will lead to some simplifications in its structure, as we will see.

Since the wavefunctional is just a way of representing the state of a quantum field theory, it can be employed in a variety of situations, including in flat space. What is special about cosmology is that there is a distinguished time slice on which to consider the wavefunction—the future boundary of de Sitter space. In this $\eta_* \rightarrow 0$ limit, fields take on time-independent spatial profiles and the fact that the symmetries of de Sitter space preserve this spatial slice means that the invariance of the vacuum wavefunctional under de Sitter symmetry is easy to implement. In many cases this makes it possible to reconstruct the wavefunctional directly on the boundary from these symmetry principles (see Section 5).

The wavefunction at a given time (which we can set to $t_* = 0$ without loss of generality) is formally computed by the following path integral

$$\Psi[\phi] = \int \mathcal{D}\Phi e^{iS[\Phi]}, \quad (4.4)$$

$\Phi(0) = \phi$
 $\Phi(-\infty^+) = 0$

which defines a sum over field configurations that interpolate between the free theory vacuum in the far past (selected via the usual $i\epsilon$ prescription) and a Dirichlet boundary condition that the field have some specified spatial profile at $t_* = 0$, $\phi(\mathbf{x}) \equiv \phi(t_*, \mathbf{x})$. Clearly, Ψ depends on this choice of late-time boundary condition for the field, making it a functional.

In practice, we compute the path integral (4.4) in perturbation theory. At tree level, the path integral can then be approximated by its saddle point

$$\Psi[\phi] \approx \exp(iS[\Phi_{\text{cl}}]), \quad (4.5)$$

where Φ_{cl} is a solution to the classical equations of motion with future boundary condition that $\Phi_{\text{cl}}(t_*) = \phi$. We will almost exclusively be interested in tree-level processes, so that this lowest-order approximation of the wavefunction will be sufficient for our purposes, but it can be systematically corrected by including quantum fluctuations around the classical saddle, as is typical in path-integral computations.

We begin by considering the evaluation of the wavefunction (4.4) in free theory, where the saddle-point approximation (4.5) is exact. We then turn to the perturbative evaluation of the wavefunction in interacting theories, and show how computations utilizing the wavefunction are equivalent to the in-in formalism.

4.2 Warmup in Quantum Mechanics

To get an intuitive understanding of the wavefunction approach, it is instructive to first apply it to a few simple examples in quantum mechanics.

4.2.1 Harmonic Oscillator

Consider a *simple harmonic oscillator*, whose action is

$$S[\Phi] = \int dt \left(\frac{1}{2} \dot{\Phi}^2 - \frac{1}{2} \omega^2 \Phi^2 \right), \quad (4.6)$$

where Φ is the deviation from equilibrium (which we called q in Exercise 2.1) and ω is the constant frequency of the oscillator. On-shell, the action can equivalently be written as a pure boundary term

$$\begin{aligned} S[\Phi_{\text{cl}}] &= \int_{t_i}^{t_*} dt \left[\frac{1}{2} \partial_t (\dot{\Phi}_{\text{cl}} \Phi_{\text{cl}}) - \frac{1}{2} \Phi_{\text{cl}} \underbrace{(\ddot{\Phi}_{\text{cl}} + \omega^2 \Phi_{\text{cl}})}_{=0} \right] \\ &= \frac{1}{2} \dot{\Phi}_{\text{cl}} \Phi_{\text{cl}} \Big|_{t=t_*}, \end{aligned} \quad (4.7)$$

where we have integrated by parts and used the fact that the classical solution satisfies the equation of motion $\ddot{\Phi}_{\text{cl}} + \omega^2 \Phi_{\text{cl}} = 0$.

To determine the classical solution $\Phi_{\text{cl}}(t)$ we have to specify two boundary conditions: We require: 1) the late-time value of the oscillator position is $\Phi_{\text{cl}}(t_* \equiv 0) = \phi$, and 2) the early-time limit is the minimum-energy solution $\Phi_{\text{cl}}(t) \sim e^{i\omega t}$. The unique solution satisfying these boundary conditions is $\Phi_{\text{cl}}(t) = \phi e^{i\omega t}$. Substituting this into (4.7), we get

$$S = \frac{i\omega}{2} \phi^2 \quad \Rightarrow \quad \exp(iS) = \exp\left(-\frac{\omega}{2}\phi^2\right) \quad \Rightarrow \quad |\Psi[\phi]|^2 = e^{-\omega\phi^2}. \quad (4.8)$$

We see the familiar fact that the ground state wavefunction of the simple harmonic oscillator is a Gaussian.²² The width of this Gaussian determines the size of the zero-point fluctuations of the oscillator:

$$\langle \phi^2 \rangle = \frac{1}{2\omega}. \quad (4.9)$$

In Exercise 2.1, we derived the same result using canonical quantization.

Free quantum field theory in Fourier space is essentially equivalent to a set of harmonic oscillators indexed by the continuous wavenumber \mathbf{k} . To see this, we write the action of a free scalar in Fourier space:

$$\begin{aligned} S &= \int dt d^3x \left(\frac{1}{2} \dot{\Phi}^2 - \frac{1}{2} (\nabla \Phi)^2 - \frac{1}{2} m^2 \Phi^2 \right) \\ &= \int dt \frac{d^3k}{(2\pi)^3} \left(\frac{1}{2} \dot{\Phi}_{\mathbf{k}} \dot{\Phi}_{-\mathbf{k}} - \frac{1}{2} (k^2 + m^2) \Phi_{\mathbf{k}} \Phi_{-\mathbf{k}} \right), \end{aligned} \quad (4.10)$$

where $\Phi_{\mathbf{k}}(t)$ are the Fourier modes of the field. We see that these Fourier modes each satisfy the equation of a simple harmonic oscillator with frequencies $\omega_k \equiv \sqrt{k^2 + m^2}$. The wavefunction, and the associated zero-point fluctuations, can then be written as a sum over the corresponding results for each harmonic oscillator:

$$\Psi[\phi] = \exp\left(-\frac{1}{2} \int \frac{d^3k}{(2\pi)^3} \omega_k \phi_{\mathbf{k}} \phi_{-\mathbf{k}}\right) \quad \Rightarrow \quad \langle \phi_{\mathbf{k}} \phi_{-\mathbf{k}} \rangle' = \frac{1}{2\omega_k}. \quad (4.11)$$

The treatment of free fields in quantum field theory is therefore as simple as that of an infinite collection of uncoupled harmonic oscillators in quantum mechanics.

4.2.2 Time-Dependent Oscillator

In Section 2.4, we showed that a free field in de Sitter space (and also the fluctuations during inflation) satisfy the equation of motion of a harmonic oscillator with a time-dependent frequency (for each Fourier mode); cf. equation (2.25). It is therefore useful to consider the the following *time-dependent oscillator*:

$$S[\Phi] = \int dt \left(\frac{1}{2} \textcolor{red}{A(t)} \dot{\Phi}^2 - \frac{1}{2} \textcolor{blue}{B(t)} \Phi^2 \right), \quad (4.12)$$

²²If we wanted to reproduce the correct phase of the wavefunction $\sim e^{i\omega t/2}$, we would have to compute the Gaussian integral for fluctuations around this classical trajectory. See, e.g. Appendix A of [?] for a discussion. Since this phase is independent of ϕ , it is not important for our purposes.

where $A(t)$ and $B(t)$ are arbitrary functions of time. On-shell, this action can again be written as a boundary term

$$\begin{aligned} S[\Phi_{\text{cl}}] &= \int_{t_i}^{t_*} dt \left[\frac{1}{2} \partial_t (A \dot{\Phi}_{\text{cl}} \Phi_{\text{cl}}) - \frac{1}{2} \Phi_{\text{cl}} \underbrace{(\partial_t (A \dot{\Phi}_{\text{cl}}) + B \Phi_{\text{cl}})}_{=0} \right] \\ &= \frac{1}{2} A \dot{\Phi}_{\text{cl}} \Phi_{\text{cl}} \Big|_{t=t_*}, \end{aligned} \quad (4.13)$$

where we have used that the classical solution satisfies $\partial_t (A \dot{\Phi}_{\text{cl}}) + B \Phi_{\text{cl}} = 0$.

We again need to find the classical solution with the correct boundary conditions to describe the ground state. We can write the desired solution abstractly as $\Phi_{\text{cl}}(t) = \phi K(t)$. Substituting this into the equation of motion, we obtain a differential equation for K :

$$\partial_t (A(t) \dot{K}(t)) + B(t) K(t) = 0. \quad (4.14)$$

The boundary conditions that we impose on the solution are that $K(t_*) = 1$ and $K(-\infty) \sim e^{i\omega t}$. Of course, the precise form of $K(t)$ depends on $A(t)$ and $B(t)$, but given those functions we can then solve the equation of motion subject to the prescribed boundary conditions to obtain K .

Substituting this solution into (4.13), we have the following expression for the ground state wavefunction

$$\Psi[\phi] = \exp(iS) = \exp \left(\frac{i}{2} (A \partial_t \log K) \Big|_{t=t_*} \phi^2 \right), \quad (4.15)$$

and hence we can compute the two-point correlator using

$$|\Psi[\phi]|^2 = \exp(-\text{Im}(A \partial_t \log K) \Big|_{t=t_*} \phi^2) \implies \boxed{\langle \phi^2 \rangle = \frac{1}{2 \text{Im}(A \partial_t \log K) \Big|_{t=t_*}}}. \quad (4.16)$$

As we will see in the next section, this result will be directly applicable to fields in de Sitter space.

4.3 Free Fields in de Sitter

Having gained some intuition for the wavefunction in the quantum-mechanical setting, we are now ready to use it to compute de Sitter correlators.

We start with the action of a free massive scalar field in a curved background:

$$S = \int d^4x \sqrt{-g} \left(-\frac{1}{2} g^{\mu\nu} \partial_\mu \Phi \partial_\nu \Phi - \frac{1}{2} m^2 \Phi^2 \right). \quad (4.17)$$

Substituting the de Sitter metric (2.15) (in conformal time), this becomes

$$\begin{aligned} S &= \int d\eta d^3x a^4(\eta) \left[\frac{1}{2a^2(\eta)} ((\Phi')^2 - (\nabla \Phi)^2) - \frac{1}{2} m^2 \Phi^2 \right] \\ &= \frac{1}{2} \int d\eta d^3k \left[\frac{1}{(H\eta)^2} \Phi'_k \Phi'_{-k} - \frac{1}{(H\eta)^2} \left(k^2 + \frac{m^2}{(H\eta)^2} \right) \Phi_k \Phi_{-k} \right], \end{aligned} \quad (4.18)$$

where, in the second line, we have written the field in terms of its Fourier components and used $a(\eta) = -1/(H\eta)$. We see that the action for each Fourier mode is the same as that of the time-dependent oscillator in (4.12), with the identifications

$$A(\eta) \equiv \frac{1}{(H\eta)^2}, \quad (4.19)$$

$$B(\eta) \equiv \frac{1}{(H\eta)^2} \left(k^2 + \frac{m^2}{(H\eta)^2} \right). \quad (4.20)$$

We can therefore apply the result (4.16) to compute the wavefunction and the variance of the field.

The classical equation of motion is

$$(A\Phi'_{\text{cl}})' + B\Phi_{\text{cl}} = 0 \implies \Phi''_{\text{cl}} + \frac{2}{\eta}\Phi'_{\text{cl}} + \left(k^2 + \frac{(m/H)^2}{\eta^2} \right)\Phi_{\text{cl}} = 0. \quad (4.21)$$

The qualitative features of the solutions to this equation were discussed in Section 2.4. We saw that on small scales, $|k\eta| \gg 1$, the equation reduces to that of simple harmonic oscillator with frequency k . On large scales, $|k\eta| \rightarrow 0$, the harmonic oscillator becomes over-damped and the fluctuations freeze-out (for $m = 0$) or decay slowly (for $m > 0$).

We write the solution to (4.21) as

$$\Phi_{\text{cl}}(\eta) \equiv \phi K(\eta), \quad (4.22)$$

where the function $K(\eta)$ approaches unity at late times and oscillates like $e^{ik\eta}$ at early times. For massless fields, we have

$$\begin{aligned} K(\eta) &= (1 - ik\eta)e^{ik\eta}, \\ \log K(\eta) &= \log(1 - ik\eta) + ik\eta. \end{aligned} \quad (4.23)$$

Substituting this into (4.16) gives

$$\begin{aligned} \text{Im}(A\partial_\eta \log K)|_{\eta=\eta_*} &= \frac{1}{(H\eta_*)^2} \text{Im} \left(\frac{-ik}{1 - ik\eta_*} + ik \right) \\ &= \frac{1}{(H\eta_*)^2} \text{Im} \left(\frac{k^2\eta + ik^3\eta_*^2}{1 + k^2\eta_*^2} \right) \xrightarrow{\eta_* \rightarrow 0} \boxed{\frac{k^3}{H^2}}, \end{aligned} \quad (4.24)$$

where we have taken $\eta_* \rightarrow 0$ at the end. The late-time two-point function of the field therefore is

$$\boxed{\langle \phi_{\mathbf{k}} \phi_{-\mathbf{k}} \rangle' = \frac{H^2}{2k^3}}, \quad (4.25)$$

which is the same as the result (??) derived by canonical quantization in Section 2.4.

For massive fields, the relevant solution to (4.21) has

$$\begin{aligned} K(\eta) &= \left(\frac{\eta}{\eta_*} \right)^{3/2} \frac{H_\nu^{(2)}(-k\eta)}{H_\nu^{(2)}(-k\eta_*)}, \\ \log K(\eta) &= \frac{3}{2} \log \eta + \log [H_\nu^{(2)}(-k\eta)], \end{aligned} \quad (4.26)$$

and hence the width of the wavefunction is given by

$$\begin{aligned}\text{Im}(A\partial_\eta \log K)|_{\eta=\eta_*} &= \frac{1}{(H\eta_*)^2} \text{Im} \left(\frac{\partial_\eta H_\nu^{(2)}(-k\eta)}{H_\nu^{(2)}(-k\eta)} \right) \Big|_{\eta=\eta_*} \\ &= \frac{1}{(H\eta_*)^2} \frac{1}{|H_\nu^{(2)}(-k\eta_*)|^2} \text{Im} \left(H_\nu^{(2)*}(-k\eta) \partial_\eta H_\nu^{(2)}(-k\eta) \right) \Big|_{\eta=\eta_*}. \end{aligned} \quad (4.27)$$

Consider first the case $m < \frac{3}{2}H$, where the order ν of the Hankel function is real. We then have $H_\nu^{(2)*} = H_\nu^{(1)}$ and hence

$$\text{Im} \left(H_\nu^{(2)*} \partial_\eta H_\nu^{(2)} \right) \Big|_{\eta=\eta_*} = \frac{1}{2i} \left(H_\nu^{(1)} \partial_\eta H_\nu^{(2)} - H_\nu^{(2)} \partial_\eta H_\nu^{(1)} \right). \quad (4.28)$$

We recognize the term in the brackets as the Wronskian of the Hankel function:

$$H_\nu^{(1)} \partial_\eta H_\nu^{(2)} - H_\nu^{(2)} \partial_\eta H_\nu^{(1)} = -\frac{4i}{\pi} \frac{1}{\eta}. \quad (4.29)$$

Substituting this into (4.27), we get

$$\text{Im}(A\partial_\eta \log K)|_{\eta=\eta_*} = \frac{1}{(H\eta_*)^2} \frac{1}{|H_\nu^{(2)}(-k\eta_*)|^2} \left(-\frac{2}{\pi} \frac{1}{\eta_*} \right). \quad (4.30)$$

The two-point function of the field is therefore

$$\langle \phi_{\mathbf{k}} \phi_{-\mathbf{k}} \rangle' = \frac{\pi}{4} H^2 (-\eta_*)^3 H_\nu^{(1)}(-k\eta_*) H_\nu^{(2)}(-k\eta_*) \Bigg], \quad (4.31)$$

which is consistent with the result obtained in Exercise 2.2.

Exercise 4.1. Prove equation (4.29).

Hint: Take a derivative of the Wronskian W and use the Bessel equation to obtain a first-order differential equation for W . Find the solution of this equation, fixing the integration constant by considering the large argument limit of the Hankel functions.

The two-point function (4.31) can actually be analytically continued to $m > \frac{3}{2}H$ by sending $\nu \rightarrow i\mu$, though showing this requires a little bit of work.

Exercise 4.2. Show that for $m > \frac{3}{2}H$, where $\nu \equiv i\mu$ is pure imaginary, the power spectrum becomes

$$\begin{aligned}\langle \phi_{\mathbf{k}} \phi_{-\mathbf{k}} \rangle' &= \frac{\pi}{4} H^2 (-\eta_*)^3 e^{\pi\mu} |H_{i\mu}^{(2)}(-k\eta_*)|^2 \\ &= \frac{\pi}{4} H^2 (-\eta_*)^3 H_{i\mu}^{(2)}(-k\eta_*) H_{i\mu}^{(1)}(-k\eta_*) . \end{aligned} \quad (4.32)$$

Note that the last expression holds both for real and imaginary orders of the Hankel function.

4.4 Interactions

Our main interest in these lectures is not in free fields, but in their interactions and the associated higher-point correlations. In this section, we will use the wavefunction approach to study higher-point correlations and show how this reproduces the in-in results of Section 3.

4.4.1 Anharmonic Oscillator

Before we study interacting field theory, it is again useful to first study a simpler example within quantum mechanics—the *anharmonic oscillator*. Consider the following action

$$S[\Phi] = \int dt \left(\frac{1}{2} \dot{\Phi}^2 - \frac{1}{2} \omega^2 \Phi^2 - \frac{1}{3} g \Phi^3 \right), \quad (4.33)$$

which is the ordinary harmonic oscillator perturbed by the addition of a cubic interaction.²³ As before, we want to determine its ground state wavefunction by computing the on-shell action, $S[\Phi_{\text{cl}}]$.²⁴ The classical solution must obey the same boundary conditions as for the unperturbed oscillator: $\Phi_{\text{cl}}(t=0) = \phi$ and $\Phi_{\text{cl}}(t \rightarrow -\infty) = e^{i\omega t}$. The complication in this case is that the equation of motion is nonlinear

$$\ddot{\Phi} + \omega^2 \Phi = -g \Phi^2, \quad (4.34)$$

and the solutions cannot be written in closed form. We can, however, write a formal solution to this equation by treating the $g\Phi^2$ term as a source:

$$\Phi_{\text{cl}}(t) = \phi e^{i\omega t} + i \int dt' G(t, t') (-g \Phi_{\text{cl}}^2(t')), \quad (4.35)$$

where $\phi e^{i\omega t}$ is the solution to the free equation of motion and $G(t, t')$ is a Green's function for the harmonic oscillator, which satisfies $(\partial_t^2 + \omega^2)G(t, t') = -i\delta(t - t')$. The boundary conditions we specify for Φ_{cl} determine what Green's function we should use. In this case, the nontrivial boundary condition that we have to impose is $G(0, t') = G(t, 0) = 0$. This guarantees that only the $\phi e^{i\omega t}$ part of the solution contributes at $t = 0$, as this piece already satisfies the boundary condition $\Phi_{\text{cl}}(0) = \phi$ by itself. The relevant Green's function is then

$$G(t, t') = \frac{1}{2\omega} \left(e^{-i\omega(t-t')} \theta(t-t') + e^{i\omega(t-t')} \theta(t'-t) - e^{i\omega(t+t')} \right), \quad (4.36)$$

which can be derived in the usual way.

Exercise 4.3. Derive the Green's function (4.36) for the the harmonic oscillator by imposing the usual continuity and jump conditions along with requiring that the field oscillate as $e^{i\omega t}$ in the far past and that the Green's function vanishes at $t = 0$.

²³This model is, of course, unstable. However, since we are only interested in perturbatively correcting the ground state of the ordinary harmonic oscillator, this instability will not be important. One could alternatively consider the ϕ^4 anharmonic oscillator if this instability is troubling.

²⁴[DB: footnote on classical approximation, reintroducing \hbar]

To derive the wavefunction of the oscillator in the saddle point approximation, we have to compute the on-shell action, $S[\Phi_{\text{cl}}]$. It is convenient to first write (4.33) in the following form

$$\begin{aligned} S[\Phi] &= \int dt \left[\frac{1}{2} \partial_t (\Phi \dot{\Phi}) - \frac{1}{2} \Phi (\ddot{\Phi} + \omega^2 \Phi) - \frac{g}{3} \Phi^3 \right] \\ &= \frac{1}{2} \Phi \dot{\Phi} \Big|_{t=0} + \int dt \left[-\frac{1}{2} \Phi (\ddot{\Phi} + \omega^2 \Phi) - \frac{g}{3} \Phi^3 \right]. \end{aligned} \quad (4.37)$$

We have to be somewhat careful when we evaluate the boundary term for the classical solution (4.35). Although the Green's function vanishes for $t = 0$ (so that $\Phi_{\text{cl}}(0) = \phi$), its derivative does not, but instead satisfies the identity

$$\lim_{t \rightarrow 0} \partial_t G(t, t') = -ie^{i\omega t'}. \quad (4.38)$$

Using this, the boundary term becomes

$$\begin{aligned} \frac{1}{2} \Phi_{\text{cl}} \dot{\Phi}_{\text{cl}} \Big|_{t=0} &= \frac{1}{2} \phi \left(i\omega \phi - ig \int dt' (-ie^{i\omega t'}) \Phi_{\text{cl}}^2(t') \right) \\ &= \frac{i\omega}{2} \phi^2 - \frac{g}{2} \phi \int dt' e^{i\omega t'} \Phi_{\text{cl}}^2(t'), \end{aligned} \quad (4.39)$$

and substituting (4.35) into (4.37) gives

$$\begin{aligned} S[\Phi_{\text{cl}}] &= \frac{i\omega}{2} \phi^2 - \frac{g}{2} \phi \int dt e^{i\omega t} \Phi_{\text{cl}}^2 \\ &\quad + \int dt \left[-\frac{1}{2} \left(\phi e^{i\omega t} - ig \int dt' G(t, t') \Phi_{\text{cl}}^2(t') \right) \left(-g \Phi_{\text{cl}}^2(t) \right) - \frac{g}{3} \Phi_{\text{cl}}^3 \right]. \end{aligned} \quad (4.40)$$

The terms linear in ϕ cancel and we get the following *on-shell action*:

$$S[\Phi_{\text{cl}}] = \frac{i\omega}{2} \phi^2 - \frac{g}{3} \int dt \Phi_{\text{cl}}^3(t) - \frac{ig^2}{2} \int dt dt' G(t, t') \Phi_{\text{cl}}^2(t') \Phi_{\text{cl}}^2(t). \quad (4.41)$$

This way of organizing the terms makes it clear that the first term contributes only to the two-point function. At higher orders both of the last two terms in (4.41) can be important.

Exercise 4.4. Consider an anharmonic oscillator with a general interaction Lagrangian L_{int} . Show that the on-shell action can be written as

$$S[\Phi_{\text{cl}}] = \frac{i\omega}{2} \phi^2 + \int dt L_{\text{int}} - \frac{i}{2} \int dt dt' G(t, t') \frac{\delta S_{\text{int}}}{\delta \Phi_{\text{cl}}(t')} \frac{\delta S_{\text{int}}}{\delta \Phi_{\text{cl}}(t)}, \quad (4.42)$$

which for $L_{\text{int}} = -\frac{1}{3}g \Phi^3$ reduces to 4.41.

Given the classical solution to the equations of motion, we can use (4.41) to compute the wavefunction. We obtain such a solution in perturbation theory by solving (4.35) order-by-order in the parameter g . To do so, we expand

$$\Phi_{\text{cl}}(t) = \Phi^{(0)}(t) + g \Phi^{(1)}(t) + g^2 \Phi^{(2)}(t) + \dots \quad (4.43)$$

The lowest order ($g = 0$) solution is just the solution to the unperturbed oscillator

$$\Phi^{(0)}(t) = \phi e^{i\omega t}. \quad (4.44)$$

At first order in g , we find

$$\begin{aligned} \Phi^{(1)}(t) &= i \int dt' G(t, t') \left(-(\Phi^{(0)}(t'))^2 \right) \\ &= i \int dt' G(t, t') \left(-\phi^2 e^{2i\omega t'} \right) = \frac{\phi^2}{3\omega^2} (e^{2i\omega t} - e^{i\omega t}), \end{aligned} \quad (4.45)$$

where we have used the lowest-order solution as a source and performed the integral using the Green's function (4.36). By plugging this solution back into (4.35) and iterating, we can perturbatively solve to any order in g desired.

Substituting (4.43) into (4.41), we obtain a perturbative expansion of the on-shell action:

$$\begin{aligned} S[\Phi_{\text{cl}}] &= \frac{i\omega}{2}\phi^2 - \frac{g}{3} \int dt \left[(\Phi^{(0)})^3 + 3g(\Phi^{(0)})^2\Phi^{(1)} + \dots \right] \\ &\quad + \frac{g^2}{2} \int dt (\Phi^{(0)}(t))^2 \int dt' iG(t, t') \left(-(\Phi^{(0)}(t'))^2 \right) + \dots, \end{aligned} \quad (4.46)$$

where we have displayed all terms up to $\mathcal{O}(g^2)$. Identifying the last integral in the second line with the solution $\Phi^{(1)}$, we can also write

$$S[\Phi_{\text{cl}}] = \frac{i\omega}{2}\phi^2 - \frac{g}{3} \int dt (\Phi^{(0)})^3 - \frac{g^2}{2} \int dt (\Phi^{(0)})^2 \Phi^{(1)} + \dots. \quad (4.47)$$

Using the explicit solutions for the zeroth and first-order solutions—equations (4.44) and (4.45)—we find that the wavefunction of the anharmonic oscillator up to this order is

$$\Psi[\phi] \approx e^{iS[\Phi_{\text{cl}}]} = \exp \left(-\frac{\omega}{2}\phi^2 - \frac{g}{9\omega}\phi^3 + \frac{g^2}{72\omega^3}\phi^4 + \dots \right). \quad (4.48)$$

We see that the anharmonic interaction induces a deviation from the Gaussian shape of the wavefunction. These terms will contribute to the moments of the distribution of ϕ defined by $|\Psi[\phi]|^2$. For example, we could compute $\langle \phi^3 \rangle$ in this theory and would get a nonzero answer, in contrast to its Gaussian counterpart where $g = 0$. Similarly, higher moments $\langle \phi^n \rangle$ receive contributions order-by-order in g . It is the analogue of these moments that we want to compute in the field theory context.

Exercise 4.5. Derive the first-order solution (4.45) by explicitly integrating the Green's function for the harmonic oscillator. Note that $\Phi^{(1)}(0) = 0$ as expected. Using (4.44) and (4.45), confirm the result (4.48) for the wavefunction.

4.4.2 Wavefunction in Field Theory

After this brief detour into quantum mechanics, we return to our main problem of interest, computing the wavefunctional in interacting field theories. In perturbation theory, we expect fluctuations to be small, and so it is convenient to expand the wavefunction (4.2) in powers of the field fluctuations as:

$$\begin{aligned} \Psi[\phi] = \exp & \left(-\frac{1}{2} \int d^3x_1 d^3x_2 \Psi_2(\mathbf{x}_1, \mathbf{x}_2) \phi(\mathbf{x}_1) \phi(\mathbf{x}_2) \right. \\ & \left. + \sum_{n=3}^{\infty} \int d^3x_1 \cdots d^3x_n \Psi_n(\underline{\mathbf{x}}) \phi(\mathbf{x}_1) \cdots \phi(\mathbf{x}_n) \right), \end{aligned} \quad (4.49)$$

where $\underline{\mathbf{x}} \equiv \{\mathbf{x}_1, \dots, \mathbf{x}_n\}$ denotes the set of all spatial coordinates and the kernels $\Psi_n(\underline{\mathbf{x}})$ are called *wavefunction coefficients*. These functions capture the statistics of the fluctuations ϕ . It is useful to write the wavefunction coefficients in momentum space,

$$\int d^3x_1 \cdots d^3x_n \Psi_n(\underline{\mathbf{x}}) \phi(\mathbf{x}_1) \cdots \phi(\mathbf{x}_n) = \int \frac{d^3k_1 \cdots d^3k_n}{(2\pi)^{3n}} \Psi_n(\underline{\mathbf{k}}) \phi_{\mathbf{k}_1} \cdots \phi_{\mathbf{k}_n}, \quad (4.50)$$

which is the natural habitat of cosmological correlations. As a consequence of translation invariance, the momentum-space wavefunction coefficients contain a momentum-conserving delta function. It is often useful to extract this delta function and write

$$\Psi_n(\underline{\mathbf{k}}) = (2\pi)^3 \delta^{(3)}(\mathbf{k}_1 + \cdots + \mathbf{k}_n) \psi_n(\underline{\mathbf{k}}). \quad (4.51)$$

These wavefunction coefficients can also be interpreted as correlation functions of operators, O , which are dual to the bulk fields, $\Psi_n = \langle O_{\mathbf{k}_1} \cdots O_{\mathbf{k}_n} \rangle$, because they have the same kinematic properties [19]. As we will see in Section 5.2, in the context of cosmology in de Sitter space, these dual operators transform like primaries in a 3d conformal field theory.²⁵

Correlators

The wavefunction coefficients $\psi_n(\underline{\mathbf{k}})$ then contain all the information about correlations in the quantum state. To see this, we parameterize the wavefunction as

$$\begin{aligned} \Psi[\phi] = \exp & \left(-\frac{1}{2} \int \frac{d^3k_1 d^3k_2}{(2\pi)^6} \langle O_{\mathbf{k}_1} O_{\mathbf{k}_2} \rangle \phi_{\mathbf{k}_1} \phi_{\mathbf{k}_2} + \int \frac{d^3k_1 d^3k_2 d^3k_3}{(2\pi)^9} \langle O_{\mathbf{k}_1} O_{\mathbf{k}_2} O_{\mathbf{k}_3} \rangle \phi_{\mathbf{k}_1} \phi_{\mathbf{k}_2} \phi_{\mathbf{k}_3} \right. \\ & \left. + \int \frac{d^3k_1 d^3k_2 d^3k_3 d^3k_4}{(2\pi)^{12}} \langle O_{\mathbf{k}_1} O_{\mathbf{k}_2} O_{\mathbf{k}_3} O_{\mathbf{k}_4} \rangle \phi_{\mathbf{k}_1} \phi_{\mathbf{k}_2} \phi_{\mathbf{k}_3} \phi_{\mathbf{k}_4} + \cdots \right). \end{aligned} \quad (4.52)$$

In order to connect to our previous discussion of correlation functions, we now want to see in perturbation theory how these wavefunction coefficients are related to correlators. To do this, we

²⁵Note that there are three sets of variables: the bulk field Φ , its boundary value ϕ and the dual boundary operator O . It is worth emphasizing that we are not requiring these O 's to literally be operators in some exact dual QFT, but rather are just exploiting the fact that they kinematically behave as such.

expand the wavefunction around a Gaussian:

$$\begin{aligned}\Psi[\phi] = \exp & \left(-\frac{1}{2} \int \frac{d^3 k_1 d^3 k_2}{(2\pi)^6} \langle O_{\mathbf{k}_1} O_{\mathbf{k}_2} \rangle \phi_{\mathbf{k}_1} \phi_{\mathbf{k}_2} \right) \\ & \times \left[1 + \int \frac{d^3 k_1 d^3 k_2 d^3 k_3}{(2\pi)^9} \langle O_{\mathbf{k}_1} O_{\mathbf{k}_2} O_{\mathbf{k}_3} \rangle \phi_{\mathbf{k}_1} \phi_{\mathbf{k}_2} \phi_{\mathbf{k}_3} \right. \\ & + \frac{1}{2} \int \frac{d^3 k_1}{(2\pi)^3} \cdots \frac{d^3 k_6}{(2\pi)^3} \langle O_{\mathbf{k}_1} O_{\mathbf{k}_2} O_{\mathbf{k}_3} \rangle \langle O_{\mathbf{k}_4} O_{\mathbf{k}_5} O_{\mathbf{k}_6} \rangle \phi_{\mathbf{k}_1} \phi_{\mathbf{k}_2} \phi_{\mathbf{k}_3} \phi_{\mathbf{k}_4} \phi_{\mathbf{k}_5} \phi_{\mathbf{k}_6} \\ & \left. + \int \frac{d^3 k_1 d^3 k_2 d^3 k_3 d^3 k_4}{(2\pi)^{12}} \langle O_{\mathbf{k}_1} O_{\mathbf{k}_2} O_{\mathbf{k}_3} O_{\mathbf{k}_4} \rangle \phi_{\mathbf{k}_1} \phi_{\mathbf{k}_2} \phi_{\mathbf{k}_3} \phi_{\mathbf{k}_4} + \cdots \right], \quad (4.53)\end{aligned}$$

where we are displaying the terms that will contribute up to the four-point function at tree level. We can then use the quantum-mechanics formula (4.3) to compute correlation functions by performing Gaussian integrals over the fields ϕ .

For example, the simplest correlation function we could compute is the two-point function, which is given by

$$\langle \phi_1 \phi_2 \rangle' = \frac{1}{2 \operatorname{Re} \langle O_1 O_2 \rangle'}, \quad (4.54)$$

where we have introduced some condensed notation $\phi_a \equiv \phi_{\mathbf{k}_a}$ (and similar for O), and where the prime on the wavefunction coefficient $\langle \cdots \rangle'$ indicates that we have removed the momentum-conserving delta function. Similarly, the three-point function is [AJ: check normalizations]

$$\langle \phi_1 \phi_2 \phi_3 \rangle = \frac{\operatorname{Re} \langle O_1 O_2 O_3 \rangle}{2 \operatorname{Re} \langle O_1 O_1 \rangle \operatorname{Re} \langle O_2 O_2 \rangle \operatorname{Re} \langle O_3 O_3 \rangle}, \quad (4.55)$$

and the four-point function becomes [DB: Exercises suggest that some factors are off]

$$\begin{aligned}\langle \phi_1 \phi_2 \phi_3 \phi_4 \rangle = & \frac{\operatorname{Re} \langle O_1 O_2 O_3 O_4 \rangle}{8 \operatorname{Re} \langle O_1 O_1 \rangle \operatorname{Re} \langle O_2 O_2 \rangle \operatorname{Re} \langle O_3 O_3 \rangle \operatorname{Re} \langle O_4 O_4 \rangle} \\ & + \frac{\langle O_1 O_2 O_I \rangle \langle O_I O_3 O_4 \rangle^* + \text{c.c.}}{8 \operatorname{Re} \langle O_I O_I \rangle \operatorname{Re} \langle O_1 O_1 \rangle \operatorname{Re} \langle O_2 O_2 \rangle \operatorname{Re} \langle O_3 O_3 \rangle \operatorname{Re} \langle O_4 O_4 \rangle} + \text{perms.} \quad (4.56) \\ & + \frac{\langle O_1 O_2 O_I \rangle \langle O_I O_3 O_4 \rangle + \text{c.c.}}{8 \operatorname{Re} \langle O_I O_I \rangle \operatorname{Re} \langle O_1 O_1 \rangle \operatorname{Re} \langle O_2 O_2 \rangle \operatorname{Re} \langle O_3 O_3 \rangle \operatorname{Re} \langle O_4 O_4 \rangle} + \text{perms.},\end{aligned}$$

where ‘‘perms.’’ denotes the sum over other permutations of the external operators (i.e. other exchange channels) because we have taken all the operators to be identical for simplicity, and we have dropped the primes on the various wavefunction coefficients to simplify notation.

Exercise 4.6. Derive the formulas (4.54)–(4.56).

On-shell action

Now that we know how to use the wavefunction, we turn to calculating it. Like we did for the harmonic oscillator, we are going to use the fact that, at tree level, the wavefunction is simply

related to the on-shell action

$$\Psi[\phi] \approx \exp(iS[\Phi_{\text{cl}}]). \quad (4.57)$$

For concreteness, we consider the action of a massive scalar field in an arbitrary spacetime background:

$$S[\Phi] = \int d^4x \sqrt{-g} \left(-\frac{1}{2} g^{\mu\nu} \partial_\mu \Phi \partial_\nu \Phi - \frac{1}{2} m^2 \Phi^2 + \mathcal{L}_{\text{int}} \right), \quad (4.58)$$

where we have isolated the free part of the action and grouped all of the interactions schematically into \mathcal{L}_{int} . The equation of motion following from this action is

$$(\square - m^2)\Phi = -\frac{1}{\sqrt{-g}} \frac{\delta S_{\text{int}}}{\delta \Phi}, \quad (4.59)$$

where $\square \equiv g^{\mu\nu} \nabla_\mu \nabla_\nu$ is the curved-space d'Alembert operator. As before, we can write a formal solution to this equation as

$$\Phi_{\text{cl}}(t, \mathbf{x}) = \int d^3x' \sqrt{\gamma} K(t, \mathbf{x}, \mathbf{x}') \phi(\mathbf{x}') + i \int d^4x' G(x, x') \frac{\delta S_{\text{int}}}{\delta \Phi(x')} \Big|_{\Phi=\Phi_{\text{cl}}}, \quad (4.60)$$

where γ_{ij} is the spatial metric and $K(t, \mathbf{x}, \mathbf{x}')$ is a solution to the free equation of motion that satisfies the boundary condition

$$K(t_*, \mathbf{x}, \mathbf{x}') = \frac{1}{\sqrt{\gamma}} \delta^{(3)}(\mathbf{x} - \mathbf{x}'), \quad (4.61)$$

and reduces to the vacuum solution as $t \rightarrow -\infty$ (we will see that this second boundary condition is most simply implemented in Fourier space). The solution $K(t, \mathbf{x}, \mathbf{x}')$ is often called the *bulk-to-boundary propagator*.²⁶ The function $G(x, x')$ is a Green's function satisfying the equation

$$(\square - m^2) G(x, x') = \frac{i}{\sqrt{-g}} \delta(t - t') \delta^{(3)}(\mathbf{x} - \mathbf{x}'). \quad (4.62)$$

The precise Green's function of interest also reduces to the vacuum in the far past and vanishes if we take one of the points to the boundary $G(x, x')|_{t=t_*} = G(x, x')|_{t'=t_*} = 0$. The latter constraint ensures that the formal solution (4.60) will satisfy the boundary condition $\Phi_{\text{cl}}(t_*, \mathbf{x}) = \phi(\mathbf{x})$. The function $G(x, x')$ is often called the *bulk-to-bulk propagator*.²⁷ The two propagators K and G are related by the identity

$$\lim_{t \rightarrow t_*} g^{tt} \partial_t G(x, x') = iK(t', \mathbf{x}, \mathbf{x}'). \quad (4.63)$$

As in the case of the anharmonic oscillator, we can substitute the formal solution (4.60) into the action (4.58). This is again most simply done by first integrating the kinetic term by parts:

$$S[\Phi] = - \int d^3x \sqrt{\gamma} \frac{1}{2} g^{tt} \Phi \dot{\Phi} \Big|_{t=t_*} + \int d^4x \sqrt{-g} \left(\frac{1}{2} \Phi (\square - m^2 \Phi) + \mathcal{L}_{\text{int}}[\Phi] \right), \quad (4.64)$$

²⁶As we will see, in the diagrammatic interpretation of the computation of the wavefunction, this object is associated to lines connecting bulk vertices to the $t = t_*$ boundary slice. The nomenclature comes from AdS/CFT, where one computes the bulk on-shell action using essentially the same procedure [?].

²⁷We will see that it is associated to internal lines in diagrams that connect two spacetime interaction vertices.

which generates a boundary term on the $t = t_*$ slice (with induced metric γ). As in the case of the anharmonic, we have to be careful when evaluating the boundary term. In particular, although $\Phi_{\text{cl}}(t_*, \mathbf{x}) = \phi(\mathbf{x})$, the time derivative of the solution (4.60) is

$$\begin{aligned}\partial_t \Phi_{\text{cl}}(t_*, \mathbf{x}) &= \int d^3x' \sqrt{\gamma} \partial_t K(t, \mathbf{x}, \mathbf{x}') \phi(\mathbf{x}') \Big|_{t=t_*} + i \int d^4x' \partial_t G(x, x') \frac{\delta S_{\text{int}}}{\delta \Phi_{\text{cl}}(x')} \\ &= \int d^3x' \sqrt{\gamma} \partial_t K(t, \mathbf{x}, \mathbf{x}') \phi(\mathbf{x}') \Big|_{t=t_*} - \int d^4x' \frac{K(t', \mathbf{x}, \mathbf{x}')}{g^{tt}} \frac{\delta S_{\text{int}}}{\delta \Phi_{\text{cl}}(x')},\end{aligned}\quad (4.65)$$

where we have used the identity (4.63). Evaluating the boundary term in (4.64) on the classical solution therefore gives

$$\begin{aligned}- \int d^3x \sqrt{\gamma} \frac{1}{2} g^{tt} \Phi_{\text{cl}} \dot{\Phi}_{\text{cl}} \Big|_{t=t_*} &= - \frac{1}{2} \int d^3x \sqrt{\gamma} d^3x' \sqrt{\gamma} \phi(\mathbf{x}) \phi(\mathbf{x}') \left(g^{tt} \partial_t K(t, \mathbf{x}, \mathbf{x}') \right) \Big|_{t=t_*} \\ &\quad + \frac{1}{2} \int d^4x' d^3x \sqrt{\gamma} K(t', \mathbf{x}, \mathbf{x}') \phi(\mathbf{x}) \frac{\delta S_{\text{int}}}{\delta \Phi_{\text{cl}}(x')},\end{aligned}\quad (4.66)$$

which should be compared to equation (4.39) in the anharmonic oscillator example. Note that the second line in (4.66) involves a bulk integral over x' . Equation (4.64) can then be written as

$$\begin{aligned}S[\Phi_{\text{cl}}] &= - \int d^3x \sqrt{\gamma} d^3x' \sqrt{\gamma} \frac{1}{2} \phi(\mathbf{x}) \phi(\mathbf{x}') \left(g^{tt} \partial_t K(t, \mathbf{x}, \mathbf{x}') \right) \Big|_{t=t_*} \\ &\quad - \frac{1}{2} \int d^4x d^3x' \sqrt{\gamma} K(t, \mathbf{x}', \mathbf{x}) \phi(\mathbf{x}') \frac{\delta S_{\text{int}}}{\delta \Phi_{\text{cl}}(x)} \\ &\quad + \int d^4x \left(-\frac{1}{2} \Phi_{\text{cl}} \frac{\delta S_{\text{int}}}{\delta \Phi_{\text{cl}}} + \sqrt{-g} \mathcal{L}_{\text{int}}[\Phi_{\text{cl}}] \right).\end{aligned}\quad (4.67)$$

We now see that if we substitute (4.60) into the first term in the last line, that the term involving ϕK will cancel with the second line and we will be left with the *on-shell action* [?]

$$\begin{aligned}S[\Phi_{\text{cl}}] &= - \int d^3x \sqrt{\gamma} d^3x' \sqrt{\gamma} \frac{1}{2} \phi(\mathbf{x}) \phi(\mathbf{x}') \left(g^{tt} \partial_t K(t, \mathbf{x}, \mathbf{x}') \right) \Big|_{t=t_*} + \int d^4x \sqrt{-g} \mathcal{L}_{\text{int}}[\Phi_{\text{cl}}] \\ &\quad - \frac{i}{2} \int d^4x d^4x' \frac{\delta S_{\text{int}}}{\delta \Phi_{\text{cl}}(x)} G(x, x') \frac{\delta S_{\text{int}}}{\delta \Phi_{\text{cl}}(x')},\end{aligned}\quad (4.68)$$

which is the analogue of (4.41) for the anharmonic oscillator. Given a formula for the classical solution Φ_{cl} , we can then plug it into (4.68) to obtain the tree-level wavefunction.

4.4.3 Perturbation Theory

We can solve (4.60) iteratively in perturbation theory. Like for the anharmonic oscillator, we imagine that there is some perturbative parameter g that we can expand the solution in

$$\Phi_{\text{cl}}(x) = \Phi^{(0)}(x) + g \Phi^{(1)}(x) + g^2 \Phi^{(2)}(x) + \dots,\quad (4.69)$$

where $\Phi^{(0)}(x)$ is the solution to the free equation of motion, $\Phi^{(1)}(x)$ is the first order correction,

$$\Phi^{(1)}(t, \mathbf{x}) = i \int d^4x' G(x, x') \frac{\delta S_{\text{int}}}{\delta \Phi(x')} \Big|_{\Phi=\Phi^{(0)}},\quad (4.70)$$

and so on.

In order to systematize the calculation, it is possible to assign a diagrammatic set of rules to the entire procedure of computing the classical solution order-by-order in perturbation theory and substituting this solution back into the action (4.68). To make this slightly more intuitive, consider the special case where $\mathcal{L}_{\text{int}} = -\frac{1}{3!}g\Phi^3$. Up to $\mathcal{O}(g^2)$, equation (4.68) can then be written as

$$\begin{aligned} iS[\Phi_{\text{cl}}] = & -i \int d^3x \sqrt{\gamma} d^3x' \sqrt{\gamma} \frac{1}{2} \phi(\mathbf{x}) \phi(\mathbf{x}') \left(g^{tt} \partial_t K(t, \mathbf{x}, \mathbf{x}') \right) \Big|_{t=t_*} - \frac{ig}{3!} \int d^4x \sqrt{-g} (\Phi^0(x))^3 \\ & - \frac{g^2}{8} \int d^4x \sqrt{-g} \int d^4x' \sqrt{-g} (\Phi^0(x))^2 G(x, x') (\Phi^0(x'))^2 + \dots . \end{aligned} \quad (4.71)$$

The first term is just the ordinary Gaussian part of the action. The other terms have the following diagrammatic interpretation:

$$-ig \int d^4x \sqrt{-g} (\Phi^{(0)}(x))^3 = \begin{array}{c} \text{---} \\ \backslash \quad / \\ \bullet \end{array} , \quad (4.72)$$

$$-g^2 \int d^4x \sqrt{-g} \int d^4x' \sqrt{-g} (\Phi^{(0)}(x))^2 G(x, x') (\Phi^{(0)}(x'))^2 = \begin{array}{c} \text{---} \\ \backslash \quad / \quad \backslash \quad / \\ \bullet \quad \bullet \end{array} , \quad (4.73)$$

and this can be continued to higher order in the boundary conditions ϕ .

In order to state the Feynman rules most simply, it is convenient to express the computation in Fourier space to trivialize the integrals over space. At this point we are specializing the background to assume that spatial translations are a symmetry. For concreteness, we will further assume isotropy so that the spacetime is of FRW form. We can then express G and K in terms of the solutions to the free equation of motion for the field Φ in Fourier space. Given the solution to the (Fourier space) free equation of motion, $f_k(t)$, which satisfies the conditions

$$f_k^*(t) \partial_t f_k(t) - \partial_t f_k^*(t) f_k(t) = i, \quad (4.74)$$

$$\lim_{t \rightarrow -\infty} f_k(t) \sim e^{ikt}, \quad (4.75)$$

we can write the bulk-to-boundary and bulk-to-bulk propagators as

$$K_k(t) = \frac{f_k(t)}{f_k(t_*)}, \quad (4.76)$$

$$G(k; t, t') = f_k^*(t) f_k(t') \theta(t - t') + f_k^*(t') f_k(t) \theta(t' - t) - \frac{f_k^*(t_*)}{f_k(t_*)} f_k(t) f_k(t'). \quad (4.77)$$

One can check that the function $G(k; t, t')$ satisfies the equation

$$(\square_k - m^2) G(k; t, t') = \frac{i}{\sqrt{-g}} \delta(t - t'), \quad (4.78)$$

where \square_k is the spatial Fourier transform of the wave operator, while $K_k(t)$ solves the homogeneous version of the same equation. The classical solution (4.60) is then expressed in Fourier space as

$$\Phi_{\text{cl}}(t, \mathbf{k}) = K_k(t) \phi_{\mathbf{k}} + i \int dt' G(k; t, t') \frac{\delta S_{\text{int}}}{\delta \Phi_{\mathbf{k}}(t')} \Big|_{\Phi=\Phi_{\text{cl}}} . \quad (4.79)$$

We can now state the rules for the computation of wavefunction coefficients.

Feynman rules

Similar to the computation of in-in correlators, wavefunctional calculations can be simplified by organizing things into a systematic expansion in Feynman diagrams. Like in-in, wavefunctional diagrams have two different types of propagators, which makes them slightly more complicated than their flat-space counterparts. However, compared to the in-in diagrams we encountered above, the wavefunction is a bit simpler, which is a benefit. Concretely, the Feynman rules are:

1. Draw the fixed-time boundary surface ($t = t_*$) on which you want to compute the wavefunction.
2. To compute the wavefunction coefficient multiplying ϕ^n , draw all diagrams with a fixed number of lines, n , ending on the boundary.
3. Assign a vertex factor, iV , to each bulk interaction, where V is obtained by functionally differentiating the action as usual. (Note that this can lead to factors of momenta or time derivatives acting on propagators if there are derivative interactions.)
4. Assign a bulk-to-bulk propagator, G , to each internal line.
5. Assign a bulk-to-boundary propagator, K , to each external line (lines that end on the boundary).
6. Integrate over the time insertions of all bulk vertices using the measure $Dt \equiv dt a^3(t)$. For diagrams involving loops, integrate over the loop momenta.

We see that all told, the Feynman rules are fairly similar to the in-in case, except that the propagators that we use are slightly different, and that there are about half as many diagrams.

A small warning: As we saw above, there are some normalization factors that appear in the on-shell action multiplying the outputs of these Feynman diagrams to give the true wavefunction coefficients. For most of our purposes, the normalizations will not end up being particularly important, but if one wants to match exactly the result of an in-in calculation, the normalizations do matter. Working out these relative normalizations in complete generality is somewhat tedious, but for the case where one is computing the wavefunction coefficient coming from a $\mathcal{L}_{\text{int}} = -g\Phi^n$ interaction, with I internal lines (at tree level), one should multiply the result of the Feynman diagram calculation by

$$c_{n,I} = \frac{\Gamma[I(n-1) + n]}{\Gamma[I+2]\Gamma[I(n-2) + n+1]\Gamma[n]^{I+1}}, \quad (4.80)$$

in order to convert it into a true wavefunction coefficient. In the following, we will often ignore these normalization factors and refer to the output of the Feynman diagram calculation as wavefunction coefficients.

Exercise 4.7. Using these Feynman rules, show explicitly that the expressions (4.55) and (4.56) are equivalent to the correlators derived in Section 3 using the in-in formalism.

Hint: You should find that the second line in (4.56) is equal to $I_{+-} + I_{-+}$, and that the first line is equal to $I_{++} + I_{--} + I_{\text{extra}}$, where I_{extra} precisely cancels against the third line.

4.4.4 Correlators in Flat Space

We are now ready to compute correlators using the wavefunction formalism. We begin with examples of flat-space correlators where all time integrals can be performed explicitly. All correlators can be evaluated at $t_* \equiv 0$ without loss of generality.

We will consider the same toy model as in Section 3.2

$$S = \int d^4x \left(-\frac{1}{2}(\partial\Phi)^2 - \frac{g}{3!}\Phi^3 \right). \quad (4.81)$$

The free equation of motion in Fourier space is $(\partial_t^2 + k^2)\phi_{\mathbf{k}} = 0$, so that the properly-normalized mode functions are

$$f_k(t) = \frac{1}{\sqrt{2k}} e^{ikt}. \quad (4.82)$$

Using this, the relevant flat-space propagators are

$$K_k(t) = e^{ikt}, \quad (4.83)$$

$$G(k; t, t') = \frac{1}{2k} \left(e^{-ik(t-t')} \theta(t-t') + e^{ik(t-t')} \theta(t'-t) - e^{ik(t+t')} \right). \quad (4.84)$$

The two-point wavefunction coefficient was computed in (4.11) and is $\langle O_1 O_2 \rangle = k_1$, which by (4.54) implies the correct two-point function $\langle \phi_1 \phi_2 \rangle = 1/(2k_1)$. Let's now compute the simplest correlators in this theory at three and four points.

Three-point function Applying the Feynman rules to the three-point wavefunction coefficient, we get

$$\begin{aligned} \langle O_1 O_2 O_3 \rangle &\equiv \begin{array}{c} \diagup \quad \diagdown \\ \text{---} \quad \text{---} \\ \diagdown \quad \diagup \end{array} \\ &= ig \int_{-\infty}^0 dt K_{k_1}(t) K_{k_2}(t) K_{k_3}(t) \\ &= ig \int_{-\infty}^0 dt e^{i(k_1+k_2+k_3)t} = \frac{g}{(k_1 + k_2 + k_3)}. \end{aligned} \quad (4.85)$$

Substituting this into (4.55), we obtain the following three-point function

$$\langle \phi_1 \phi_2 \phi_3 \rangle = -\frac{\text{Re} \langle O_1 O_2 O_3 \rangle}{4k_1 k_2 k_3} = -\frac{g}{4k_1 k_2 k_3} \frac{1}{k_1 + k_2 + k_3}, \quad (4.86)$$

which agrees with (3.46), the result of the in-in computation.

Four-point function Applying the Feynman rules to the four-point wavefunction coefficient, we get

$$\begin{aligned}
\langle O_1 O_2 O_3 O_4 \rangle &\equiv \text{Diagram} \\
&= -g^2 \int_{-\infty}^0 dt' dt'' K_{k_1}(t') K_{k_2}(t') G(k_I; t', t'') K_{k_3}(t'') K_{k_4}(t'') \\
&= -g^2 \int_{-\infty}^0 dt' dt'' e^{ik_{12}t'} \left[G_F(k_I; t', t'') - \frac{1}{2k_I} e^{ik_I(t'+t'')} \right] e^{ik_{34}t''}, \quad (4.87)
\end{aligned}$$

where we have split the bulk-to-bulk propagator into the Feynman propagator and an extra term. Up to a rescaling, the integral involving the Feynman propagator is the same as the one we computed in (3.47) to get the I_{++} contribution to the in-in correlator. We therefore have

$$\begin{aligned}
\langle O_1 O_2 O_3 O_4 \rangle &= 16 k_1 k_2 k_3 k_4 \times I_{++} + \frac{g^2}{2k_I} \int_{-\infty}^0 dt' e^{i(k_{12}+k_I)t'} \int_{-\infty}^0 dt'' e^{i(k_{34}+k_I)t''} \\
&= 16 k_1 k_2 k_3 k_4 \times I_{++} - \frac{g^2}{2k_I} \frac{1}{(k_{12} + k_I)(k_{34} + k_I)}. \quad (4.88)
\end{aligned}$$

Substituting (3.49) for I_{++} , this gives

$$\begin{aligned}
\langle O_1 O_2 O_3 O_4 \rangle &= \frac{g^2}{2k_I} \left(\frac{1}{k_{12} + k_{34}} \left(\frac{1}{k_{12} + k_I} + \frac{1}{k_{34} + k_I} \right) - \frac{1}{(k_{12} + k_I)(k_{34} + k_I)} \right) \\
&= \frac{g^2}{(k_{12} + k_{34})(k_{12} + k_I)(k_{34} + k_I)}. \quad (4.89)
\end{aligned}$$

In summary, we have obtained the following wavefunction coefficients [AJ: Fix normalizations]

$$\langle O_1 O_2 \rangle = k_1, \quad (4.90)$$

$$\langle O_1 O_2 O_3 \rangle = \frac{g}{(k_1 + k_2 + k_3)} \quad (4.91)$$

$$\langle O_1 O_2 O_3 O_4 \rangle = \frac{g^2}{(k_{12} + k_{34})(k_{12} + k_I)(k_{34} + k_I)}. \quad (4.92)$$

Note the simplicity of these expressions relative to the corresponding in-in correlation functions.

Finally, let us confirm that these results reproduce the four-point function that we derived in Section 3.2 using the in-in formalism. Since the wavefunction coefficients are real, equation (4.56) reduces to

$$\langle \phi_1 \phi_2 \phi_3 \phi_4 \rangle = \frac{1}{8 k_1 k_2 k_3 k_4} \left(\langle O_1 O_2 O_3 O_4 \rangle + \frac{\langle O_1 O_2 O_I \rangle \langle O_I O_3 O_4 \rangle}{k_I} \right) \quad (4.93)$$

$$= \frac{g^2}{8 k_1 k_2 k_3 k_4} \left(\frac{1}{(k_{12} + k_{34})(k_{12} + k_I)(k_{34} + k_I)} + \frac{1}{k_I} \frac{1}{(k_{12} + k_I)(k_{34} + k_I)} \right), \quad (4.94)$$

where we substituted (4.91) and (4.92) in the second line. It is not hard to confirm that (4.94) is the same as (3.56), so that we precisely recover the result of the in-in computation.

4.4.5 Correlators in de Sitter

It is now straightforward to extend the computations to de Sitter space. The relevant propagators are given by (4.76) and (4.77), with

$$f_k(\eta) = H \sqrt{\frac{\pi}{4}} e^{-\frac{i\pi}{4}(1+2\nu)} (-\eta)^{3/2} H_\nu^{(2)}(-k\eta). \quad (4.95)$$

While the computations are conceptually exactly the same as in flat space, for generic fields the time integrals involving Hankel functions typically cannot be performed explicitly. As in Section 3.3, we will therefore often specialize to situations involving scalars with conformal mass $m^2 = 2H^2$, whose mode functions are

$$f_k(\eta) = H(-\eta) \frac{e^{ik\eta}}{\sqrt{2k}}, \quad (4.96)$$

corresponding to $\nu = 1/2$ in (4.95). The simplicity of these functions will enable analytic results in many cases.

Contact diagrams We first consider contact diagrams coming from polynomial bulk interactions of the form Φ^n . For example, the three-point wavefunction coefficient is [AJ: check sign]

$$\begin{aligned} \langle O_1 O_2 O_3 \rangle &\equiv \text{Diagram: three vertical lines meeting at a central point} \\ &= ig \int_{-\infty}^{\eta_*} D\eta K_{k_1}(\eta) K_{k_2}(\eta) K_{k_3}(\eta) \\ &= \frac{ig}{f_{k_1}(\eta_*) f_{k_2}(\eta_*) f_{k_3}(\eta_*)} \int_{-\infty}^{\eta_*} \frac{d\eta}{(H\eta)^4} f_{k_1}(\eta) f_{k_2}(\eta) f_{k_3}(\eta). \end{aligned} \quad (4.97)$$

In the generic case, this involves an integral over a product of three Hankel functions whose result in terms of an Appell F_4 function is not very illuminating.

Specializing to conformal scalars, and taking the limit $\eta_* \rightarrow 0$, we get

$$\langle O_1 O_2 O_3 \rangle = -\frac{ig}{H^4(-\eta_*)^3} \int_{-\infty}^{\eta_*} \frac{d\eta}{\eta} e^{iK\eta} = \boxed{\frac{ig}{H^4\eta_*^3} \log(iK\eta_*)}, \quad (4.98)$$

where $K = k_1 + k_2 + k_3$. As in (3.61) the factors of i come from the $i\epsilon$ prescription used to regulate the integral. Using $2\text{Re}\langle O_n O_n \rangle = |f_{k_n}(\eta_*)|^{-2}$, the three-point correlator (4.55) becomes [AJ: fix normalization here]

$$\begin{aligned} \langle \phi_1 \phi_2 \phi_3 \rangle &= -\frac{H^6 \eta_*^6}{8k_1 k_2 k_3} \left(\langle O_1 O_2 O_3 \rangle + \langle O_1 O_2 O_3 \rangle^* \right) \\ &= -\frac{g}{8} \frac{H^2 \eta_*^3}{k_1 k_2 k_3} \left(i \log(iK\eta_*) - i \log(-iK\eta_*) \right) = \boxed{\frac{\pi}{8} g \frac{H^2 \eta_*^3}{k_1 k_2 k_3}}. \end{aligned} \quad (4.99)$$

which is the same as the in-in result (3.62). Notice that the two contributions from the different branches of the in-in contour are reproduced from the wavefunction perspective by the contributions from Ψ and Ψ^* .

Another case where the integrals can be explicitly computed involves two conformally coupled scalar fields and one scalar with general mass.

Exercise 4.8. Derive the three-point wavefunction coefficient of two conformally coupled scalars and one scalar of generic mass. You should find

$$\langle OOX \rangle = \left(\frac{\pi}{2 \cosh(\pi\mu)} \right)^{\frac{1}{2}} k_3^{i\mu - \frac{1}{2}} {}_2F_1 \left[\begin{matrix} \frac{1}{2} + i\mu, & \frac{1}{2} - i\mu \\ 1 & \end{matrix} \middle| \frac{u-1}{2u} \right], \quad (4.100)$$

where ${}_2F_1$ is the Gauss hypergeometric function. Show that this result is consistent with the in-in correlator found in Exercise 3.4.

Computing higher-point contact diagrams involving conformally coupled scalars is completely straightforward as well.

Exercise 4.9. Show that the contact n -point wavefunction coefficient and correlator for conformal scalars arising from a $-g\Phi^n/n!$ interaction are ($n \geq 4$):

$$\langle O_1 \cdots O_n \rangle_c = -i^n \frac{g}{H^4 \eta_*^n} \frac{\Gamma[n-3]}{n!} \frac{1}{K^{n-3}}, \quad (4.101)$$

$$\langle \phi_1 \cdots \phi_n \rangle_c = \begin{cases} (-1)^{\frac{n}{2}+1} \Gamma[n-3] \frac{g H^{2n-4} \eta_*^n}{2^{n-1} k_1 \cdots k_4} \frac{1}{K^{n-3}}, & n \text{ even}, \\ 0, & n \text{ odd}, \end{cases} \quad (4.102)$$

where $K \equiv k_1 + k_2 + \cdots + k_n$. Since the Φ^4 interaction preserves the conformal symmetry of the free theory, the result for $n=4$ is essentially the same as in flat space (except for a factor of $H\eta_*$ for each external field).

Exchange diagrams Next, we look at exchange diagrams. For example, the four-point wavefunction coefficient arising from the exchange of a massive scalar:

$$\begin{aligned} \langle O_1 O_2 O_3 O_4 \rangle &\equiv \begin{array}{c} \text{---} \\ \backslash \quad / \\ \bullet \quad \bullet \end{array} \\ &= -g^2 \int_{-\infty}^{\eta_*} D\eta' D\eta'' K_{k_1}(\eta') K_{k_2}(\eta') G(k_I; \eta', \eta'') K_{k_3}(\eta'') K_{k_4}(\eta''). \end{aligned} \quad (4.103)$$

We first consider the case of a conformal scalar, for which the bulk-to-boundary and bulk-to-bulk propagators (for $\eta_* \rightarrow 0$) are

$$K_k(\eta) = \frac{\eta}{\eta_*} e^{ik\eta}, \quad (4.104)$$

$$G(k_I; \eta', \eta'') = \frac{H^2 \eta' \eta''}{2k_I} \left[e^{-ik|\eta' - \eta''|} - e^{ik_I(\eta' + \eta'')} \right]. \quad (4.105)$$

Equation (4.103) then becomes

$$\langle O_1 O_2 O_3 O_4 \rangle = -\frac{g^2}{H^6 \eta_*^4} \frac{1}{2k_I} \int_{-\infty}^0 \frac{d\eta'}{\eta'} \int_{-\infty}^0 \frac{d\eta''}{\eta''} e^{ik_{12}\eta'} e^{ik_{34}\eta''} \left[e^{-ik|\eta' - \eta''|} - e^{ik_I(\eta' + \eta'')} \right]$$

$$\begin{aligned}
&= -\frac{g^2}{H^6 \eta_*^4} \frac{1}{2k_I} \int_{k_{12}}^\infty dx \int_{k_{34}}^\infty dy \int_{-\infty}^0 d\eta' d\eta'' e^{ix\eta'} e^{iy\eta''} \left[e^{-ik|\eta'-\eta''|} - e^{ik_I(\eta'+\eta'')} \right] \\
&= \frac{1}{H^6 \eta_*^4} \int_{k_{12}}^\infty dx \int_{k_{34}}^\infty dy \langle O_1 O_2 O_3 O_4 \rangle_{(\text{flat})}(x, y, k_I),
\end{aligned} \tag{4.106}$$

where we have used the same trick as in Section 3.3 to write the expression as an integral over the corresponding flat-space result. Substituting (4.89) for $\langle O_1 O_2 O_3 O_4 \rangle_{(\text{flat})}$, gives the same integral as for $I_{++}^{(c)}$ in (3.78). We therefore get

$$\begin{aligned}
\langle O_1 O_2 O_3 O_4 \rangle &= -\frac{g^2}{H^6 \eta_*^4} \int_{k_{12}}^\infty dx \int_{k_{34}}^\infty dy \frac{1}{(x+y)(x+k_I)(y+k_I)} \\
&= \boxed{\frac{g^2}{2H^6 \eta_*^4} \frac{1}{k_I} \left[\text{Li}_2\left(\frac{k_{12}-k_I}{E}\right) + \text{Li}_2\left(\frac{k_{34}-k_I}{E}\right) + \log\left(\frac{k_{12}+k_I}{E}\right) \log\left(\frac{k_{34}+k_I}{E}\right) - \frac{\pi^2}{6} \right]}.
\end{aligned} \tag{4.107}$$

Notice that the wavefunction coefficient (4.107) is very similar to the full correlator (3.83). The primary difference is in the π^2 term (along with some overall normalization factors), which comes from the disconnected contributions to the correlator from $\langle O_1 O_2 O_3 \rangle$.

Exercise 4.10. Using the wavefunction coefficient that you just computed along with the three-point result (4.98), check that the correlator derived from the wavefunction reproduces the in-in result (3.83).

It is also straightforward to include the effects of derivative interactions in the vertices of diagrams. In many of the most phenomenologically interesting cases, the interactions of fields break the de Sitter symmetries of the background. Processes involving time derivatives of massless scalar fields are particularly simple [?].

Exercise 4.11. Consider the (de Sitter breaking) interaction

$$L_{\text{int}} = -\frac{g}{2} a^3(t) \dot{\Phi}^2 \chi, \tag{4.108}$$

where Φ is a massless scalar and χ is a conformally coupled scalar. Compute the four-point wavefunction coefficient $\langle OOOO \rangle'$ for massless scalars coming from the exchange of χ . You should find

$$\langle O_1 O_2 O_3 O_4 \rangle' = -\frac{g^2}{H^2} k_1^2 k_2^2 k_3^2 k_4^2 \frac{2E_L E_R + E(E_L + E_R) + E^2}{E^3 E_L^2 E_R^2}, \tag{4.109}$$

where $E \equiv k_{12} + k_{34}$, $E_L \equiv k_{12} + k_I$, $E_R \equiv k_{34} + k_I$. Can you relate this to the four-point function of a massless scalar in flat space?

4.5 A Challenge

So far, most of our explicit computations in de Sitter space were for conformally coupled scalars. However, as soon as we allow for generic massive fields, the resulting integrals typically cannot be evaluated analytically. A simple example is the exchange of a generic massive scalar χ between

two pairs of conformally coupled scalars Φ . The corresponding wavefunction coefficient is of the form (4.103) and can explicitly be written as

$$F \equiv \langle O_1 O_2 O_3 O_4 \rangle = -g^2 \int \frac{d\eta'}{\eta'^2} \int \frac{d\eta''}{\eta''^2} e^{ik_{12}\eta'} e^{ik_{34}\eta''} G_\nu(k_I; \eta', \eta''), \quad (4.110)$$

where the propagator of the massive field is

$$\begin{aligned} G_\nu(k_I; \eta', \eta'') = & \frac{\pi}{4} (\eta' \eta'')^{3/2} \left[H_\nu^{(1)}(-k\eta') H_\nu^{(2)}(-k\eta'') \right. \\ & \left. - \frac{H_\nu^{(1)}(-k\eta_*)}{H_\nu^{(2)}(-k\eta_*)} H_\nu^{(2)}(-k\eta') H_\nu^{(2)}(-k\eta'') \right], \quad \text{for } \eta'' < \eta'. \end{aligned} \quad (4.111)$$

The expression for $\eta' < \eta''$ is the same but with η' and η'' interchanged. Here, ν can either be real or complex ($\nu = i\mu$), depending on the mass of the exchanged field.

The wavefunction coefficient (4.110) captures some of the physics of the on-shell production and decay of massive particles in de Sitter space, and can be used as a seed to compute the phenomenological signatures of these heavy particles [13, 24, 28]. Unfortunately, however, the time integrals involved cannot be evaluated by elementary means. Instead of trying to compute the integrals directly, we note that G_ν satisfies the differential equation

$$\left(\eta^2 \frac{\partial^2}{\partial \eta^2} - 2\eta \frac{\partial}{\partial \eta} + k_I^2 \eta^2 + \frac{m^2}{H^2} \right) G_\nu(k_I; \eta, \eta') = -iH^2 \eta^2 \eta'^2 \delta(\eta - \eta'), \quad (4.112)$$

which is just the explicit form of the Green's function equation (4.78). The fact that G_ν satisfies this differential equation can be used to derive a differential equation for the function F . To do this, we consider the auxiliary object

$$\tilde{F} \equiv -g^2 \int \frac{d\eta'}{\eta'^2} \frac{d\eta''}{\eta''^2} e^{ik_{12}\eta'} e^{ik_{34}\eta''} \left(\eta'^2 \frac{\partial^2}{\partial \eta'^2} - 2\eta' \frac{\partial}{\partial \eta'} + k_I^2 \eta'^2 + \frac{m^2}{H^2} \right) G_\nu(k_I, \eta', \eta''), \quad (4.113)$$

and evaluate it in two ways. First, we use (4.112) to write

$$\tilde{F} = ig^2 H^2 \int_{-\infty}^0 d\eta' e^{iE\eta'} = \frac{g^2 H^2}{E}, \quad (4.114)$$

with $E \equiv k_{12} + k_{34}$. Next, we integrate the time derivatives by parts in (4.113) and trade factors of η' for $-i\partial_{k_{12}}$ to obtain²⁸

$$\begin{aligned} \tilde{F} &= -g^2 \int_{-\infty}^0 \frac{d\eta'}{\eta'^2} \frac{d\eta''}{\eta''^2} \left((k_I^2 - k_{12}^2) \eta'^2 + 2ik_{12}\eta' + \frac{m^2}{H^2} - 2 \right) e^{ik_{12}\eta'} e^{ik_{34}\eta''} G_\nu(k_I, \eta', \eta'') \\ &= -g^2 \int_{-\infty}^0 \frac{d\eta'}{\eta'^2} \frac{d\eta''}{\eta''^2} \left((k_{12}^2 - k_I^2) \partial_{k_{12}}^2 + 2k_{12} \partial_{k_{12}} + \frac{m^2}{H^2} - 2 \right) e^{ik_{12}\eta'} e^{ik_{34}\eta''} G_\nu(k_I, \eta', \eta'') \\ &= \left((k_{12}^2 - k_I^2) \partial_{k_{12}}^2 + 2k_{12} \partial_{k_{12}} + \frac{m^2}{H^2} - 2 \right) F, \end{aligned} \quad (4.115)$$

²⁸We can drop the boundary term, because the bulk-to-bulk propagator vanishes on the boundary.

where, in the second line, we have pulled the differential operator outside the integral, which we then recognize as being precisely (4.110). Comparing (4.114) and (4.115), we find that F satisfies the following differential equation

$$\boxed{\left((k_{12}^2 - k_I^2) \partial_{k_{12}}^2 + 2k_{12} \partial_{k_{12}} + \frac{m^2}{H^2} - 2 \right) F = \frac{g^2 H^2}{E}}. \quad (4.116)$$

This equation is rather interesting. Time evolution in the bulk spacetime has been traded for a differential operator in terms of the external energy k_{12} . When this operator acts on the exchange solution it produces a conformally coupled scalar contact solution (cf. (4.101)). We can therefore think of the operator as collapsing the internal propagator, creating a contact interaction.

Exercise 4.12. Show that $\hat{F} = k_I F$ satisfies

$$\left(u^2(1-u^2)\partial_u^2 - 2u^3\partial_u + \frac{m^2}{H^2} - 2 \right) \hat{F} = g^2 H^2 \frac{uv}{u+v}, \quad (4.117)$$

where $u \equiv k_I/k_{12}$ and $v = k_I/k_{34}$.

This strategy of turning the integrals for the late-time wavefunction coefficients into differential equations is applicable in a wide range of situations. In the following exercise, you will derive an analogous differential equation for a three-point function.

Exercise 4.13. Derive a differential equation for the three-point wavefunction coefficient involving two conformally coupled scalars and one massive scalar, $G \equiv \langle OOX \rangle$. Write the equation in terms of $u \equiv k_3/k_{12}$.

Notice that “time” has completely disappeared from the problem. The differential equation (4.116) is formulated purely in terms of the boundary momenta (or energies k_{12} , k_{34} and k_I). This suggests that there should be a more efficient way of understanding the correlations on the late-time boundary of de Sitter without ever explicitly referring to the (unobservable) bulk time evolution. In the next section, we will first show how the differential equation (4.116) can be derived directly on the boundary and then discuss its solutions.

5 The Cosmological Bootstrap

In the previous two sections, we have presented two methods for computing inflationary correlations by evolving the fluctuations through the bulk spacetime and evaluating the resulting correlators on the future boundary. This has resulted in complex time integrals (one for each vertex in a diagram) that in general cannot be computed analytically. Numerical integration is possible, but comes at the cost of masking the physical structure of the answers.

In this section, we describe a new approach to deriving the correlations directly on the boundary by imposing consistency with unitarity, locality and symmetry assumptions. Although “time” will make no appearance, the effects of the time-dependent bulk physics (such as the production and decay of massive particle) will be reflected in the momentum scalings of the resulting correlators (see Fig. 8). The cosmological bootstrap is a very active area of current research which we will *not* be able to fully review in these lectures. Instead, we will try to give a pedagogical introduction to a few selected topics that hopefully will provide students with a useful entry point into the subject. More details and further references can be found in [1, 4, 5].

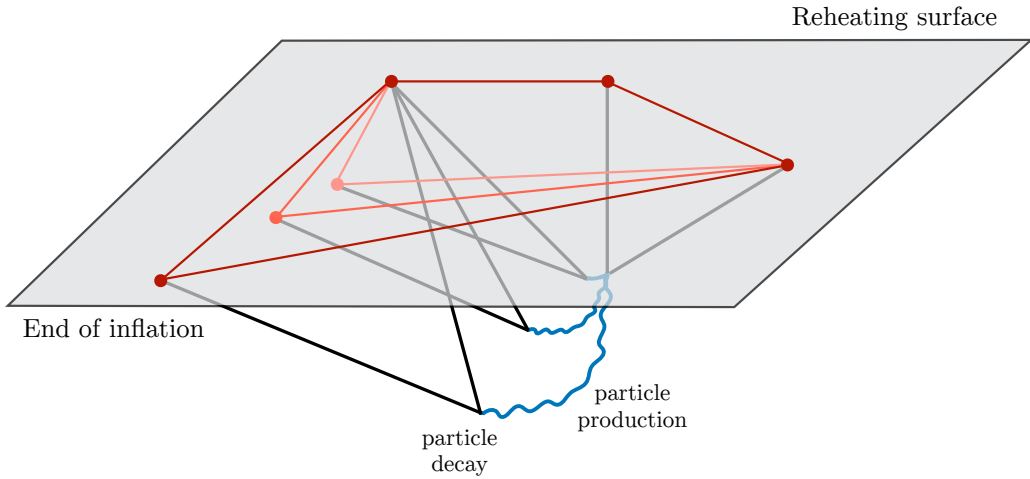


Figure 8: All cosmological correlations can be traced back to the spacelike boundary of the inflationary quasi-de Sitter spacetime. The time dependence of bulk interactions is encoded in the momentum dependence of these boundary correlators. The cosmological bootstrap is a way to derive these correlators purely from a boundary perspective.

5.1 Bootstrap Philosophy

Let us start with a few general remarks on the bootstrap philosophy and then illustrate them with the example of the S-matrix bootstrap.

You have probably learned that theories are defined by their Lagrangians. In particular, Lagrangians are a transparent way of encoding local and causal interactions between particles, which in relativistic quantum mechanics requires the introduction of fields. However, as illustrated in Fig. 9, Lagrangians are not really the fundamental starting point, but instead are intermediate objects that take us from a set of physical principles to a set of observables guaranteed to be consistent with these principles. The way that Lagrangians guarantee consistency often requires

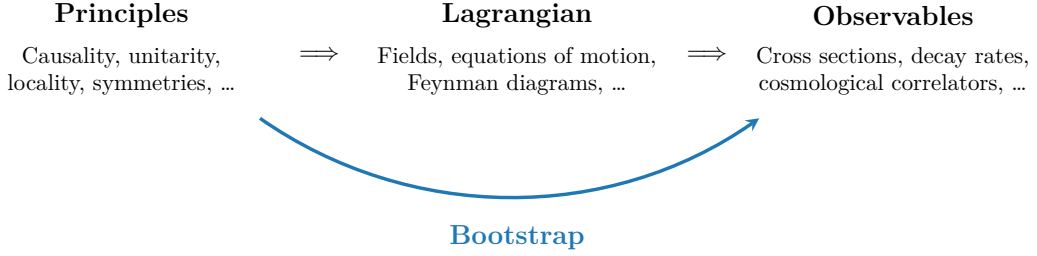


Figure 9: Graphical illustration of the bootstrap philosophy. Instead of encoding physical principles in a Lagrangian, the basic idea of the bootstrap is to take us directly from these principles to the final observables.

the introduction of additional, unphysical, degrees of freedom that are not observable, but nevertheless must be tracked in detail throughout the calculation. This introduces a substantial complication, and so the basic bootstrap philosophy is to go directly from the physical principles to final observables, without the intermediate step of introducing a Lagrangian and computing Feynman diagrams.

5.1.1 S-matrix Bootstrap

The textbook approach to computing scattering amplitudes involves a perturbative expansion in terms of Feynman diagrams. Unfortunately, these calculations can quickly become very complicated, especially in gauge theories. For example, the five-point gluon amplitude involves 25 diagrams and the associated mathematical expressions span many pages. Similar, the four-point gravity amplitude involves thousands of diagrams, each involving hundreds of terms. In these case, it required truly heroic efforts (by Parke and Taylor [?] and DeWitt [?], respectively) to compute these amplitudes explicitly. Yet, when restricted to physical configurations, the final answers are remarkably simple one-line expressions. This suggested that there should be a better way to obtain these results. Part of the problem is that individual Feynman diagrams are not truly physical, in the sense that they carry along unphysical gauge degrees of freedom that must cancel in the final answers.²⁹ In the modern amplitudes bootstrap, the focus is instead on the external on-shell data (like the momenta and helicity of the external particle) and the space of consistent amplitudes is reconstructed from consistency requirements alone, dispensing with the need for Lagrangians, Feynman diagrams and unphysical gauge degrees of freedom.

As a concrete example, consider the tree-level scattering of four identical scalars of mass m . Firstly, *Lorentz symmetry* implies that the amplitude must be a function of the Mandelstam invariants $s \equiv -(p_1 + p_2)^2$, $t \equiv -(p_1 + p_4)^2$ and $u \equiv -(p_1 + p_3)^2$, which satisfy the constraint $s + t + u = 4m^2$ (because of momentum conservation). Secondly, *locality* dictates that tree-level amplitudes can at most have simple poles (and not higher-order poles or branch cuts) at locations where an exchanged particle goes *on-shell*. For example, in the s -channel, this corresponds to a pole at $s \rightarrow M^2$, where M is the mass of the exchanged particle. Finally, *unitarity* demands that,

²⁹Even in scalar theories, Feynman diagrams are not invariant under field redefinitions. An infinite number of different Lagrangians and their corresponding Feynman diagrams can map to the same S -matrix. In that case, a poor choice of field basis can complicate the calculation and obscure important structures of the theory.

on the pole, the amplitude factorizes into a product of on-shell three-particle amplitudes:

$$\lim_{s \rightarrow M^2} A_4(s, t, u) = \frac{1}{s - M^2} \sum_h A_3^{-h}(p_1, p_2, -p_I) \times A_3^{-h}(p_1, p_2, p_I), \quad (5.1)$$

where $p_I \equiv p_1 + p_2$ is the four-momentum of the exchanged particles and we have summed over its helicities h . The three-particle amplitudes are completely fixed by symmetries: for example, if the exchange particle has spin J then

$$A_3^h(p_1, p_2, p_3) = g(p_1 - p_2)^{\mu_1} \cdots (p_1 - p_2)^{\mu_J} \epsilon_{\mu_1 \dots \mu_J}^J, \quad (5.2)$$

where g is the coupling constant and $\epsilon_{\mu_1 \dots \mu_J}^h$ is the polarization tensor. Substituting this into (5.1), and performing the sum over helicities, one then obtains the final form of the amplitude

$$A(\textcolor{red}{s}, \textcolor{blue}{t}) = \textcolor{orange}{g^2} \frac{(4m^2 - M^2)^J}{s - \textcolor{teal}{M}^2} P_J \left(1 + \frac{2t}{M^2 - 4m^2} \right) + \text{t- and u-channel}, \quad (5.3)$$

where P_J is a Legendre polynomial of order the spin J . Note that no Lagrangian and Feynman diagrams were needed to derive this, and that basic principles allowed only a small menu of possibilities. [DB: more]

Can we obtain a similar understanding of cosmological correlators?

5.1.2 Cosmological Bootstrap

- What are the rules for consistent correlators?
- How are these rules implemented?

5.2 Symmetries

The importance of symmetries in physics is hard to overstate. In this section, we review the role of symmetries to constrain the functional form of the boundary correlators in the inflationary quasi-de Sitter spacetime. We will first present the set of symmetries of a perfect de Sitter space and then describe some of their important consequences: We first derive the unitary representations associate to the de Sitter group and show how these representations are realized by bulk fields and boundary operators. We then demonstrate that the de Sitter isometries become a conformal symmetry on the late-time boundary and we derive the associated Ward identities.

5.2.1 De Sitter Isometries

We can view D -dimensional de Sitter space as a hypersurface in $(D + 1)$ -dimensional Minkowski space defined by the equation

$$\eta_{AB} X^A X^B = -X_0^2 + X_1^2 + \cdots + X_D^2 = H^{-2}, \quad (5.4)$$

where A, B run from $0, \dots, D$ and $\eta_{AB} = \text{diag}(-1, 1, \dots, 1)$. We will also frequently refer to the dimension of the spatial slices, $d \equiv D - 1$. The symmetries of de Sitter space correspond to the higher-dimensional Poincaré transformations that leave the embedded hypersurface invariant

which are Lorentz transformations. The generators of the Lorentz symmetry, J_{AB} , satisfy the $\text{so}(D, 1)$ algebra:

$$[J_{AB}, J_{CD}] = \eta_{BC} J_{AD} - \eta_{AC} J_{BD} + \eta_{AD} J_{BC} - \eta_{BD} J_{AC}. \quad (5.5)$$

It is natural, particularly in the inflationary slicing, to define

$$\begin{aligned} D &\equiv J_{D0}, \\ P_i &\equiv J_{Di} - J_{0i}, \\ K_i &\equiv J_{Di} + J_{0i}, \end{aligned} \quad (5.6)$$

so that the de Sitter algebra is given by

$$\begin{aligned} [J_{ij}, J_{kl}] &= \delta_{jk} J_{il} - \delta_{ik} J_{jl} + \delta_{il} J_{jk} - \delta_{jl} J_{ik}, & [D, P_i] &= P_i, \\ [J_{ij}, K_l] &= \delta_{jl} K_i - \delta_{il} K_j, & [D, K_i] &= -K_i, \\ [J_{ij}, P_l] &= \delta_{jl} P_i - \delta_{il} P_j, & [K_i, P_j] &= 2\delta_{ij} D - 2J_{ij}. \end{aligned} \quad (5.7)$$

Given a particular choice of coordinates, we can pull back the ambient space Lorentz generators to find explicit expressions for the Killing vectors that realize these symmetries on coordinates. In the following, we will work with the flat slicing

$$ds^2 = \frac{1}{H^2 \eta^2} (-d\eta^2 + d\mathbf{x}^2), \quad (5.8)$$

where the Killing vectors are given by

$$\begin{aligned} P_i &= \partial_i, \\ J_{ij} &= x_i \partial_j - x_j \partial_i, \\ D &= -\eta \partial_\eta - x^i \partial_i, \\ K_i &= 2x_i \eta \partial_\eta + \left(2x^j x_i + (\eta^2 - x^2) \delta_i^j \right) \partial_j. \end{aligned} \quad (5.9)$$

One can check directly that they these satisfy the commutation relations in (5.7).

Exercise 5.1. The flat slicing corresponds to the embedding

$$\begin{aligned} X^0 &= \frac{\rho}{2(-\eta)} (1 - \eta^2 + x^2), & X^i &= \frac{\rho}{(-\eta)} x^i, \\ X^D &= \frac{\rho}{2(-\eta)} (1 + \eta^2 - x^2), \end{aligned} \quad (5.10)$$

which foliates $\mathbb{R}^{D,1}$ by de Sitter hyperboloids of radius ρ . Using these embedding functions, pull back the ambient space Lorentz transformations to derive the Killing vectors in (5.9).

De Sitter space is a maximally symmetric spacetime, so it has $D(D+1)/2$ symmetries. Some of these are obvious: the metric (5.8) has \mathbb{R}^d spatial slices, so the translations and rotations of these spatial slices will be symmetries. There are d such translations and $d(d-1)/2$ rotations. The

remaining D transformations are somewhat less familiar. One of them is a *dilatation symmetry*, whose finite form is

$$\begin{aligned}\eta &\mapsto \lambda\eta, \\ \mathbf{x} &\mapsto \lambda\mathbf{x},\end{aligned}\tag{5.11}$$

while the final $D - 1$ symmetries are the de Sitter analogue of Lorentz boost transformations, which act similarly to *special conformal transformations* (SCTs):

$$\begin{aligned}\eta &\mapsto \frac{\eta}{1 + 2(\mathbf{b} \cdot \mathbf{x}) + b^2(x^2 - \eta^2)}, \\ \mathbf{x} &\mapsto \frac{\mathbf{x} + (x^2 - \eta^2)\mathbf{b}}{1 + 2(\mathbf{b} \cdot \mathbf{x}) + b^2(x^2 - \eta^2)}.\end{aligned}\tag{5.12}$$

In fact, as we will see, the transformations (5.12) act precisely as special conformal transformations on the spacelike boundary of de Sitter, motivating the naming convention. This is no accident, and is a manifestation of the fact that the de Sitter group $\text{SO}(D, 1)$ is exactly the Euclidean conformal group in $D - 1$ dimensions.

We want to understand how the symmetries of de Sitter space manifest themselves in the physics of cosmological correlations. We first study the unitary representations of the de Sitter group.

5.2.2 Unitary Representations

The Hilbert space of a quantum field theory in de Sitter space arranges itself into representations of the de Sitter group. In this section, we will present the essential properties of these unitary irreducible representations (in the bosonic case), leaving their derivations to Appendix A. Further details can be found in [29? , 30].

The goal is to realize the generators J_{AB} as anti-Hermitian operators on a vector space with positive-definite norm. It is natural to label representations by their eigenvalues of the quadratic and quartic Casimir operators [29? –31]

$$\begin{aligned}\mathcal{C}_2 &\equiv \frac{1}{2}J^{AB}J_{AB} = \hat{D}(d - \hat{D}) + P^iK_i + \frac{1}{2}J^{ij}J_{ij}, \\ \mathcal{C}_4 &\equiv J_{AB}J^{BC}J_{CD}J^{DA},\end{aligned}\tag{5.13}$$

since these commute with all the generators of the de Sitter symmetries. (We have put a hat on the D operator in just this equation to avoid confusion with the D of the $\text{SO}(D, 1)$ group.) The expression for \mathcal{C}_4 in terms of the generators in (5.6) is fairly long and unilluminating.

Unitary representations of the de Sitter group can then be constructed by starting from a *primary state* $|\bar{\Delta}\rangle_s$, which is annihilated by the SCT operator K_i , has dilatation eigenvalue $\bar{\Delta} = d - \Delta$, and $\text{so}(D)$ spin weight s . Since Δ and s completely determine the Casimirs in (5.13), we can label representations by these quantum numbers. In Appendix A.2, we describe the explicit construction of unitary scalar representations (the techniques are similar for spinning representations). Here, we just record the list of unitary representations (specializing to $D \geq 3$ spacetime dimensions).

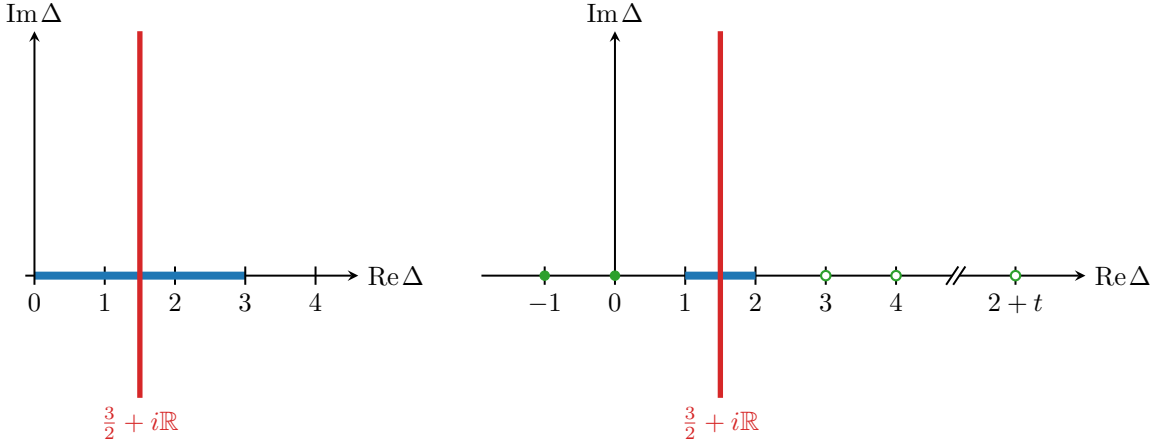


Figure 10: Illustration of scalar (*left*) and spin- ℓ (*right*) representations of $\text{SO}(4, 1)$ in the complex Δ plane. The red lines corresponds to the principal series, while the blue lines mark the complementary series. The green circles for the spin- ℓ case denote the representations of the exceptional series (which coincide with the discrete series in this case). Open circles are the shadows of the filled ones.

Scalar representations: There are three families of unitary irreducible scalar representations on de Sitter space:³⁰

- **Principal series:** This family is generated by a primary with conformal dimension $\Delta = \frac{d}{2} + i\mu$, with $\mu \in \mathbb{R}$. We will see that these representations correspond to heavy fields in de Sitter with $m^2 > \frac{d^2}{4}H^2$.
- **Complementary series:** This family is generated by a primary with conformal dimension in the range $0 < \Delta < d$. We will see that these representations are carried by light fields with $0 < m^2 < \frac{d}{4}H^2$.
- **Exceptional series:** These representations have a primary state with $\Delta = -k$ with $k \in \mathbb{Z}_{\geq 0}$. The representation obtained from this primary state is reducible and so must be projected. It is unclear what field theory carries these representations.³¹

It is interesting to compare these representations to the unitary scalar representations of the group $\text{SO}(D - 1, 2)$, which is the group of isometries of anti-de Sitter space. The representations are built in a somewhat similar manner, starting from a primary state, and in the AdS context, unitarity places a lower bound of the value of Δ for scalar representations: $\Delta \geq \frac{d}{2} - 1$.

Spinning representations: Fields with spin have a slightly different classification, which is somewhat richer than that of scalars. Along with the principal and complementary series, there are additional families of unitary representations, whose weights take on discrete values. The

³⁰Note that this is already richer than in flat space, where there are only two families: the ordinary scalar representations with $m^2 \geq 0$ and the tachyons with $m^2 < 0$.

³¹A reasonable guess is that the shift-symmetric scalar fields considered in [?] carry these representations if they are quantized treating the shift symmetries like gauge redundancies. The mass values of these fields are $m^2 = -k(d + k)H^2$.

classification of general mixed-symmetry fields is rather intricate [29?], so we will focus on spin- ℓ fields whose spin weight is $\mathbf{s} = (\ell, 0, \dots, 0)$.³²

- **Principal series:** Spinning representations in the principal series have conformal dimensions satisfying $\Delta = \frac{d}{2} + i\mu$, with $\mu \in \mathbb{R}$. The corresponding bulk fields are heavy fields with

$$m^2 \geq (\frac{d}{2} + \ell - 2)^2 H^2. \quad (5.14)$$

- **Complementary series:** Fields in this family have conformal dimensions in the range $1 < \Delta < d - 1$. Note that this is bounded away from $\Delta = 0$. These representations correspond to bulk fields with masses in the range

$$(\ell - 1)(\ell + d - 3)H^2 < m^2 < (\frac{d}{2} + \ell - 2)^2 H^2. \quad (5.15)$$

A qualitative difference from the scalar case is that spinning representations with $\ell \geq 2$ have a lower bound on their mass in order to remain unitary. This lower bound is typically called the *Higuchi bound* [?].

- **Exceptional series:** These representations have a primary state with $\Delta = 1 - t$ with $t \in \{0, 1, \dots, \ell - 1\}$, where t is called the depth. The corresponding bulk gauge fields have spin ℓ and mass

$$m^2 = (\ell - 1 - t)(\ell + t + d - 3)H^2. \quad (5.16)$$

The representation with $t = \ell - 1$ is a massless field, the other depths are known as *partially massless* fields, have gauge invariances with t -index gauge parameters, and have no flat-space analogues.

The unitary scalar and spin- ℓ representations of $\text{SO}(4, 1)$ —which is the physically relevant case—are depicted in Fig. 10.

5.2.3 Realization on Bulk Fields

Next, we want to understand how the symmetries of de Sitter space are realized on bulk fields, and in particular what representation of $\text{SO}(D, 1)$ they carry. As before, we will focus mostly on the scalar case and comment only briefly on the generalization to fields with spin.

Recall that a scalar field in de Sitter is described by the action

$$S = \int d^D x \sqrt{-g} \left(-\frac{1}{2} (\partial \Phi)^2 - \frac{m^2}{2} \Phi^2 \right). \quad (5.17)$$

³²In odd d , general mixed-symmetry fields have another family of representations, called the *discrete series*. However, these representations require all spin weights to be activated [?], so they do not appear for spin- ℓ representations, except in $d = 3$, where they happen to coincide with the exceptional series.

It is straightforward to derive the transformation of Φ under the isometries generated by the Killing vectors (5.9), it just transforms by the Lie derivative

$$P_i \Phi = \partial_i \Phi, \quad (5.18)$$

$$J_{ij} \Phi = (x_i \partial_j - x_j \partial_i) \Phi, \quad (5.19)$$

$$D\Phi = -(\eta \partial_\eta + x^i \partial_i) \Phi, \quad (5.20)$$

$$K_i \Phi = 2x_i \eta \partial_\eta \Phi + \left(2x^j x_i + (\eta^2 - x^2) \delta_i^j \right) \partial_j \Phi. \quad (5.21)$$

From this, we can work out the action of the quadratic Casimir (5.13):

$$\mathcal{C}_2 \Phi = -\eta^2 \left(\frac{\partial^2}{\partial \eta^2} - \frac{d-1}{\eta} \frac{\partial}{\partial \eta} - \nabla^2 \right) \Phi. \quad (5.22)$$

This is exactly the wave operator acting on the scalar: $H^2 \mathcal{C}_2 \Phi = \square \Phi$, so that the equation of motion can be read as an eigenvalue equation

$$\mathcal{C}_2 \Phi = \frac{m^2}{H^2} \Phi. \quad (5.23)$$

Equating this to the Casimir of a scalar representation $\mathcal{C}_2 = \Delta(d - \Delta)$, we can solve for Δ :

$$\Delta_\pm = \frac{d}{2} \pm \sqrt{\frac{d^2}{4} - \frac{m^2}{H^2}}. \quad (5.24)$$

Notice first that the two branches Δ_+ and Δ_- are related by $\Delta_+ = d - \Delta_-$. Scaling weights with this relation are so-called *shadows* of each other (see Appendix A.2), and correspond to equivalent representations, which makes sense because we anticipate that a scalar should carry a single representation that could be labeled by either of these two choices.

Notice that there are two qualitative regimes:

- **Complementary series:** For $0 \leq m^2/H^2 < d^2/4$, the values of Δ_\pm lie in the interval $[0, d]$, which are the values corresponding to the complementary series. We therefore see that “light” fields in de Sitter carry complementary series representations.
- **Principal series:** For $m^2/H^2 > d^2/4$, the values of Δ_\pm are of the form $\frac{d}{2} + i\mu$, with μ a real number. These are precisely the principal series values. Hence, “heavy” fields in de Sitter carry principal series representations.

We note in passing that fields with the (tachyonic) masses $m^2/H^2 = -k(D - 1 + k)$ have the correct weights to be the exceptional series scalars, but they have shift symmetries that are naively de Sitter symmetry-violating zero modes. It would therefore seem that they have to be quantized in some nonstandard way. Other tachyonic mass values do not correspond to any representations on the list in Section 5.2.2 and so are not unitary.

Cosmological correlations naturally live on the boundary of de Sitter space, so we now want to understand the action of these symmetries on the boundary.

5.2.4 Boundary Conformal Symmetry

There is a distinguished spatial slice in de Sitter space—the future boundary—which is invariant under the symmetries of de Sitter space. The points on this surface get mapped into each other, but the surface itself does not move. In the flat slicing, this is the $\eta = 0$ surface. In the idealized inflationary picture, this is where the universe reheats and the standard hot Big Bang cosmology starts. The fluctuations on this surface serve as the initial conditions for the universe, and therefore the correlations at $\eta = 0$ have a distinguished status. We would like to understand how de Sitter symmetry acts on them.

Consider a scalar field, Φ , with mass m . The action (5.17) implies the following equation of motion

$$\Phi'' - \frac{(d-1)}{\eta} \Phi' - \nabla^2 \Phi + \frac{m^2}{H^2} \frac{1}{\eta^2} \Phi = 0. \quad (5.25)$$

At late times ($\eta \rightarrow 0$), we can neglect the spatial gradient term and the solutions become power laws in time. The complete solution has two contributions with two different fall-offs

$$\Phi(\mathbf{x}, \eta \rightarrow 0) = \phi(\mathbf{x}) \eta^\Delta + \bar{\phi}(\mathbf{x}) \eta^{\bar{\Delta}}, \quad (5.26)$$

where $\bar{\Delta} = d - \Delta$ and the *scaling dimension* (sometimes also called the scaling weight) is

$$\Delta \equiv \frac{d}{2} - \sqrt{\frac{d^2}{4} - \frac{m^2}{H^2}}. \quad (5.27)$$

For “light fields”, with $m < \frac{d}{2}H$, the scaling dimension is purely real and the first term in (5.26) dominates at late times. Near the boundary, we can then replace time derivatives by $\eta \partial_\eta \mapsto \Delta, \bar{\Delta}$ and the de Sitter isometries (in the limit $\eta \rightarrow 0$) act as

$$\begin{aligned} P_i \phi &= \partial_i \phi, \\ J_{ij} \phi &= (x_i \partial_j - x_j \partial_i) \phi, \\ D \phi &= -(\Delta + x^i \partial_i) \phi, \\ K_i \phi &= \left[2x_i \Delta + \left(2x^j x_i - x^2 \delta_i^j \right) \partial_j \right] \phi, \end{aligned} \quad (5.28)$$

and similarly for $\bar{\phi}$. As you will show in the following exercise, these are precisely the transformation rules for a primary operator of conformal weight Δ in a conformal field theory (CFT). The late-time correlations of the field Φ can be thought of as being captured by the correlations of the spatial coefficients $\phi, \bar{\phi}$. Since these coefficients transform like operators in a CFT, late-time cosmological correlators are constrained by conformal symmetry.

Exercise 5.2. Consider \mathbb{R}^d , with $ds^2 = g_{ij} dx^i dx^j$. A conformal transformation is a coordinate transformation $x^i \mapsto \tilde{x}^i$ that leaves the metric invariant up to a scale change,

$$g_{ij}(x) \mapsto \tilde{g}_{ij}(\tilde{x}) = \Omega^2(x) g_{ij}(x). \quad (5.29)$$

For $d > 2$, show that the infinitesimal transformation $x^i \mapsto x^i + \epsilon^i(x)$ is a conformal transfor-

mation if

$$\epsilon^i(x) = a^i + r^{ij}x_j + \alpha x^i + x^2 b^i - 2(\mathbf{b} \cdot \mathbf{x})x^i, \quad (5.30)$$

where $r_{ij} = -r_{ji}$. The corresponding finite transformations are

$$T: \quad \tilde{x}^i = a^i \quad \Omega(x) = 1 \quad (5.31)$$

$$R: \quad \tilde{x}^i = R^{ij}x_j \quad \Omega(x) = 1 \quad (5.32)$$

$$D: \quad \tilde{x}^i = \lambda x^i \quad \Omega(x) = \lambda^{-1} \quad (5.33)$$

$$SCT: \quad \tilde{x}^i = \frac{x^i - b^i x^2}{1 - 2\mathbf{b} \cdot \mathbf{x} + b^2 x^2} \quad \Omega(x) = 1 - 2\mathbf{b} \cdot \mathbf{x} + b^2 x^2. \quad (5.34)$$

Note that the special conformal transformation can also be written as

$$\frac{\tilde{x}^i}{\tilde{x}^2} = \frac{x^i}{x^2} - b^i, \quad (5.35)$$

i.e. it can be thought of as a translation, preceded and followed by an inversion (at least in parity-invariant CFTs).

Conformal symmetry is surprisingly powerful. In the following exercise, you will prove the famous fact that the two- and three-point functions of primary operators in a CFT is completely fixed by symmetry [?]. In the cosmological context, this will mean that some correlation functions in de Sitter space are also entirely fixed by symmetry.

Exercise 5.3. Acting on *scalar primary operators*, O , a conformal transformation implies

$$O(x) \mapsto \tilde{O}(\tilde{x}) = \Omega(x)^\Delta O(x), \quad (5.36)$$

where Δ is the *scaling dimension* of the operator. Correlators in a CFT must then satisfy

$$\langle O_1(\tilde{x}_1) \dots O_n(\tilde{x}_n) \rangle = \Omega(x_1)^{\Delta_1} \dots \Omega(x_N)^{\Delta_N} \langle O_1(x_1) \dots O_n(x_n) \rangle, \quad (5.37)$$

which is the requirement of conformal covariance. Show that (5.37) implies

$$\langle O_1 O_2 \rangle = \frac{1}{x_{12}^{2\Delta_1}} \delta_{\Delta_1, \Delta_2}, \quad (5.38)$$

$$\langle O_1 O_2 O_3 \rangle = \frac{c_{123}}{x_{12}^{\Delta_t - 2\Delta_3} x_{23}^{\Delta_t - 2\Delta_1} x_{31}^{\Delta_t - 2\Delta_2}}, \quad (5.39)$$

with $O_a \equiv O_a(\mathbf{x}_a)$, $x_{ab} \equiv |\mathbf{x}_a - \mathbf{x}_b|$ and $\Delta_t \equiv \sum \Delta_a$.

Four-point functions are less constrained than two- and three-point functions. There is a full function's worth of freedom that is consistent with conformal invariance. We therefore typically need some additional input in order to uniquely fix the form of these correlators.

Exercise 5.4. Show that the four-point function of scalar operators is constrained to take the form

$$\langle O_1 O_2 O_3 O_4 \rangle = f(u, v) \prod_{n < m}^4 x_{nm}^{\Delta_t/3 - \Delta_n - \Delta_m}, \quad (5.40)$$

where we have introduced the conformally-invariant “cross-ratios”

$$u \equiv \left(\frac{x_{12}x_{34}}{x_{13}x_{24}} \right)^2, \quad v \equiv \left(\frac{x_{12}x_{34}}{x_{23}x_{14}} \right)^2. \quad (5.41)$$

Notice that the left-hand side of (5.40) is invariant under permutations of all of the operators, but the right hand is not manifestly invariant. Consider swapping the points 2 and 4, what constraint does this place on the function $f(u, v)$?

Now that we understand how de Sitter symmetry acts on the late-time fields, we turn to deriving the consequences of these symmetries.

5.2.5 Conformal Ward Identities

Our primary interest is in late-time cosmological correlators, and so we want to understand the constraints of de Sitter symmetry for these objects. In general, symmetries imply that correlation functions satisfy differential equations called *Ward identities*, which express invariance under symmetry transformations. We will now derive these Ward identities for both cosmological correlation functions and wavefunction coefficients.

Correlators: We can think of in-in correlation functions as directly correlating the late-time field profiles of the bulk fields Φ . As such, they are essentially correlation functions of the coefficients of the field fall-offs in (5.26). Under a de Sitter transformation, these coefficients transform as in (5.28). For light fields (in the complementary series), only the leading fall-off ϕ survives at late times, because the other branch decays more quickly. In this case, the requirements of de Sitter invariance can be phrased as

$$\sum_{a=1}^N \langle \phi_1 \cdots \delta\phi_a \cdots \phi_N \rangle = 0, \quad (5.42)$$

where $\delta\phi_a$ can stand for any of the field transformations (5.28). The constraints of translation and rotation invariance are very easy to implement and simply require that the correlator is a function only of separations $|\mathbf{x}_a - \mathbf{x}_b|$. The constraints of dilation and SCT invariance are more nontrivial, and lead to the equations

$$D : \quad 0 = \sum_{a=1}^N \left(\Delta_a + x_a^j \frac{\partial}{\partial x_a^j} \right) \langle \phi_1 \cdots \phi_N \rangle, \quad (5.43)$$

$$SCT : \quad 0 = \sum_{a=1}^N \left(2\Delta_a x_a^i + 2x_a^i x_a^j \frac{\partial}{\partial x_a^j} - x_a^2 \frac{\partial}{\partial x_{a,i}} \right) \langle \phi_1 \cdots \phi_N \rangle. \quad (5.44)$$

Correlation functions computed directly from the bulk will satisfy these equations. The idea of the bootstrap approach is to shortcut this procedure and solve these equations directly in order

to construct the output of the bulk time evolution. However, solving these equations in general is rather difficult, and there are many solutions, so we require some additional input in order to know which solutions are physically relevant.

Exercise 5.5. Show that (5.38) and (5.39) are solutions of these Ward identities.

Wavefunction coefficients: Next, we will determine how these conformal transformations act on the wavefunction coefficients. Consider the n -th order term in the perturbative expansion of the late-time wavefunction (4.49):

$$\Psi[\phi] = \exp \left(\cdots + \int d^d x_1 \cdots d^d x_N \Psi_N(\underline{\mathbf{x}}) \phi(\mathbf{x}_1) \cdots \phi(\mathbf{x}_N) + \cdots \right). \quad (5.45)$$

Under a de Sitter transformation, we have

$$\delta \Psi \supset \sum_{a=1}^N \int d^d x_1 \cdots d^d x_N \Psi_N(\underline{\mathbf{x}}) \phi(\mathbf{x}_1) \cdots \delta \phi(\mathbf{x}_a) \cdots \phi(\mathbf{x}_N), \quad (5.46)$$

where the transformations of the late-time field profiles are given by (5.28). (We are again assuming that ϕ is a complementary series field, so that it only has a single fall-off, otherwise we should also keep track of $\bar{\phi}$.) We now integrate this expression by parts, so that the generator of the transformation acts on the wavefunction coefficient $\Psi_N(\underline{\mathbf{x}})$. For example, for the dilatation symmetry, we get

$$\begin{aligned} \delta \Psi &\supset \sum_{a=1}^N \int d^d x_1 \cdots d^d x_N \Psi_N(\underline{\mathbf{x}}) \phi(\mathbf{x}_1) \cdots \left(-\Delta_a - x_a^j \partial_{x_a^j} \right) \phi(\mathbf{x}_a) \cdots \phi(\mathbf{x}_N) \\ &= \sum_{a=1}^N \int d^d x_1 \cdots d^d x_N \left((d - \Delta_a) + x_a^j \partial_{x_a^j} \right) \Psi_N(\underline{\mathbf{x}}) \phi(\mathbf{x}_1) \cdots \phi(\mathbf{x}_N), \end{aligned} \quad (5.47)$$

and hence the wavefunction coefficients transform as

$$\delta \Psi_N(\underline{\mathbf{x}}) = \sum_{a=1}^N \left((d - \Delta_a) + x_a^j \partial_{x_a^j} \right) \Psi_N(\underline{\mathbf{x}}). \quad (5.48)$$

If we think of the wavefunction coefficients as being correlation functions in some putative dual, $\Psi_N(\underline{\mathbf{x}}) = \langle O(\mathbf{x}_1) \cdots O(\mathbf{x}_N) \rangle$, then the operators, O_a , transform as fields of weight $\bar{\Delta}_a = d - \Delta_a$. (There is also a flip of sign of the parameter of the transformation, but this is not important.) The same is true for the special conformal transformations, so that O_a behaves like a primary of weight $d - \Delta_a$. Explicitly, the action of de Sitter symmetry on the late-time wavefunction coefficients is captured by the following transformation rules for the dual operators

$$D O = ((d - \Delta) + x^j \partial_{x^j}) O, \quad (5.49)$$

$$K_i O = \left(2(d - \Delta)x^i + 2x^i x^j \frac{\partial}{\partial x^j} - x^2 \frac{\partial}{\partial x_i} \right) O. \quad (5.50)$$

If we assume that the wavefunction Ψ is *invariant* under conformal symmetry, then the wavefunction coefficients must be annihilated by the action of the symmetry generators:

$$\sum_{a=1}^N D_a \langle O_1 \cdots O_N \rangle = 0, \quad (5.51)$$

$$\sum_{a=1}^N b_i \cdot K_a^i \langle O_1 \cdots O_N \rangle = 0, \quad (5.52)$$

where the operators D and K_i are given by (5.49) and (5.50), respectively. These equations are the analogue for the wavefunction coefficients of equations (5.43) and (5.44).

For the most part, we will be interested in solving these equations for the wavefunction because, as we have seen, wavefunction coefficients are somewhat simpler than in-in correlators and contain the same information.

Fourier space: In cosmology, we typically work in Fourier space, so it will be useful to have expressions for the action of the dilatation (5.49) and special conformal (5.50) symmetries in Fourier space.³³ On a scalar operator, they act as [13, 25, 34]

$$DO_{\mathbf{k}} = \left[-(\Delta - d) + k^i \partial_{k^i} \right] O_{\mathbf{k}}, \quad (5.53)$$

$$K_i O_{\mathbf{k}} = - \left[2(\Delta - d) \partial_{k^i} + k_i \partial_{k^j} \partial_{k^j} - 2k^j \partial_{k^j} \partial_{k^i} \right] O_{\mathbf{k}}. \quad (5.54)$$

One further subtlety arises when writing the Ward identities (5.51) and (5.52) in Fourier space. The derivatives with respect to momenta can hit the momentum-conserving delta function which appears in front of a correlator:

$$\langle O_1 \cdots O_N \rangle = (2\pi)^d \delta^{(d)}(\mathbf{k}_1 + \cdots + \mathbf{k}_n) \langle O_1 \cdots O_N \rangle'. \quad (5.55)$$

We can deal with this subtlety by treating the delta function distributionaly and integrating by parts the terms where the derivatives hit the delta function. The SCT operator (5.54) ends up passing through the delta function unchanged, but the dilation operator becomes

$$\sum_{a=1}^N D_a \langle O_1 \cdots O_N \rangle' = \left[d(N-1) - \sum_{a=1}^N \Delta_a + \sum_{a=1}^{N-1} k_a^i \partial_{k_a^i} \right] \langle O_1 \cdots O_N \rangle', \quad (5.56)$$

where we have imposed the constraint that the delta function implements by setting $\mathbf{k}_N = -\sum_{a=1}^{N-1} \mathbf{k}_a$. Concretely, this means that wavefunction coefficients (in Fourier space) satisfy

$$\left[-d + \sum_{a=1}^N D_a \right] \langle O_1 \cdots O_N \rangle'(\underline{\mathbf{k}}) = 0, \quad (5.57)$$

$$\sum_{a=1}^N K_a^i \langle O_1 \cdots O_N \rangle'(\underline{\mathbf{k}}) = 0, \quad (5.58)$$

where D is given by (5.53) and K_i is given by (5.54), where the Fourier-space wavefunction coefficients are understood to be defined with the momentum-conserving delta functions removed.

³³Reference [32] has an explanation of how to derive these transformations in Fourier space, though beware of some sign errors. See also [33] for details.

Exercise 5.6. Derive the Fourier-space action of the dilatation (5.53) and SCT (5.54) operators. Then, verify that their action on the wavefunction with the momentum-conserving delta function removed is given by (5.57) and (5.58).

Warning: This is relatively tedious.

Dilatation symmetry is simply reflected in the overall scaling dimension of the correlator: a general n -point function has scaling dimension $\Delta_t \equiv \sum_a \Delta_a$ in position space. This implies that the momentum-space correlator has dimension $\Delta_t - d \times n$. After stripping off the momentum-conserving delta function, the dimension of the remaining function is $\Delta_t - d(n - 1)$. This fixes the overall momentum scaling of the correlator, allowing us to make an ansatz for $\langle O_1 \cdots O_n \rangle'$ that automatically solves the dilatation Ward identity (5.57). All the juice is in the SCT Ward identity (5.58). We now want to see how solving this Ward identity directly in a couple simple situations can reproduce the de Sitter physics that we previously derived directly from the bulk.

Two-point functions

We first derive the constraints of conformal symmetry on the two-point functions of scalar operators. Following the above argument, it is straightforward to see that an ansatz that solves the dilatation Ward identity (5.57) is that

$$\langle O_1 O_2 \rangle' \propto k_1^\alpha, \quad (5.59)$$

with $\alpha \equiv \Delta_1 + \Delta_2 - d$. Since the two-point function depends only on the magnitude of momenta, the SCT operator takes the simplified form:

$$b_i K^i O_{\mathbf{k}} = \mathbf{b} \cdot \mathbf{k} \left[\frac{\partial^2}{\partial k^2} + \frac{(d+1-2\Delta)}{k} \frac{\partial}{\partial k} \right] O_{\mathbf{k}}. \quad (5.60)$$

Demanding SCT invariance of the two-point function then implies

$$\alpha + d - 2\Delta_1 = 0, \quad (5.61)$$

which forces the scaling dimensions of the two operators to be equal, $\Delta_1 = \Delta_2$. We therefore get

$$\langle O_1 O_2 \rangle' \propto k_1^{2\Delta_1 - d} \delta_{\Delta_1, \Delta_2}. \quad (5.62)$$

We have learned that the two-point function of two scalar vanishes unless their scaling dimensions are equal and that their momentum scaling is fixed in terms of that scaling dimension.

Exercise 5.7. Show that (5.62) is consistent with the explicit result for the power spectrum of a massive particle derived in Exercise 2.2, which consists of one term with scaling weight Δ_+ and one with weight Δ_- .

Three-point functions

As a more nontrivial example—which is still completely fixed by symmetry—we consider the three-point function of scalar fields interacting in exact de Sitter space. The constraints of

conformal invariance on the corresponding momentum space three-point function were treated comprehensively in [25]. An ansatz that solves the dilatation Ward identity (5.57) is

$$\langle O_1 O_2 O_3 \rangle' = k_3^{\Delta_1 + \Delta_2 + \Delta_3 - 2d} \hat{G}(p, q), \quad (5.63)$$

where $p \equiv k_1/k_3$ and $q \equiv k_2/k_3$. Although it looks like k_3 is special here, it is not because of the presence of an arbitrary function, \hat{G} . The SCT Ward identity (5.58) then implies two differential equation for the dimensionless function $\hat{G}(p, q)$, whose solution can be expressed in terms of the Appell F_4 function.³⁴

For our purpose, it will be useful to work out more explicitly the special case of two conformally coupled fields Φ (with $\Delta = 2$) and a generic field χ (with arbitrary Δ), in $d = 3$ dimensions. A dilatation-invariant ansatz for the wavefunction coefficient is

$$\langle O_1 O_2 X_3 \rangle' = k_3^{\Delta-2} \hat{G}(u, w), \quad (5.65)$$

where $u \equiv k_3/(k_1 + k_2)$ and $w \equiv k_3/(k_1 - k_2)$. This is a slightly different ansatz from (5.63), but is convenient for this situation because the variables u, w have definite parity under $1 \leftrightarrow 2$. We can now act with the SCT operator in the form (5.60) and choose $\mathbf{b} \cdot \mathbf{k}_3 = 0$. After using momentum conservation, we then find

$$\left(\frac{\partial^2}{\partial k_1^2} - \frac{\partial^2}{\partial k_2^2} \right) \hat{G}(u, w) = 0 \implies \frac{4u^2 w^2}{k_3^2} \partial_u \partial_w \hat{G}(u, w) = 0. \quad (5.66)$$

We can therefore take $\hat{G}(u, w) = \hat{G}(u)$.³⁵ Next, we consider the SCT Ward identity with $\mathbf{b} \cdot \mathbf{k}_2 = 0$, which leads to

$$\left(\frac{\partial^2}{\partial k_1^2} - \frac{\partial^2}{\partial k_3^2} - \frac{4-2\Delta}{k_3} \frac{\partial}{\partial k_3} \right) \left(k_3^{\Delta-2} \hat{G}(u) \right) = 0. \quad (5.67)$$

Changing the derivatives to ones with respect to u , this implies the equation

$$\left[\Delta_u + \left(\mu^2 + \frac{1}{4} \right) \right] \hat{G}(u) = 0, \quad (5.68)$$

where $\Delta_u \equiv u^2(1-u^2)\partial_u^2 - 2u^3\partial_u$ is the same differential operator as in (4.117) and $\mu^2 + \frac{1}{4} = -(\Delta - 2)(\Delta - 1)$. In terms of the mass parameter of the bulk field χ , we have $\mu^2 + \frac{1}{4} = m^2/H^2 - 2$. Notice that this differential equation is precisely the one obtained for this wavefunction coefficient in Exercise 4.13 from the bulk perspective.

³⁴This special function is not so familiar, but there are relatively nice representations in terms of an integral over products of modified Bessel functions. Using this integral representation, one can derive the Fourier space expression for the correlation function of three scalar operators [25]:

$$\langle O_1 O_2 O_3 \rangle' \propto k_1^{\Delta_1 - \frac{d}{2}} k_2^{\Delta_2 - \frac{d}{2}} k_3^{\Delta_3 - \frac{d}{2}} \int_0^\infty dx x^{\frac{d}{2}-1} K_{\nu_1}(k_1 x) K_{\nu_2}(k_2 x) K_{\nu_3}(k_3 x), \quad (5.64)$$

where K_ν , with $\nu = \Delta - \frac{d}{2}$, is the modified Bessel function of the second kind. See [35?] for more details of the evaluation of integrals of this type for special mass values.

³⁵There is, in principle, another solution that depends only on w , but we can obtain it from this one by sending $k_2 \rightarrow -k_2$.

Equation (5.89) is of hypergeometric type and is solved by

$$\hat{G}_+(u) \propto {}_2F_1\left[\frac{1}{2} + i\mu, \frac{1}{2} - i\mu \mid \frac{u-1}{2u}\right] = P_{i\mu-\frac{1}{2}}^0(u^{-1}), \quad (5.69)$$

where we have written the solution both in terms of the Gauss hypergeometric function and as an associated Legendre function. A linearly-independent solution is given by $\hat{G}_-(u) \propto P_{i\mu-\frac{1}{2}}^0(-u^{-1})$. The solution G can then be written as

$$\begin{aligned} G_+(u) &= \left(\frac{\pi}{2 \cosh(\pi\mu)}\right)^{\frac{1}{2}} k_3^{i\mu-\frac{1}{2}} {}_2F_1\left[\frac{1}{2} + i\mu, \frac{1}{2} - i\mu \mid \frac{u-1}{2u}\right] \\ &= \left(\frac{\pi}{2 \cosh(\pi\mu)}\right)^{\frac{1}{2}} k_3^{i\mu-\frac{1}{2}} P_{i\mu-\frac{1}{2}}^0(u^{-1}), \end{aligned} \quad (5.70)$$

where \hat{G} has been normalized so that its Wronskian is $1/(1-u^2)$.³⁶ This solution is exactly the same as the wavefunction coefficient obtained in Exercise 4.8, and is simply related to the in-in correlator from Exercise 3.4.

The solution (5.70) has a more complicated analytic structure than many of the examples we have encountered so far. In particular, it has branch points at $u = 0, 1$ (it is natural to choose the cut to not lie in the physical region, which is the interval between $u = 0$ and $u = 1$). This branch cut can be thought of as a signature of the production of massive particles with a continuum of possible relative momenta in the bulk spacetime. Note also that for special values of μ , the equation (5.89) is not satisfied exactly in momentum space, due to the presence of anomalies.³⁷

5.3 Singularities

An important feature of cosmology is that energy is not conserved. As we will see, this leads to cosmological correlators possessing characteristic singularities at special points in kinematic space. These singularities will be an important input for the bootstrap procedure.

5.3.1 Flat-Space Examples

It is useful to start with a few concrete examples and then try to draw some general lessons from them. In Section 4.4.4, we computed wavefunction coefficients in flat space. It is instructive to look back at some of the results.

³⁶The Wronskian of the associated Legendre function satisfies

$$(P_\nu^{-\mu}(x), P_\nu^{-\mu}(-x)) = P_\nu^{-\mu}(x)\partial_x P_\nu^{-\mu}(-x) - \partial_x P_\nu^{-\mu}(x)P_\nu^{-\mu}(-x) = \frac{2}{\Gamma[\mu-\nu]\Gamma[\nu+\mu+1]} \frac{1}{1-x^2}, \quad (5.71)$$

which we can use to normalize the solution of interest.

³⁷For example, this happens when the third field also has $\Delta = 2$. In Section 4.4.5, we derived the three-point wavefunction coefficient of three conformally coupled fields:

$$\langle O_1 O_2 O_3 \rangle' \propto \log(K/\bar{\mu}). \quad (5.72)$$

This expression solves the Ward identities “anomalously.” The scale variation of the logarithm does not vanish, but is instead a function that is analytic in the momenta (in this case it is just a constant), indicating that it is a contact term in position space. This correlation function therefore satisfies the conformal Ward identities at separated points, which is all that is required. (The failure of the conformal Ward identities at coincident points is a reflection of an anomaly.) Note that we can freely add an arbitrary constant to this correlation function by shifting the (arbitrary) scale $\bar{\mu}$.

The three-point wavefunction coefficient is

$$\langle O_1 O_2 O_3 \rangle \equiv \begin{array}{c} \text{---} \\ \backslash \quad / \\ \bullet \end{array} = ig \int_{-\infty}^0 dt e^{i(k_1+k_2+k_3)t} = \frac{g}{(k_1 + k_2 + k_3)}. \quad (5.73)$$

We see that this has a singularity when the total energy of the process vanishes, $K \equiv k_1 + k_2 + k_3 \rightarrow 0$. For a four-point contact interaction, we would get a similar result with a singularity at $E \equiv k_1 + k_2 + k_3 + k_4 \rightarrow 0$. We call these *total energy singularities*. These singularities are the avatar of the energy-conserving δ -functions for amplitudes, which arise because we integrate from $t = -\infty$ to $+\infty$:

$$\int_{-\infty}^{\infty} dt e^{i(E_1 + \dots + E_N)t} = \delta(E_1 + \dots + E_N). \quad (5.74)$$

The flat-space wavefunction, instead, involves integration from $t = -\infty$ to 0, so instead of a delta function, we get a singularity at $E = 0$. Remarkably, we will find that the residues of these singularities are the corresponding scattering amplitudes. For the above contact examples, this is rather trivial since the residue of the total energy singularity is the coupling constant g which is the amplitude for a polynomial contact interaction. However, the fact that amplitudes live at the loci of energy singularities will be true more generally. It is important to point out that these singularities cannot be accessed for physical kinematics, since for correlators all energies have to positive. (For amplitudes, in contrast, energies can be positive or negative corresponding to incoming or outgoing particles.) Nevertheless, the fact that the analytic continuation of correlation functions must have these singularities will be an important constraint. Using this as input for the bootstrap procedure will allow us to reconstruct the full correlator and extract answers in the physical domain.

A more interesting example is the four-point wavefunction coefficient arising from an exchange diagram:

$$\langle O_1 O_2 O_3 O_4 \rangle \equiv \begin{array}{c} \text{---} \\ \backslash \quad / \\ \bullet \quad \bullet \\ \text{---} \end{array} = -g^2 \int_{-\infty}^0 dt' dt'' e^{ik_{12}t'} G(k_I; t', t'') e^{ik_{34}t''} = \frac{g^2}{E E_L E_R}, \quad (5.75)$$

where $E_L \equiv k_{12} + k_I$ and $E_R \equiv k_{34} + k_I$. In addition to the total energy singularity at $E = 0$, we now also have *partial energy singularities* at $E_L = 0$ and $E_R = 0$. We first confirm that the residue of the total energy singularity is indeed the corresponding exchange amplitude in the s -channel. Taking the limit $E \rightarrow 0$, we get

$$\lim_{E \rightarrow 0} \frac{g^2}{E E_L E_R} = \frac{1}{E} \frac{g^2}{(k_{12} + k_I)(-k_{12} + k_I)} = -\frac{1}{E} \frac{\cancel{g^2}}{\cancel{s}} = \frac{\cancel{A}_4}{E},$$

where $s \equiv k_{12}^2 - k_I^2$ is the Mandelstam invariant. This time, it is rather more nontrivial to find that the residue of the $E = 0$ pole is the scattering amplitude corresponding to the process. Moreover, in the limit $E_L \rightarrow 0$, the correlator becomes

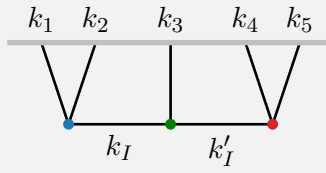
$$\lim_{E_L \rightarrow 0} \frac{g^2}{E E_L E_R} = \frac{\cancel{g}}{E_L} \frac{g}{(\cancel{k}_{34} + k_I)(\cancel{k}_{34} - k_I)} = \frac{\cancel{A}_3 \times \tilde{\psi}_3}{E_L}. \quad (5.76)$$

We see that the residue of this partial energy singularity is the product of a three-point scattering amplitude $A_3 = g$ and a new object which we call the *shifted wavefunction coefficient*

$$\tilde{\psi}_3 \equiv \frac{1}{2k_I} [\psi_3(k_{34}, -k_I) - \psi_3(k_{34}, k_I)], \quad (5.77)$$

where ψ_3 is the three-point wavefunction coefficient given in (5.73). In fact, these simple flat-space correlators are completely fixed by their singularities. In particular, the result (5.75) is the unique function that has the correct factorization singularities. This is rather interesting, because it implies that the answer can be assembled from simpler building blocks (amplitudes and lower-point shifted wavefunctions).

Exercise 5.8. Derive the wavefunction coefficient for the following five-point diagram:



You should find:

$$\langle O_1 O_2 O_3 O_4 O_5 \rangle' = \frac{1}{E} \frac{1}{E_L E_M E_R} \left[\frac{1}{k_{123} + k'_I} + \frac{1}{k_{345} + k_I} \right], \quad (5.78)$$

where $E_L \equiv k_{12} + k_I$, $E_M \equiv k_3 + k_I + k'_I$ and $E_R \equiv k_{45} + k'_I$ are the energies running into the three different vertices. Discuss the different singularities of the solution.

5.3.2 Generalization to de Sitter

The singularities of the wavefunction in de Sitter space are actually somewhat similar to the ones in flat space. In order to see this, it is useful to take a step back and examine the origin of the singularities that we noticed in the flat-space wavefunction.

[DB: include]

5.3.3 Singularities as Input

The patterns we have seen in these examples are a general feature:

- Correlators have singularities at points of would-be energy conservation.
- The residues of these singularities are scattering amplitudes and shifted correlators.

We will use these singularities as an input for the bootstrap.

5.4 Example: Massive Exchange

As a concrete example of the bootstrap approach, we now revisit the challenge posed in Section 4.5: We would like to derive the four-point function of conformally coupled scalars, mediated by the tree-level exchange of a generic massive scalar. We will focus on the s -channel contribution, from which the t - and u -channels can be obtained as simple permutations. The description below follows closely the treatment in [28], which should be consulted for further details.

5.4.1 Ward Identities

A priori, the four-point function $F \equiv \langle O_1 O_2 O_3 O_4 \rangle'$ depends on four three-momenta, $\mathbf{k}_{n=1,2,3,4}$, and hence 12 scalar variables. Translational and rotational invariance reduce this to six independent variables before imposing conformal symmetry. It is convenient to take these variables to be $k_{n=1,2,3,4} \equiv |\mathbf{k}_n|$, $k_I \equiv |\mathbf{k}_1 + \mathbf{k}_2|$ and $k'_I \equiv |\mathbf{k}_2 + \mathbf{k}_3|$. Constraints from dilatation symmetry and SCTs reduce these six independent variables to just two, which in position space are the conformally-invariant cross ratios. In momentum space, we will use the dimensionless variables

$$u \equiv \frac{k_I}{k_1 + k_2}, \quad v \equiv \frac{k_I}{k_3 + k_4}. \quad (5.79)$$

In Section 5.2.5, we explained that dilatation invariance forces an n -point function in d dimensional momentum space to have scaling dimension $\Delta_t - d(n - 1)$. For the four-point function of conformally coupled scalars ($\Delta = 2$), this implies that F has dimension $4 \times 2 - 3 \times (4 - 1) = -1$. This motivates us to define

$$\langle O_1 O_2 O_3 O_4 \rangle' = \frac{1}{k_I} \hat{F}(u, v). \quad (5.80)$$

As you will show in the following exercise, this ansatz automatically solves the dilatation Ward identity.

Exercise 5.9. Show that (5.80) solves the dilatation Ward identity (5.57).

At this point, the dimensionless function $\hat{F}(u, v)$ is still completely undetermined. Its functional form will be constrained by the special conformal Ward identity and the allowed singularities of a given perturbative process. After quite some work (see Appendix A of [28]), the conformal Ward identity (5.58) can be written as

$$(\nabla_u - \nabla_v) \hat{F} = 0, \quad (5.81)$$

where $\Delta_u \equiv u^2(1 - u^2)\partial_u^2 - 2u^3\partial_u$ is our old friend the hypergeometric differential operator.

Exercise 5.10. Derive the result (5.81).

Warning: This is algebraically quite involved and tedious.

Equation (5.81) is a purely kinematic constraint that must be satisfied by *all* de Sitter four-point functions. We will classify the physical distinct solutions to (5.81) by the expected singularities of different processes.

5.4.2 Contact Solutions

The simplest solutions to equation (5.81) correspond to the four-point functions arising from contact interactions:

$$\hat{F}_c = \begin{array}{c} \text{---} \\ \backslash \quad \backslash \quad \backslash \end{array}$$

These solutions are characterized by the simplest possible singularity structure with only total energy singularities. Consider first the case of a bulk Φ^4 interaction. As we have seen in Exercise 4.9, the four-point wavefunction coefficient coming from a Φ^4 interaction in both flat space and de Sitter space is proportional to $1/E$, where $E \equiv k_1 + k_2 + k_3 + k_4$ is the total energy. Up to an overall constant factor, we therefore have

$$\hat{F}_{c,0} = \frac{k_I}{E} = \frac{uv}{u+v}. \quad (5.82)$$

It is easy to confirm that this is indeed a solution of (5.81).

Solutions corresponding to higher-derivative contact interactions in the bulk are created by the repeated application of the operator Δ_u :³⁸

$$\hat{F}_{c,n} \equiv \Delta_u^n \hat{F}_{c,0}, \quad (5.83)$$

where the functional form of $\hat{f}_n(u, v)$ is fixed by conformal invariance. It is easy to see that these are indeed solutions to (5.81). For example,

$$\begin{aligned} (\Delta_u - \Delta_v) \hat{F}_{c,1} &= (\Delta_u - \Delta_v) \Delta_u \hat{F}_{c,0} \\ &= (\Delta_u^2 - \Delta_v \Delta_u) \hat{F}_{c,0} \\ &= (\Delta_u^2 - \Delta_u \Delta_v) \hat{F}_{c,0} \\ &= \Delta_u (\Delta_u - \Delta_v) \hat{F}_{c,0} = 0, \end{aligned} \quad (5.84)$$

where we used that $\Delta_v \Delta_u \hat{F}_{c,0} = \Delta_u \Delta_v \hat{F}_{c,0}$ because the seed solution $\hat{F}_{c,0}$ is symmetric in u and v .

Exercise 5.11. By acting with Δ_u on the seed solution (5.82), show that

$$\hat{F}_{c,1} = -2 \left(\frac{uv}{u+v} \right)^3 \frac{1+uv}{uv}, \quad (5.85)$$

$$\hat{F}_{c,2} = -4 \left(\frac{uv}{u+v} \right)^5 \frac{u^2 + v^2 + uv(3u^2 + 3v^2 - 4) - 6(uv)^2 - 6(uv)^3}{(uv)^3}. \quad (5.86)$$

³⁸This only captures the contact solutions arising from integrating out massive scalars. Integrating out particles with spin can produce contact solutions with dependence on additional kinematic invariants.

We see that even these contact solutions are relatively intricate functions of the momenta, but are fully controlled by symmetries and singularities without any reference to a Lagrangian.

The sum of contact solutions can be written as

$$\hat{F}_c = \sum_{n=0}^{\infty} \left(\frac{k_I}{E} \right)^{2n+1} \hat{f}_n(u, v) + \text{perms}, \quad (5.87)$$

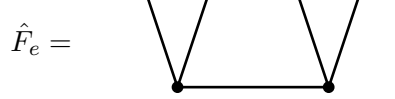
where the expansion in powers of E^{-1} corresponds to the derivative expansion of the bulk EFT. The limit $E \rightarrow 0$ of the individual contact solutions is

$$\lim_{E \rightarrow 0} \hat{F}_{c,n} = (2n)! \frac{s^{2n}}{E^{2n+1}}, \quad (5.88)$$

where s is the Mandelstam invariant. This confirms the expected relation between the singularity of the correlator at $E = 0$ and the scattering amplitude for contact interactions.

5.4.3 Exchange Solutions

Next, we look for solutions of the Ward identity corresponding to the tree-level exchange of a scalar particle:



We will proceed by inspired guesswork. In Section 5.2.5, we have seen that the three-point function of two conformally coupled scalars and a generic scalar, $\langle O_1 O_2 X_3 \rangle' = k_3^{\Delta-2} \hat{G}(u)$, with $u \equiv k_3/k_{12}$, satisfies

$$\left[\Delta_u + \left(\mu^2 + \frac{1}{4} \right) \right] \hat{G} = 0, \quad (5.89)$$

where Δ_u is the same operator as that appearing in the four-point Ward identity (5.81). It is therefore easy to see that a product of two three-point functions, $\hat{F}(u, v) = \hat{G}(u)\hat{H}(v)$, is also a solution of (5.81):

$$\begin{aligned} (\Delta_u - \Delta_v) \hat{G}(u) \hat{H}(v) &= (\Delta_u \hat{G}) \hat{H} - \hat{G}(\Delta_v \hat{H}) \\ &= - \left(\mu^2 + \frac{1}{4} \right) \hat{G} \hat{H} - \hat{G} \left[- \left(\mu^2 + \frac{1}{4} \right) \hat{H} \right] \\ &= - \left(\mu^2 + \frac{1}{4} \right) (\hat{G} \hat{H} - \hat{G} \hat{H}) \\ &= 0. \end{aligned} \quad (5.90)$$

This isn't surprising since a four-point function factorizes into a product of three-point functions in the OPE limit.

This motivates us to find a more general solution of (5.81), not of the factorized form, but obeying

$$\begin{aligned} \left[\Delta_u + \left(\mu^2 + \frac{1}{4} \right) \right] \hat{F}_e &= \hat{C}, \\ \left[\Delta_v + \left(\mu^2 + \frac{1}{4} \right) \right] \hat{F}_e &= \hat{C}. \end{aligned} \quad (5.91)$$

Note that these are two *ordinary* differential equations in u and v separately. The solution corresponding to a product of three-point functions are the homogeneous solutions to these equations, which explains the introduction of the μ -dependent terms, to dictate the mass of the exchanged particle.

Exercise 5.12. Show that for consistency the functions $\hat{C}(u, v)$ appearing on the right-hand side of (5.91) must satisfy $(\nabla_u - \nabla_v)\hat{C} = 0$ and are thus themselves conformally invariant.

What is the physical interpretation of the inhomogeneous source function $\hat{C}(u, v)$? Consider the limit of large μ , for which we expect the interaction to effectively reduce to a contact interaction, $\hat{F}_e \rightarrow \hat{F}_c = \mu^{-2}\hat{C}$. The source on the right-hand side of (5.91) is therefore just one of our previously found contact solutions. Given our classification of these contact solutions, we can therefore also classify the corresponding exchange solutions. In Lagrangian language, this classification corresponds to choosing the bulk interactions of the theory.

Another way of understanding (5.91) is by considering the example of tree-exchange amplitudes. Multiplying the s -channel amplitude by the inverse propagator, we get

$$(s + m^2)A_e = A_c(s, t), \quad (5.92)$$

where the right-hand side is a rational function of the Mandelstam variables, i.e. a sum of contact amplitudes. The structure of (5.92) is similar to (5.91) except that it is an algebraic equation rather than a differential equation.

Exercise 5.13. In Section 4.4.5, we derived the four-point wavefunction coefficient of conformally coupled scalars:

$$\langle O_1 O_2 O_3 O_4 \rangle_c = \frac{g}{H^4 \eta_*^4} \frac{1}{K}, \quad (5.93)$$

$$\begin{aligned} \langle O_1 O_2 O_3 O_4 \rangle_e = & \frac{g^2}{2H^6 \eta_*^4} \left[\text{Li}_2 \left(\frac{k_{12} - k_I}{E} \right) + \text{Li}_2 \left(\frac{k_{34} - k_I}{E} \right) \right. \\ & \left. + \log \left(\frac{k_{12} + k_I}{E} \right) \log \left(\frac{k_{34} + k_I}{E} \right) - \frac{\pi^2}{6} \right], \end{aligned} \quad (5.94)$$

where the subscripts denote the contact (c) and exchange (e) contributions. Show that these solutions solve the differential equations in (5.91). Verify also that the solutions have the correct singularities.

A formal solution of (5.81) can be obtained by inverting the differential operator:

$$\begin{aligned} \hat{F} = \frac{\hat{C}_0}{\Delta_u + M^2} &= \sum_n \frac{1}{n!} \left(\frac{\Delta_u}{M^2} \right)^n \frac{\hat{C}_0}{M^2} \\ &= \hat{F}_{c,0} + \frac{\hat{F}_{c,1}}{M^2} + \frac{1}{2} \frac{\hat{F}_{c,2}}{M^4} + \dots, \end{aligned} \quad (5.95)$$

where $M^2 \equiv \mu^2 + \frac{1}{4}$. We see that the solution has been written as an infinite expansion of contact solutions, which corresponds to the *EFT expansion* of the correlator as expected from

the integration out of a massive particle. However, as we will see, this EFT expansion misses nonperturbative terms associated with particle production in the expanding spacetime.

In the rest of this section, we will find an explicit solution to (5.91) corresponding to the exchange of a generic massive particle, thereby addressing the challenge posed in Section 4.5. For concreteness, we consider the simplest contact interaction, $\hat{F}_{c,0}$, as a source. The solutions for other sources, $\hat{F}_{c,n}$, can then simply be found by acting with Δ_u . The equation we would like to solve then is

$$\left[u^2(1-u^2)\partial_u^2 - 2u^3\partial_u + \left(\mu^2 + \frac{1}{4}\right) \right] \hat{F} = \frac{uv}{u+v}, \quad (5.96)$$

where we have rescaled \hat{F} to set the normalization of the source function to unity. Note that this is the same as (4.117) if we recall that $\mu^2 + 1/4 = m^2/H^2 - 2$.

The homogeneous solutions of (5.96), which we will denote by \hat{F}_\pm , can be expressed as hypergeometric functions (or associated Legendre polynomials). The Wronksian of these solutions, $W \equiv \hat{F}_+ \partial_u \hat{F}_- - \hat{F}_- \partial_u \hat{F}_+$, satisfies $\partial_u W = 2u/(1-u^2)W$, so it is natural to normalize the solutions, so that $W = 1/(1-u^2)$. The correctly normalized homogeneous solutions are then

$$\hat{F}_\pm(u) = \left(\frac{iu}{2\mu}\right)^{\frac{1}{2}\pm i\mu} {}_2F_1\left[\begin{array}{c} \frac{1}{4} \pm \frac{i\mu}{2}, \frac{3}{4} \pm \frac{i\mu}{2} \\ 1 \pm i\mu \end{array} \middle| u^2\right], \quad (5.97)$$

and equivalent solutions for the differential equation in terms of v .

Singularities

To find the full solution for the inhomogeneous equation, we must impose boundary conditions for specific values of u and v . We will do this by looking at the singular points of the differential equation. First, we note that the differential operator on the left-hand side of (5.96) becomes singular at $u \rightarrow 0$ and $u \rightarrow \pm 1$. Let us discuss the physical meaning of these singularities:

- *Factorization limit:* In the limit $u \rightarrow -1$, the equation has a logarithmic singularity

$$\lim_{u \rightarrow -1} \hat{F} \propto A_3 \log(1+u). \quad (5.98)$$

This is precisely the partial energy singularity at $E_L = 0$ that we discussed in Section 5.3. Correctly normalizing this singularity (together with the corresponding singularity at $E_R = 0$ or $v \rightarrow -1$) will be one of the boundary conditions for our differential equation.

- *Folded limit:* Similarly, in the limit $u \rightarrow +1$, we have

$$\lim_{u \rightarrow +1} \hat{F} \propto \log(1-u). \quad (5.99)$$

This is a singularity in the folded limit, $k_I \rightarrow k_1 + k_2$, where two of the momenta become collinear. As we discussed in Section 5.3, this singularity should be absent for Bunch–Davies initial conditions. We will take this as a second boundary conditions for our differential equation.

- *Collapsed limit:* Imposing the boundary conditions at $u = \pm 1$ will completely fix the solution and the behavior at the remaining singularities becomes an output. For example, in the limit $u \rightarrow 0$, the solution becomes

$$\lim_{u \rightarrow 0} \hat{F} \propto u^{\frac{1}{2} + i\mu}. \quad (5.100)$$

This is the so-called collapsed limit of the correlator where the internal momentum becomes soft, $k_I \rightarrow 0$. As we will see, the boundary conditions of the problem will force us add a fixed amount of the homogeneous solutions (5.97) which has this oscillatory behavior in the collapsed limit. Physically, the non-analytic scaling for $u \rightarrow 0$ is the signature of particle production in the bulk spacetime. We will have more to say about this below.

- *Flat-space limit:* Finally, the source term in (5.96) has a singularity for $u = -v$. Of course, this is simply the total energy singularity of the contact solution. We therefore expect the full exchange solution also to have this singularity:

$$\lim_{u \rightarrow -v} \hat{F} = A_4 (u + v) \log(u + v). \quad (5.101)$$

The coefficient of this singularity must be the correct four-point exchange amplitude (in the high-energy limit), $A_4 = 1/s$. Reproducing this singularity will be an important consistency check for our solution.

Harmonic oscillator limit

Before discussing the general solution of (5.96), it is instructive to consider a simple limit where it reduces to a forced harmonic oscillator. Consider therefore the limit $v \rightarrow 0$, where the source term is small. Writing $u = \xi v$ and $\tilde{F} = v \tilde{F}$, the differential equation (5.96) then takes the form

$$\left[\xi^2 \partial_\xi^2 + \left(\mu^2 + \frac{1}{4} \right) \right] \tilde{F} = \frac{\xi}{1 + \xi}. \quad (5.102)$$

Defining $t \equiv \ln \xi$ and $f \equiv \tilde{F}/\sqrt{\xi}$, this becomes

$$\left[\frac{d^2}{dt^2} + \mu^2 \right] f = \frac{1}{2 \cosh(\frac{1}{2}t)}, \quad (5.103)$$

which is the equation of a forced harmonic oscillator. The homogeneous solutions of this equation are those of the simple harmonic oscillator:

$$f_\pm = e^{\pm i\mu t} = \xi^{\pm i\mu}. \quad (5.104)$$

We would now like to construct a particular solution of the inhomogeneous equation. Our strategy will be to find two series solutions around $\xi = 0$ and $\xi = \infty$, and then match the two solutions at $\xi = 1$ (where both solutions are convergent). The matching will force us to add a fixed amount of the homogeneous solution.

Around $\xi = 0$, the inhomogeneous equation has the following series solution

$$f_<(\xi) = \sqrt{\xi} \sum_{n=0}^{\infty} (-1)^n \frac{\xi^n}{(n + \frac{1}{2})^2 + \mu^2}, \quad (5.105)$$

which is convergent for $\xi \leq 1$ and divergent for $\xi > 1$. Modulo the overall factor of $\sqrt{\xi}$, this solution is analytic around $\xi = 0$. We would like to extend the solution into the regime $\xi > 1$. In this simple case, the solution can be written as a hypergeometric function and we could rely on the known analytic structure of the hypergeometric functions to find the solution for general ξ . However, as a warmup for the general case it will be useful to proceed by finding a series solution to the differential equation ourselves.

Around $\xi = \infty$, the solution can be written as a power series in ξ^{-1} :

$$f_>(\xi) = \frac{1}{\sqrt{\xi}} \sum_{n=0}^{\infty} (-1)^n \frac{\xi^{-n}}{(n + \frac{1}{2})^2 + \mu^2}, \quad (5.106)$$

which is convergent for $\xi \geq 1$ and divergent for $\xi < 1$. Modulo the overall factor of $1/\sqrt{\xi}$, this solution is analytic around $\xi = \infty$. Importantly, the two solutions $f_<(\xi)$ and $f_>(\xi)$ are both convergent at $\xi = 1$. We therefore find the full solution by matching the solutions at $\xi = 1$. Consider first the difference $f_<(\xi) - f_>(\xi)$, which must be a solution of the homogeneous equation:

$$f_<(\xi) - f_>(\xi) = \sum_{\pm} A_{\pm} \xi^{\pm i\mu}, \quad (5.107)$$

where continuity at $\xi = 1$ requires that $A_+ = -A_- \equiv A$ and

$$2i\mu A = \sum_n^{\infty} (-1)^n \frac{(2n+1)}{(n + \frac{1}{2})^2 + \mu^2} = \frac{\pi}{\cosh \pi\mu}. \quad (5.108)$$

We have therefore obtained an explicit form for the solution of the differential equation which is analytic around the origin:

$$\tilde{F}_<(\xi) = \begin{cases} \sum_{n=0}^{\infty} (-1)^n \frac{\xi^{n+1}}{(n + \frac{1}{2})^2 + \mu^2} & \xi \leq 1, \\ \sum_{n=0}^{\infty} (-1)^n \frac{\xi^{-n}}{(n + \frac{1}{2})^2 + \mu^2} + \frac{\pi}{\cosh \pi\mu} \frac{\xi^{\frac{1}{2}-i\mu} - \xi^{\frac{1}{2}+i\mu}}{2i\mu} & \xi \geq 1. \end{cases} \quad (5.109)$$

We see that it is impossible for the solution which is analytic around $\xi = 0$ to be analytic around $\xi = \infty$. This important feature will persist in the general solution.

General solution

The general solution can be derived in a similar way. To avoid losing the forest for the trees, we will delegate some of the algebraic details to the exercises. The solutions to these exercises can be found in Appendix B.

Around $u = 0$, the inhomogeneous solution is

$$\hat{F}_<(u, v) \sum_{m,n=0}^{\infty} c_{mn}(\mu) u^{2m+1} (u/v)^n, \quad (5.110)$$

where the series coefficients are [28]

$$c_{mn}(\mu) = \frac{(-1)^n(n+1)(n+2)\cdots(n+2m)}{[(n+\frac{1}{2})^2 + \mu^2][(n+\frac{5}{2})^2 + \mu^2]\cdots[(n+\frac{1}{2}+2m)^2 + \mu^2]}. \quad (5.111)$$

Note that (5.110) is the unique particular solution that is regular at the origin, since both homogeneous solutions are non-analytic at $u = 0$. In contrast, regularity around $u = \infty$ does not uniquely fix $\hat{F}_>(u, v)$. Instead, we will demand that the full particular solution is symmetric under the exchange $u \leftrightarrow v$. For $u > v$, the solution therefore is $\hat{F}_>(u, v) = \hat{F}_<(v, u)$, or

$$\hat{F}_>(u, v) = \sum_{m,n=0}^{\infty} c_{mn}(\mu) v^{2m+1} (v/u)^n, \quad (5.112)$$

where $c_{mn}(\mu)$ are same coefficients as in (5.111). It is straightforward to check that (5.112) solves (5.96).

Exercise 5.14. By matching the two solutions (5.110) and (5.112) at $u = v$, show the particular solution that is regular around $u = 0$ is

$$\hat{F}_<(u, v) = \begin{cases} \sum_{m,n=0}^{\infty} c_{mn} u^{2m+1} (u/v)^n & u \leq v, \\ \sum_{m,n=0}^{\infty} c_{mn} v^{2m+1} (v/u)^n + \frac{\pi}{\cosh \pi \mu} \hat{F}_h(u, v) & u \geq v, \end{cases} \quad (5.113)$$

where $\hat{F}_h(u, v) \equiv \hat{F}_+(v) \hat{F}_-(u) - \hat{F}_-(v) \hat{F}_+(u)$.

We still have the freedom to add homogeneous solutions. In fact, we *must* add them to satisfy the boundary conditions [DB: fix]

$$\lim_{u \rightarrow +1} \hat{F} = \text{regular}, \quad (5.114)$$

$$\lim_{u,v \rightarrow -1} \hat{F} = \frac{1}{2} \log(1+u) \log(1+v). \quad (5.115)$$

It is easy to check that the homogeneous solution (5.97) has the following singular behavior in the limit $u \rightarrow 1$:

$$\lim_{u \rightarrow 1} \hat{F}_{\pm}(u) = \alpha_{\pm} \log(1-u), \quad \text{where} \quad \alpha_{\pm} \equiv -\left(\frac{i}{2\mu}\right)^{\frac{1}{2} \pm i\mu} \frac{\Gamma(1 \pm i\mu)}{\Gamma(\frac{1}{4} \pm \frac{i\mu}{2}) \Gamma(\frac{3}{4} \pm \frac{i\mu}{2})}. \quad (5.116)$$

By adding an appropriate amount of the homogeneous solution we can cancel off any potential singularity in this. Finally, the solution in (5.113) isn't symmetric in $u \leftrightarrow v$, as required by consistency of the bulk evolution (and the symmetry of the conformally-invariant contact terms). In particular, the nonperturbative correction is absent as $u \rightarrow 0$, and as a result the solution is analytic in this limit. In the following exercise you will fix these deficiencies. The final result then is

$$\hat{F}(u, v) = \begin{cases} \sum_{m,n=0}^{\infty} c_{mn} u^{2m+1} (u/v)^n + \frac{\pi}{2 \cosh \pi \mu} \hat{g}(u, v) & u \leq v, \\ \sum_{m,n=0}^{\infty} c_{mn} v^{2m+1} (v/u)^n + \frac{\pi}{2 \cosh \pi \mu} \hat{g}(v, u) & u \geq v, \end{cases} \quad (5.117)$$

where we have defined [DB: fix]

$$\begin{aligned} \hat{g}(u, v) \equiv & \hat{F}_h(u, v) - \frac{\alpha_-}{\alpha_+} (\beta_0 + 1) \hat{F}_+(u) \hat{F}_+(v) - \frac{\alpha_+}{\alpha_-} (\beta_0 - 1) \hat{F}_-(u) \hat{F}_-(v) \\ & + \beta_0 [\hat{F}_-(u) \hat{F}_+(v) + \hat{F}_-(v) \hat{F}_+(u)], \end{aligned} \quad (5.118)$$

with $\beta_0 = (i \sinh \pi \mu)^{-1}$ and the parameters α_{\pm} were defined in (5.116).

It is interesting that the only solutions that are symmetric and free of spurious singularities are necessarily non-analytic around $u \rightarrow 0$ and $v \rightarrow 0$. This is how particle production in the time-dependent bulk spacetime is encoded in the boundary correlators.

Exercise 5.15. Derive the result (5.117).

Analytic structure

The solution (5.117) has an interesting analytic structure, illustrated in Fig. 11. The function is analytic in the physical domain, $0 < u < 1$, but has a branch cut for $-1 < u \leq 0$. The existence of this branch cut is to be contrasted with the case of scattering amplitude which at tree level can only have poles. As we alluded to above, the discontinuity at $E = 0$ (or $u \rightarrow -v$) contains the flat-space scattering amplitude. In the following, we will show this explicitly.

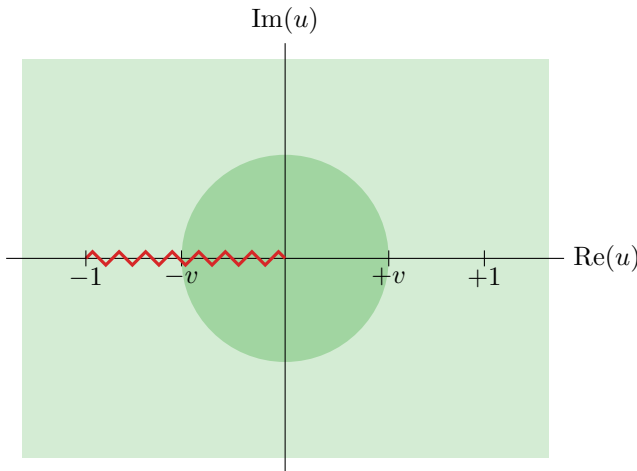


Figure 11: Analytic structure of the result (5.117). Note that the physical regime corresponds to $0 < u < 1$, and the branch cut for negative u is a signal of particle production.

To study the $E \rightarrow 0$ limit, we go back to the differential equation (5.96), which, in the limit $u \rightarrow -v$, becomes

$$\lim_{u \rightarrow -v} \frac{\partial^2 \hat{F}}{\partial u^2} = -\frac{1}{1-v^2} \frac{1}{u+v}. \quad (5.119)$$

This integrates to

$$\lim_{u \rightarrow -v} \hat{F} = -\frac{1}{k_I(1-v^2)} (u+v) \log(u+v) = -\frac{1}{s} E \log E, \quad (5.120)$$

where $s = k_{12}^2 - k_I^2$ is the Mandelstam variable. We see that the coefficient of the $E = 0$ singularity is indeed given by the high-energy limit of the flat-space amplitude, $A_4 = 1/s$.

5.4.4 Particle Production

In the collapsed limit $u \rightarrow 0$, the particle production piece dominates and the function (5.117) becomes

$$\lim_{u,v \rightarrow 0} \hat{F}(u,v) = g^2 \left(\frac{uv}{4}\right)^{\frac{1}{2}+i\mu} (1+i \sinh \pi \mu) \frac{\Gamma(\frac{1}{2}+i\mu)^2 \Gamma(-i\mu)^2}{2\pi} + \text{c.c.} \quad (5.121)$$

We see that the signal oscillates with a frequency given by the mass of the new particles. This is the analog of resonances in collider physics (see Fig. 12). [DB: more]

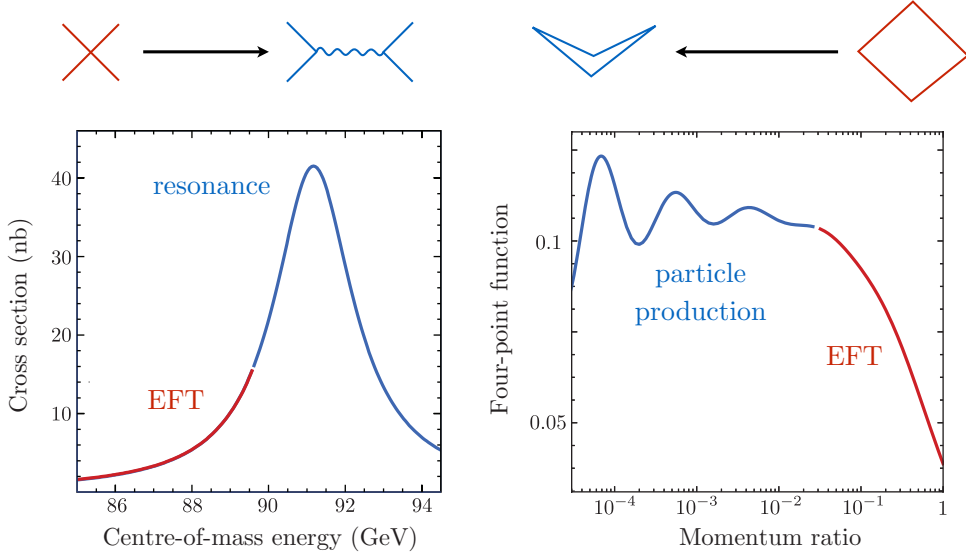


Figure 12: Oscillations in the soft limit of cosmological correlators (*right*) are the analog of resonances in scattering experiments (*left*).

5.5 Unitarity

5.5.1 Optical Theorem

Describe Goodhew, Jazayeri, Gordon Lee and Pajer [36].

5.5.2 Cutting Rules

5.6 Example: Boostbreaking Correlators

5.7 Summary of Recent Progress

6 Conclusions and Outlook

Quantum field theory in cosmological spacetimes is still an active area of research. ...

Beyond Feynman xxx ... xxx xxx xxx xxx xxx
xxx xxx xxx xxx ... xxx ... xxx xxx xxx xxx xxx xxx
xxx xxx xxx ... xxx ... xxx xxx xxx xxx xxx xxx
xxx xxx ... xxx xxx xxx xxx xxx xxx xxx xxx xxx ... xxx xxx xxx xxx xxx xxx xxx
xxx ... xxx xxx xxx xxx xxx xxx xxx xxx ... xxx xxx xxx xxx xxx xxx xxx
... xxx xxx xxx xxx xxx xxx xxx xxx ... xxx xxx xxx xxx xxx xxx xxx
... xxx xxx xxx xxx xxx xxx xxx xxx ... xxx xxx xxx xxx xxx xxx
... xxx xxx xxx xxx xxx xxx xxx ... xxx xxx xxx xxx xxx xxx
... xxx xxx xxx xxx xxx xxx ... xxx xxx xxx xxx xxx
... xxx xxx xxx xxx xxx ...

Beyond Perturbation Theory xxx ... xxx xxx xxx
xxx xxx xxx xxx xxx xxx ... xxx xxx xxx xxx xxx xxx xxx xxx xxx ... xxx xxx xxx xxx
xxx xxx xxx xxx xxx ... xxx xxx xxx xxx xxx xxx xxx xxx xxx ... xxx xxx xxx xxx
xxx xxx xxx xxx ... xxx xxx xxx xxx xxx xxx xxx xxx ... xxx xxx xxx xxx xxx
xxx xxx ... xxx xxx xxx xxx xxx xxx ... xxx xxx xxx xxx xxx xxx ... xxx xxx
xxx ... xxx xxx xxx xxx xxx xxx ... xxx xxx xxx xxx xxx xxx ... xxx xxx
... xxx xxx xxx xxx xxx ... xxx xxx xxx xxx xxx ... xxx xxx xxx xxx xxx
xxx xxx ... xxx xxx xxx xxx ... xxx xxx xxx xxx ... xxx xxx
xxx ... xxx xxx xxx ...

Beyond Spacetime xxx xxx xxx xxx xxx xxx xxx xxx xxx ... xxx xxx xxx xxx xxx
xxx xxx xxx ... xxx xxx xxx xxx xxx xxx xxx xxx xxx ... xxx xxx xxx xxx xxx xxx
xxx xxx ... xxx xxx xxx xxx xxx xxx xxx xxx ... xxx xxx xxx xxx xxx xxx xxx
xxx ... xxx xxx xxx xxx xxx xxx xxx ... xxx xxx xxx xxx xxx xxx xxx
xxx ... xxx xxx xxx xxx xxx xxx xxx ... xxx xxx xxx xxx xxx xxx xxx
... xxx xxx xxx xxx xxx xxx ... xxx xxx xxx xxx xxx xxx xxx xxx ...
xxx xxx xxx ... xxx xxx xxx xxx xxx ... xxx xxx xxx xxx xxx xxx ...
xxx ... xxx xxx xxx xxx ... xxx xxx xxx xxx ... xxx xxx xxx
xxx ... xxx xxx ...

References

- [1] C. Duaso Pueyo, A Bootstrap Approach to Cosmology. PhD thesis, University of Amsterdam, 2022.
- [2] X. Chen, “Primordial Non-Gaussianities from Inflation Models,” *Adv. Astron.* **2010** (2010) 638979, [arXiv:1002.1416 \[astro-ph.CO\]](#).
- [3] Y. Wang, “Inflation, Cosmic Perturbations and Non-Gaussianities,” *Commun. Theor. Phys.* **62** (2014) 109–166, [arXiv:1303.1523 \[hep-th\]](#).
- [4] P. Benincasa, “Amplitudes meet Cosmology: A (Scalar) Primer,” [arXiv:2203.15330 \[hep-th\]](#).
- [5] D. Baumann, D. Green, A. Joyce, E. Pajer, G. L. Pimentel, C. Sleight, and M. Taronna, “Snowmass White Paper: The Cosmological Bootstrap,” in 2022 Snowmass Summer Study. 3, 2022. [arXiv:2203.08121 \[hep-th\]](#).
- [6] D. Baumann, *Cosmology*. Cambridge University Press, 7, 2022.
- [7] S. Dodelson, *Modern Cosmology*. Academic Press, Amsterdam, 2003.
- [8] P. Creminelli, M. A. Luty, A. Nicolis, and L. Senatore, “Starting the Universe: Stable Violation of the Null Energy Condition and Non-standard Cosmologies,” *JHEP* **12** (2006) 080, [arXiv:hep-th/0606090](#).
- [9] C. Cheung, P. Creminelli, A. L. Fitzpatrick, J. Kaplan, and L. Senatore, “The Effective Field Theory of Inflation,” *JHEP* **03** (2008) 014, [arXiv:0709.0293 \[hep-th\]](#).
- [10] D. Baumann, “Inflation,” in Theoretical Advanced Study Institute in Elementary Particle Physics: Physics of the Large and the Small, pp. 523–686. 2011. [arXiv:0907.5424 \[hep-th\]](#).
- [11] E. Mottola, “Particle Creation in de Sitter Space,” *Phys. Rev. D* **31** (1985) 754.
- [12] B. Allen, “Vacuum States in de Sitter Space,” *Phys. Rev. D* **32** (1985) 3136.
- [13] N. Arkani-Hamed and J. Maldacena, “Cosmological Collider Physics,” [arXiv:1503.08043 \[hep-th\]](#).
- [14] J. S. Schwinger, “Brownian motion of a quantum oscillator,” *J. Math. Phys.* **2** (1961) 407–432.
- [15] P. M. Bakshi and K. T. Mahanthappa, “Expectation value formalism in quantum field theory. 1.,” *J. Math. Phys.* **4** (1963) 1–11.
- [16] L. V. Keldysh, “Diagram technique for nonequilibrium processes,” *Zh. Eksp. Teor. Fiz.* **47** (1964) 1515–1527.
- [17] R. D. Jordan, “Effective Field Equations for Expectation Values,” *Phys. Rev. D* **33** (1986) 444–454.
- [18] E. Calzetta and B. L. Hu, “Closed Time Path Functional Formalism in Curved Space-Time: Application to Cosmological Back Reaction Problems,” *Phys. Rev. D* **35** (1987) 495.
- [19] J. M. Maldacena, “Non-Gaussian features of primordial fluctuations in single field inflationary models,” *JHEP* **05** (2003) 013, [arXiv:astro-ph/0210603 \[astro-ph\]](#).
- [20] S. Weinberg, “Quantum contributions to cosmological correlations,” *Phys. Rev. D* **72** (2005) 043514, [arXiv:hep-th/0506236 \[hep-th\]](#).
- [21] S. Weinberg, *The Quantum theory of fields. Vol. 1: Foundations*. Cambridge University Press, 6, 2005.
- [22] M. E. Peskin and D. V. Schroeder, *An Introduction to quantum field theory*. Addison-Wesley, Reading, USA, 1995.
- [23] S. B. Giddings and M. S. Sloth, “Cosmological diagrammatic rules,” *JCAP* **1007** (2010) 015, [arXiv:1005.3287 \[hep-th\]](#).

- [24] D. Baumann, C. Duaso Pueyo, A. Joyce, H. Lee, and G. L. Pimentel, “The Cosmological Bootstrap: Weight-Shifting Operators and Scalar Seeds,” *JHEP* **12** (2020) 204, [arXiv:1910.14051 \[hep-th\]](#).
- [25] A. Bzowski, P. McFadden, and K. Skenderis, “Implications of conformal invariance in momentum space,” *JHEP* **03** (2014) 111, [arXiv:1304.7760 \[hep-th\]](#).
- [26] P. Creminelli, “Conformal invariance of scalar perturbations in inflation,” *Phys. Rev. D* **85** (2012) 041302, [arXiv:1108.0874 \[hep-th\]](#).
- [27] C. Cheung, A. L. Fitzpatrick, J. Kaplan, and L. Senatore, “On the consistency relation of the 3-point function in single field inflation,” *JCAP* **02** (2008) 021, [arXiv:0709.0295 \[hep-th\]](#).
- [28] N. Arkani-Hamed, D. Baumann, H. Lee, and G. L. Pimentel, “The Cosmological Bootstrap: Inflationary Correlators from Symmetries and Singularities,” *JHEP* **04** (2020) 105, [arXiv:1811.00024 \[hep-th\]](#).
- [29] V. K. Dobrev, G. Mack, V. B. Petkova, S. G. Petrova, and I. T. Todorov, *Harmonic Analysis on the n-Dimensional Lorentz Group and Its Application to Conformal Quantum Field Theory*, vol. 63. 1977.
- [30] Z. Sun, “A note on the representations of $\text{SO}(1, d+1)$,” [arXiv:2111.04591 \[hep-th\]](#).
- [31] S. Deser and A. Waldron, “Arbitrary spin representations in de Sitter from dS / CFT with applications to dS supergravity,” *Nucl. Phys.* **B662** (2003) 379–392, [arXiv:hep-th/0301068 \[hep-th\]](#).
- [32] P. Creminelli, A. Joyce, J. Khoury, and M. Simonovic, “Consistency Relations for the Conformal Mechanism,” *JCAP* **1304** (2013) 020, [arXiv:1212.3329](#).
- [33] L. Berezhiani, J. Khoury, and J. Wang, “Non-Trivial Checks of Novel Consistency Relations,” *JCAP* **1406** (2014) 056, [arXiv:1401.7991 \[hep-th\]](#).
- [34] J. M. Maldacena and G. L. Pimentel, “On graviton non-Gaussianities during inflation,” *JHEP* **09** (2011) 045, [arXiv:1104.2846 \[hep-th\]](#).
- [35] A. Bzowski, P. McFadden, and K. Skenderis, “Scalar 3-point functions in CFT: renormalisation, beta functions and anomalies,” *JHEP* **03** (2016) 066, [arXiv:1510.08442 \[hep-th\]](#).
- [36] H. Goodhew, S. Jazayeri, M. H. Gordon Lee, and E. Pajer, “Cutting Cosmological Correlators,” *JCAP* **08** (2021) 003, [arXiv:2104.06587 \[hep-th\]](#).
- [37] P. Adshead, R. Easther, and E. A. Lim, “The ‘in-in’ Formalism and Cosmological Perturbations,” *Phys. Rev. D* **80** (2009) 083521, [arXiv:0904.4207 \[hep-th\]](#).
- [38] L. Senatore and M. Zaldarriaga, “On Loops in Inflation,” *JHEP* **12** (2010) 008, [arXiv:0912.2734 \[hep-th\]](#).
- [39] A. Kaya, “On $i\epsilon$ Prescription in Cosmology,” *JCAP* **04** (2019) 002, [arXiv:1810.12324 \[gr-qc\]](#).
- [40] M. Baumgart and R. Sundrum, “Manifestly Causal In-In Perturbation Theory about the Interacting Vacuum,” *JHEP* **03** (2021) 080, [arXiv:2010.10785 \[hep-th\]](#).
- [41] M. Baumgart and R. Sundrum, “De Sitter Diagrammar and the Resummation of Time,” *JHEP* **07** (2020) 119, [arXiv:1912.09502 \[hep-th\]](#).
- [42] S. Coleman, “Notes from Sidney Coleman’s Physics 253a: Quantum Field Theory,” [arXiv:1110.5013 \[physics.ed-ph\]](#).
- [43] X. Chen, Y. Wang, and Z.-Z. Xianyu, “Schwinger-Keldysh Diagrammatics for Primordial Perturbations,” *JCAP* **12** (2017) 006, [arXiv:1703.10166 \[hep-th\]](#).
- [44] A. Abolhasani and H. Goodhew, “Derivative interactions during inflation: a systematic approach,”

JCAP **06** no. 06, (2022) 032, arXiv:2201.05117 [hep-th].

- [45] T. Falk, R. Rangarajan, and M. Srednicki, “The Angular dependence of the three point correlation function of the cosmic microwave background radiation as predicted by inflationary cosmologies,” *Astrophys. J. Lett.* **403** (1993) L1, arXiv:astro-ph/9208001.
- [46] C. Sleight, “A Mellin Space Approach to Cosmological Correlators,” *JHEP* **01** (2020) 090, arXiv:1906.12302 [hep-th].